

IJEST

Special Issue

ISSN: 0973-6255
Vol. 10 No.1
January - June 2016

Indian Journal of Engineering, Science, and Technology

A Refereed Research Journal



Published by

BANNARI AMMAN INSTITUTE OF TECHNOLOGY

(Autonomous Institution Affiliated to Anna University of Technology, Coimbatore -

Approved by AICTE - Accredited by NBA and NAAC with "A" Grade)

Sathyamangalam - 638 401 Erode District Tamil Nadu India

Ph: 04295-226340 - 44 Fax: 04295-226666

www.bitsathy.ac.in E-mail: ijest@bitsathy.ac.in



Indian Journal of Engineering, Science, and Technology

IJEST is a refereed research journal published half-yearly by Bannari Amman Institute of Technology. Responsibility for the contents rests upon the authors and not upon the IJEST. For copying or reprint permission, write to Copyright Department, IJEST, Bannari Amman Institute of Technology, Sathyamangalam, Erode District - 638 401, Tamil Nadu, India.

Advisor

Dr. A.M. Natarajan
Chief Executive

Editor

Dr. D. Saravanan
Principal

Associate Editors

Dr. S. Valarmathy
Professor & Head/ECE
Dr. Lakshmi Narayana M Mohan
Associate Professor/ECE

Bannari Amman Institute of Technology, Sathyamangalam, Erode District - 638 401, Tamil Nadu, India

Editorial Board

Dr. Srinivasan Alavandar

Department of Electronics and Computer Engineering
Caledonian (University) College of Engineering
PO Box: 2322, CPO Seeb-111, Sultanate of Oman

Dr. H.S. Jamadagni

Centre for Electronics Design and Technology
Indian Institute of Science
Bangalore - 560 012

Dr. V.K. Kothari

Department of Textile Technology
Indian Institute of Technology-Delhi
New Delhi - 110 016

Dr. S. Mohan

National Institute of Technical Teachers Training and
Research
Taramani, Chennai - 600 113

Dr. P. Nagabhushan

Department of Studies in Computer Science
University of Mysore
Mysore - 570 006

Dr. Edmond C. Prakash

Department of Computing and Mathematics
Manchester Metropolitan University
Chester Street, Manchester M1 5GD, United Kingdom

Dr. E.G. Rajan

Pentagram Research Centre Pvt. Ltd.
Hyderabad - 500 028
Andhra Pradesh

Dr. Seshadri S.Ramkumar

Nonwovens & Advanced Materials Laboratory
The Institute of Environmental & Human Health
Texas Tech University, Box 41163
Lubbock, Texas 79409-1163, USA

Dr. T.S. Ravi Sankar

Department of Electrical Engineering
University of South Florida
Sarasota, FL 34243, USA

Dr. T.S. Jagannathan Sankar

Department of Mechanical and Chemical Engineering
North Carolina A&T State University
NC 27411, USA

Dr. A.K. Sarje

Department of Electronics & Computer Engineering
Indian Institute of Technology, Roorkee
Roorkee - 247 667

Dr. R. Sreeramkumar

Department of Electrical Engineering
National Institute of Technology - Calicut
Calicut - 673 601

Dr. Talabatulla Srinivas

Department of Electrical & Communication Engineering
Indian Institute of Science
Bangalore - 560 012

Dr. Dinesh K. Sukumaran

Magnetic Resonance Centre
Department of Chemistry
State University of New York Buffalo, USA - 141 214

Dr. Prahlad Vadakkepat

Department of Electrical and Computer Engineering
National University of Singapore
4 Engineering Drive 3, Singapore 117576

Dr. S. Srikanth

AU-KBC Research Centre
Madras Institute of Technology Campus
Anna University
Chennai-600 044

CONTENTS

Excerpt from the Proceeding of National Conference

S.No.	Title	Page.No.
1	Realization of Aging Aware Reliable Multiplier Design Using Verilog R.Rathna Devi and R.Ganesan	01
2	Bloom Filter Based Data Management With Error Detection And Correction V. K. Juvilna, S. Amalorpava Mary Rajee and R.Ganesan	08
3	Comparative Analysis of Different Wheeling Charge Methodologies N. Selvam and P.L. Somasundaram	14
4	Analysis on Various Optimization Techniques for Selecting Gain Parameters in FOC of an E-Drive Meher Anusha Vanapalli, Raja Sekhar Kammala and Sathish Laxmanan	20
5	Automated Gesture Recognition System Using Raspberry Pi N. Geraldine Shirley and Neethu Krishna	25
6	Assessment and Enhancement of Transient Stability in Power system using ETAP Software A.Maria Sindhuja and D. Raj Kumar	31
7	Antioxidant Activities of A Few Common Seaweeds from the Gulf of Mannar and the Effect of Drying As the Method of Preservation R.Charu Deepika, J.Madhusudhanan and T.Charles John Bhaskar	37
8	Optimization, Standardization of extraction and Characterization of Lutein S. Gayathri, S.R. Radhika Rajasree, L. Aranganathan and T.Y. Suman	44
9	Biopharmaceuticals and Nutraceuticals from Marine Species and Marine Waste T. Charles John Bhaskar	49
10	Analysis and Comparison of Mechanical Properties of Alloy Steel gr.22 Material Welded by GMAW Process with Conventional SMAW Process K. Karthikeyan, V. Anandakrishnan and R. Alagesan	53
11	A Finite Element Investigation on Nonlinear Elastic Material for Anthropomorphic Robotic Fingertips J. Pugalenthil, M.Raguraman, L.Vijayakumar, S. Sankar, S. Yuvaraj and K. Venkatesh Raja	59
12	Experimental Study on a Solar Water Desalination System K.Selvakannan and P.Prashanth	64

Realization of Aging Aware Reliable Multiplier Design Using Verilog

R.Rathna Devi¹ and R.Ganesan²

¹PG Scholar, ²PG Scholar Head, Sethu Institute of Technology, Kariapatti - 626 115, Virudhunagar District, Tamil Nadu

E-mail: r.rathnadevi@gmail.com, ganesanhod@gmail.com

Abstract

Digital multipliers are among the most critical arithmetic functional units. The overall performance of these systems depends on the throughput of the multiplier. Meanwhile, the negative bias temperature instability effect occurs when a PMOS transistor is under negative bias ($V_{gs} = -V_{dd}$), increasing the threshold voltage of the PMOS transistor, and reducing multiplier speed. The similar phenomenon, positive bias temperature instability, occurs when an NMOS transistor is under positive bias. Both effects degrade transistor speed, and in the long term, the system may fail due to timing violations. Therefore, it is important to design reliable high-performance multipliers. In this paper, we propose an aging-aware multiplier design with a novel adaptive hold logic (AHL) circuit. The multiplier is able to provide higher throughput through the variable latency and can adjust the AHL circuit to mitigate performance degradation that is due to the aging effect. Moreover, the proposed architecture can be applied to a column- or row-bypassing multiplier. The experimental results show that proposed architecture can attain performance improvement.

Keywords: Adaptive hold logic (AHL), Column By-Passing Multiplier(CBPM), Row By-Passing Multiplier(RBPM), Variable latency.

1. INTRODUCTION

Multipliers are key components of many high performance systems such as FIR filters, microprocessors, digital signal processors, etc. A system's performance is generally determined by the performance of the multiplier because the multiplier is generally the slowest element in the system. Furthermore, it is generally the most area consuming. Hence, optimizing the speed and area of the multiplier is a major design issue. However, area and speed are usually conflicting constraints so that improving speed results mostly in larger areas. As a result, a whole spectrum of multipliers with different area-speed constraints have been designed with fully parallel. Multipliers at one end of the spectrum and fully serial multipliers at the other end. In between, the digit serial multipliers where single digits consisting of several bits are operated on. These multipliers have moderate performance in both speed and area. Power dissipation is recognized as a critical parameter in modern VLSI design field. To satisfy Moore's law and to produce consumer electronics goods with more backup and less weight, low power VLSI design is necessary. Dynamic power dissipation which is the major part of total power dissipation is due to the charging and discharging capacitance in the circuit.

Fast multipliers are essential parts of digital signal processing systems. The speed of multiply operation is of great importance in digital signal processing as well as in the general purpose processors today, especially since the media processing took off. In the past multiplication was generally implemented via a sequence of addition, subtraction, and shift operations. Multiplication can be considered as a series of repeated additions. The number to be added is the multiplicand, the number of times that it is added is the multiplier, and the result is the product. Each step of addition generates a partial product.

The basic multiplication principle is two fold i.e., evaluation of partial products and accumulation of the shifted partial products. It is performed by the successive additions of the columns of the shifted partial product matrix. The 'multiplier' is successfully shifted and gates the appropriate bit of the 'multiplicand'. The delayed, gated instance of the multiplicand must all be in the same column of the shifted partial product matrix. They are then added to form the product bit for the particular form. Multiplication is therefore a multi operand operation.

1.1 Methods and Performances

There are number of techniques that to perform binary multiplication. In general, the choice is based upon factors such as latency, throughput, area, and design complexity. More efficient parallel approach uses some sort of array or tree of full adders to sum partial products. Array multiplier, Booth Multiplier and Wallace Tree multipliers are some of the standard approaches to have hardware implementation of binary multiplier which are suitable for VLSI implementation at CMOS level.

1.1.1 Array Multiplier

Array multiplier is an efficient layout of a combinational multiplier. Multiplication of two binary number can be obtained with one micro-operation by using a combinational circuit that forms the product bit all at once thus making it a fast way of multiplying two numbers since only delay is the time for the signals to propagate through the gates that forms the multiplication array.

In array multiplier, consider two binary numbers A and B, of m and n bits. There are mn summands that are produced in parallel by a set of mn AND gates. n x n multiplier requires n (n-2) full adders, n half-adders and n² AND gates. Also, in array multiplier worst case delay would be (2n+1) td.

Array Multiplier gives more power consumption as well as optimum number of components required, but delay for this multiplier is larger. It also requires larger number of gates because of which area is also increased; due to this array multiplier is less economical. Thus, it is a fast multiplier but hardware complexity is high.

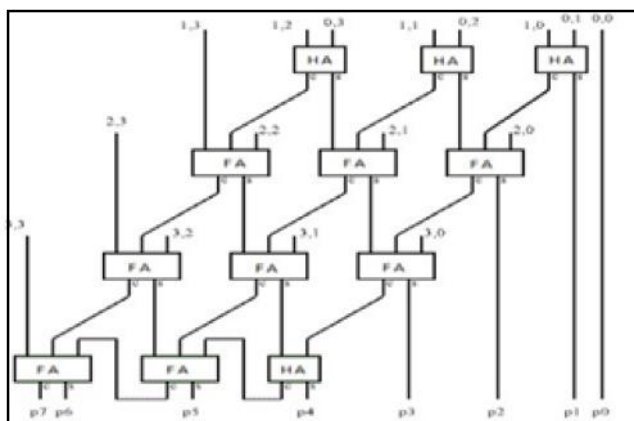


Fig.1 Array multiplier

2. EXISTING SCHEME

Digital multipliers are among the most critical arithmetic functional units in many applications, such as the Fourier transform, discrete cosine transforms, and digital filtering. The throughput of these applications depends on multipliers, and if the multipliers are too slow, the performance of entire circuits will be reduced. Furthermore, negative bias temperature instability (NBTI) occurs when PMOS transistor is under -ve bias ($V_{gs} = -V_{dd}$).

In this situation, the interaction between inversion layer holes and hydrogen-passivated Si atoms breaks the Si-H bond generated during the oxidation process, generating H or H₂ molecules. When these molecules diffuse away, interface traps are left. The accumulated interface traps between silicon and the gate oxide interface result in increased threshold voltage (V_{th}), reducing the circuit switching speed. When the biased voltage is removed, the reverse reaction occurs, reducing the NBTI effect. However, the reverse reaction does not eliminate all the interface traps generated during the stress phase, and V_{th} is increased in the long term. Hence, it is important to design a reliable high-performance multiplier.

2.1 Column-Bypassing Multiplier

A column-bypassing multiplier is an improvement on the normal array multiplier (AM). The AM is a fast parallel AM and is shown in Fig. 1. The multiplier array consists of (n - 1) rows of carry save adder (CSA), in which each row contains (n - 1) full adder (FA) cells. Each FA in the CSA array has two outputs:

- 1) the sum bit goes down and
- 2) the carry bit goes to the lower left F

The FAs in the AM are always active regardless of input states. A low-power column-bypassing multiplier design is proposed in which the FA operations are disabled if the corresponding bit in the multiplicand is 0. Figure shows a 4 x 4 column-bypassing multiplier. Supposing the inputs are 10102 * 11112, it can be seen that for the FAs in the first and third diagonals, two of the three input bits are 0: the carry bit from its upper right FA and the partial product $a_i b_i$. Therefore, the output of the adders in both diagonals is 0, and the output sum bit is simply equal to the third bit, which is the sum output of its upper FA. Hence, the FA is modified to add two tristate gates and one multiplexer.

The multiplicand bit a_i can be used as the selector of the multiplexer to decide the output of the FA, and a_i can also be used as the selector of the tristate gate to turn off the input path of the FA. If a_i is 0, the inputs of FA are disabled, and the sum bit of the current FA is equal to the sum bit from its upper FA, thus reducing the power consumption of the multiplier. If a_i is 1, the normal sum result is selected. More details for the column-bypassing multiplier can be found.

2.2 Row-Bypassing Multiplier

A low-power row-bypassing multiplier is also proposed to reduce the activity power of the AM. The operation of the low-power row-bypassing multiplier is similar to that of the low-power column-bypassing multiplier, but the selector of the multiplexers and the tristate gates use the multiplier.

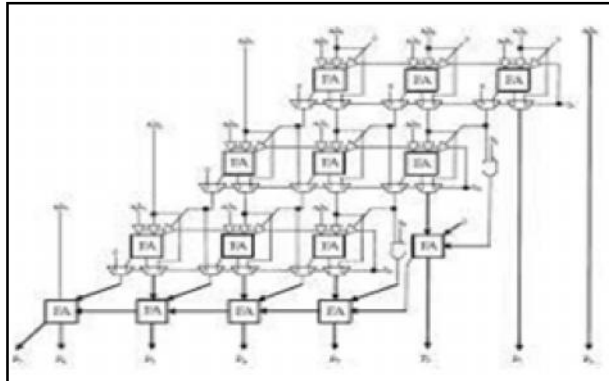


Fig.2 Row-By Passing Multiplier

In a 4×4 row-bypassing multiplier each input is connected to an FA through a tristate gate. When the inputs are $1112 * 10012$, the two inputs in the first and second rows are 0 for FAs. Because b_1 is 0, the multiplexers in the first row select $a_i b_0$ as the sum bit and select 0 as the carry bit. The inputs are bypassed to FAs in the second rows, and the tristate gates turn off the input paths to the FAs. Therefore, no switching activities occur in the first-row FAs; in return, power consumption is reduced. Similarly, because b_2 is 0, no switching activities will occur in the second-row FAs. However, the FAs must be active in the third row because the b_3 is not zero. More details for the row-bypassing multiplier can also be found in Row By passing Multiplier.

3. PROPOSED SCHEME

The multiplier is based on the variable-latency technique and can adjust the AHL circuit to achieve

reliable operation under the influence of NBTI and PBTI effects. To be specific, the contributions of this paper are summarized as follows: 1) novel variable-latency multiplier architecture with an AHL circuit. The AHL circuit can decide whether the input patterns require one or two cycles and can adjust the judging criteria to ensure that there is minimum performance degradation after considerable aging occurs; 2) comprehensive analysis and comparison of the multiplier’s performance under different cycle periods to show the effectiveness of our proposed architecture; 3) an aging-aware reliable multiplier design method that is suitable for large multipliers. Although the experiment is performed in 16- and 32-bit multipliers, our proposed architecture can be easily extended to large designs;

3.1 Proposed Aging-Aware Multiplier

Proposed aging-aware multiplier architecture, which includes two m -bit inputs (m is a positive number), one $2m$ -bit output, one column- or row-bypassing multiplier, $2m$ 1-bit Razor flip-flops, and an AHL circuit.

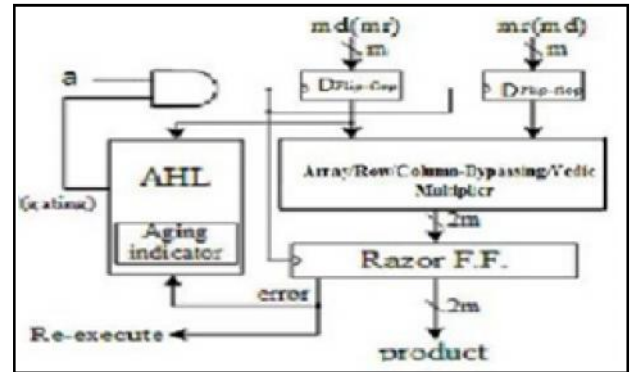


Fig. 3 Proposed architecture (md means multiplicand; mr means multiplier)

Hence, the two aging-aware multipliers can be implemented using similar architecture, and the difference between the two bypassing multipliers lies in the input signals of the AHL. According to the bypassing selection in the column or rowbypassing multiplier, the input signal of the AHL in the architecture with the column-bypassing multiplier is the multiplicand, whereas of the row-bypassing multiplier is the multiplier

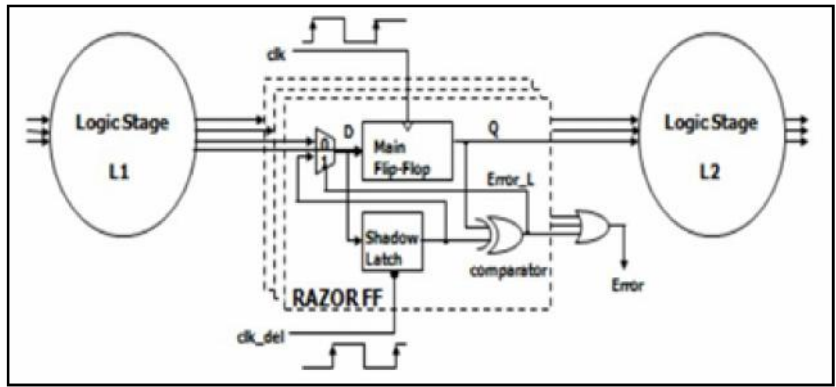


Fig.4 Razor Flipflop

Razor flip-flops can be used to detect whether timing violations occur before the next input pattern arrives. A 1-bit Razor flip-flop contains a main flip-flop, shadow latch, XOR gate, and mux. The main flip-flop catches the execution result for the combination circuit using a normal clock signal, and the shadow latch catches the execution result using a delayed clock signal, which is slower than the normal clock signal. If the latched bit of the shadow latch is different from that of the main flip-flop, this means the path delay of the current operation exceeds the cycle period, and the main flip-flop catches an incorrect result. If errors occur, the Razor flip-flop will set the error signal to 1 to notify the system to reexecute the operation and notify the AHL circuit that an error has occurred. We use Razor flip-flops to detect whether an operation that is considered to be a one-cycle pattern can really finish in a cycle. If not, the operation is reexecuted with two cycles. Although the reexecution may seem costly, the overall cost is low because the reexecution frequency is low.

More details for the Razor flip-flop can be found. The AHL circuit is the key component in the aging-ware variable-latency multiplier.

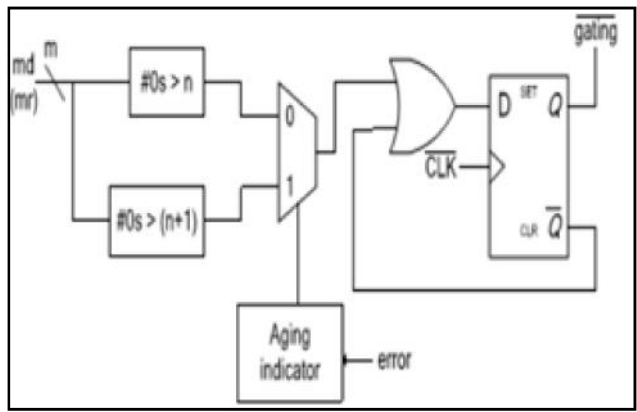


Fig.5 AHL (md means multiplicand; mr means multiplier)
IJEST Vol.10 No.1 January - June 2016

The AHL circuit contains an aging indicator, two judging blocks, one mux, and one D flip-flop. The aging indicator indicates whether the circuit has suffered significant performance degradation due to the aging effect. The aging indicator is implemented in a simple counter that counts the number of errors over a certain amount of operations and is reset to zero at the end of those operations. If the cycle period is too short, the column- or row-bypassing multiplier is not able to complete these operations successfully, causing timing violations. These timing violations will be caught by the Razor flip-flops, which generate error signals. If errors happen frequently and exceed a predefined threshold, it means the circuit has suffered significant timing degradation due to the aging effect, and the aging indicator will output signal 1; otherwise, it will output 0 to indicate the aging effect is still not significant, and no actions are needed.

The first judging block in the AHL circuit will output 1 if the number of zeros in the multiplicand (multiplier for the row-bypassing multiplier) is larger than n (n is a positive number, which will be discussed in Section IV), and the second judging block in the AHL circuit will output 1 if the number of zeros in the multiplicand (multiplier) is larger than $n + 1$. They are both employed to decide whether an input pattern requires one or two cycles, but only one of them will be chosen at a time. In the beginning, the aging effect is not significant, and the aging indicator produces 0, so the first judging block is used. After a period of time when the aging effect becomes significant, the second judging block is chosen. Compared with the first judging block, the second judging block allows a smaller number of patterns to become one-cycle patterns because it requires more zeros in the multiplicand (multiplier).

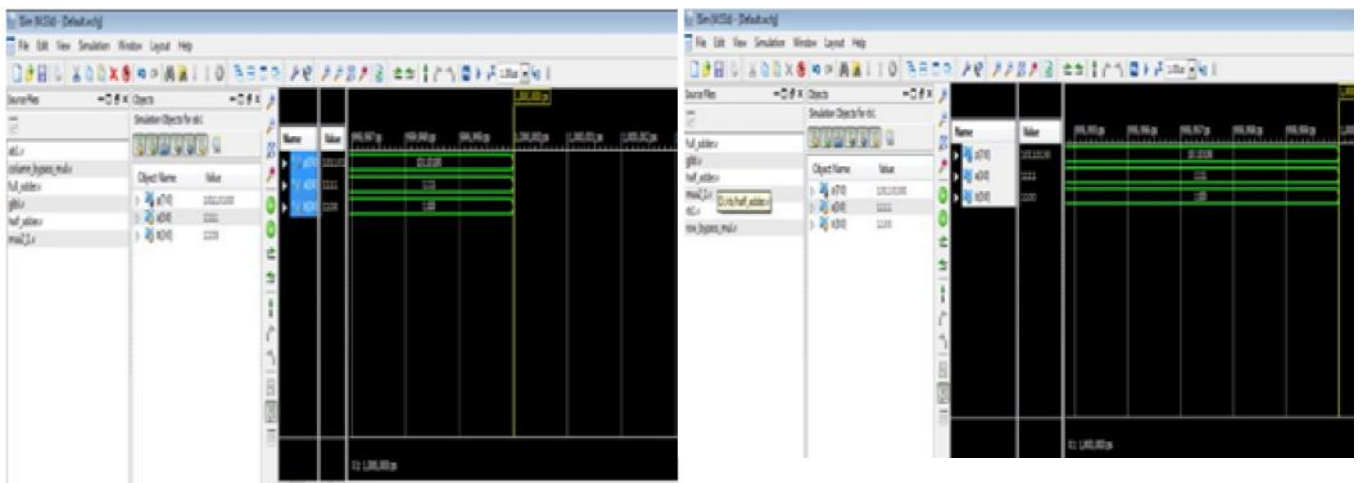
The details of the operation of the AHL circuit are as follows: when an input pattern arrives, both judging blocks will decide whether the pattern requires one cycle or two cycles to complete and pass both results to the multiplexer. The multiplexer selects one of either result based on the output of the aging indicator. Then an OR operation is performed between the result of the multiplexer, and the Q signal is used to determine the input of the D flip-flop. When the pattern requires one cycle, the output of the multiplexer is 1. The $!(gating)$ signal will become 1, and the input flip flops will latch new data in the next cycle. On the other hand, when the output of the multiplexer is 0, which means the input pattern requires two cycles to complete, the OR gate will output 0 to the D flip-flop. Therefore, the $(gating)$ signal will be 0 to disable the clock signal of the input flip-flops in the next cycle.

Note that only a cycle of the input flip-flop will be disabled because the D flip-flop will latch 1 in the next cycle. The overall flow of our proposed architecture is as follows: when input patterns arrive, the column- or row-bypassing multiplier, and the AHL circuit execute simultaneously. According to the number of zeros in the multiplicand (multiplier), the AHL circuit decides if the input patterns require one or two cycles. If the input pattern requires two cycles to complete, the AHL will output 0 to disable the clock signal of the flip-flops. Otherwise, the AHL will output 1 for normal operations. When the column- or row-bypassing multiplier finishes the operation, the result will be passed to the Razor flip-flops. The Razor flipflops check whether there is the path delay timing violation. If timing violations occur, it means the cycle period is not long enough for the current operation to complete and that the execution

result of the multiplier is incorrect. Thus, the Razor flip-flops will output an error to inform the system that the current operation needs to be reexecuted using two cycles to ensure the operation is correct. In this situation, the extra reexecution cycles caused by timing violation incurs a penalty to overall average latency. However, our proposed AHL circuit can accurately predict whether the input patterns require one or two cycles in most cases. Only a few input patterns may cause a timing variation when the AHL circuit judges incorrectly. In this case, the extra reexecution cycles did not produce significant timing degradation.

4. EXPERIMENTAL RESULTS

In the variable-latency design, the average latency is affected by both the percentage of one-cycle patterns and the cycle period. If more patterns only require one cycle, the average latency is reduced. Similarly, if the cycle period is reduced, the average latency is also reduced. However, the cycle period cannot be too small. If the cycle period is too small, large amounts of timing violations will be detected by the Razor flip-flops, and the average latency will increase. Hence, it is important to analyze the tradeoff between the percentage of one-cycle patterns and the cycle period. To achieve this, we analyze three scenarios for both 16×16 and 32×32 variable latency column-bypassing (VLCB) and variable-latency rowbypassing (VLRB) multipliers. We also compare the results with the AM, a FLCB multiplier, and a fixed-latency rowbypassing (FLRB) multiplier.



Timing constraint: Default path analysis
Total number of paths / destination ports: 614 / 8

Delay: 13.940ns (Levels of Logic = 10)
Source: a<1> (PAD)
Destination: p<7> (PAD)

Data Path: a<1> to p<7>

Cell:in->out	Fanout	Gate Delay	Net Delay	Logical Name (Net Name)
IBUF:I->O	11	0.849	1.076	a_1_IBUF (a_1_IBUF)
LUT4:I0->O	2	0.648	0.527	U_mux2_1bb/data_out1 (r1_mux2_op<1>)
LUT3:I1->O	1	0.643	0.000	U_mux2_1ee/data_out66_G (N50)
MUXF8:I1->O	4	0.276	0.667	U_mux2_1ee/data_out66 (z2_mux2_op<1>)
LUT4:I1->O	1	0.643	0.000	U_mux2_1gg/data_out2 (U_mux2_1gg/data_out1)
MUXF8:I0->O	2	0.276	0.479	U_mux2_1gg/data_out_f5 (r3_mux2_op<0>)
LUT3:I2->O	2	0.648	0.527	U_full_adder11/carry1 (w_carry<11>)
LUT3:I1->O	2	0.643	0.450	U_full_adder12/carry1 (w_carry<12>)
LUT4:I3->O	1	0.648	0.420	U_full_adder13/carry1 (p_7_OBUF)
OBUF:I->O		4.520		p_7_OBUF (p<7>)
Total		13.940ns	9.794ns	(9.794ns logic, 4.146ns route) (70.3% logic, 29.7% route)

Timing constraint: Default path analysis
Total number of paths / destination ports: 330 / 8

Delay: 11.976ns (Levels of Logic = 7)
Source: b<1> (PAD)
Destination: p<7> (PAD)

Data Path: b<1> to p<7>

Cell:in->out	Fanout	Gate Delay	Net Delay	Logical Name (Net Name)
IBUF:I->O	7	0.849	0.881	b_1_IBUF (b_1_IBUF)
LUT4:I0->O	2	0.648	0.590	U_full_adder1/U_half_adder2/carry1 (U_full_adder1/carry1)
LUT4:I0->O	2	0.648	0.450	U_full_adder4/carry1 (w_carry<3>)
LUT4:I3->O	3	0.648	0.611	gnt_0_and00001 (gnt<0>)
LUT4:I1->O	2	0.643	0.450	U_full_adder11/carry1 (w_carry<10>)
LUT4:I3->O	1	0.648	0.420	U_full_adder12/carry1 (p_7_OBUF)
OBUF:I->O		4.520		p_7_OBUF (p<7>)
Total		11.976ns	8.46ns	(8.46ns logic, 3.372ns route) (71.0% logic, 28.3% route)

Timing constraint: Default period analysis for Clock 'clk_del'
Clock period: 2.013ns (frequency: 496.771MHz)
Total number of paths / destination ports: 8 / 8

Delay: 2.013ns (Levels of Logic = 1)
Source: U_razor8/U_shadow_ff/q_out (FF)
Destination: U_razor8/U_shadow_ff/q_out (FF)
Source Clock: clk_del rising
Destination Clock: clk_del rising

Data Path: U_razor8/U_shadow_ff/q_out to U_razor8/U_shadow_ff/q_out

Cell:in->out	Fanout	Gate Delay	Net Delay	Logical Name (Net Name)
FDC:C->Q	2	0.591	0.527	U_razor8/U_shadow_ff/q_out (U_razor8/U_shadow_ff/q_out)
LUT3:I1->O	2	0.643	0.000	U_razor8/U_mux2_1/data_out1 (U_razor8/mx_0)
FDC:D		0.252		U_razor8/U_shadow_ff/q_out
Total		2.013ns	1.486ns	(1.486ns logic, 0.527ns route) (73.8% logic, 26.2% route)

Timing constraint: Default period analysis for Clock 'clk'
Clock period: 2.054ns (frequency: 486.855MHz)

Table 1 Experimental Results

Parameters	Multipliers	Percentage
Look-up tables	Row-by pass	40
	Column-by pass	26
	Razor Flip-flop	14
Delay	Row-by pass	13.940ns
	Column-by pass	11.976ns
	Razor Flip-flop	2.013ns

5. CONCLUSION

An aging aware design of a novel Adaptive Hold Logic (AHL) circuit is proposed in this paper. The AHL circuit adjusts itself to mitigate performance degradation which is caused due to aging effects. This proposed work can be used in various VLSI applications to perform operations like addition, multiplication etc. The AHL circuit will produce output which will be both power and area efficient. The results will be in terms of Latency and Power consumption which will improve the circuit performance.

REFERENCE

- [1] A. Calimera and E. Macii, "Design Techniques for NBTI Tolerant Power-gating Architecture," *IEEE Transactions on Circuits System*, Exp. Briefs, Vol.59, No.4, Apr. 2012, pp. 249-253.
- [2] A. Mohanra and M. Poncino, "Design techniques for NBTI Tolerant Power-Gating Architecture", *IEEE Transactions on Circuits System, Exp. Briefs*, Vol.59, No.4, Apr. 2012, pp. 249-253.
- [3] N. V. Mujadiya, "Instruction Scheduling On Variable Latency Functional Units of VLIW Processors", in *Proc. ACM/IEEE ISED*, Dec. 2011, pp.307-312.
- [4] M. Olivieri, "Design of Synchronous and Asynchronous Variable-Latency Pipelined Multipliers", *IEEE Transactions on Very Large Scale Integr. (VLSI) Syst.*, Vol. 9, No.4, Aug. 2001, pp.365-376.
- [5] K. Du, P. Varman and K. Mohanram, "High Performance Reliable Variable Latency Carry Select Addition", in *Proc. DATE*, 2012, pp. 1257–1262.
- [6] M.C. Wen, S.-J. Wang and Y.-N. Lin, "Low Power Parallel Multiplier with Column Bypassing", in *Proc. IEEE ISCAS*, May 2005, pp. 1638–1641.
- [7] H.I. Yang, S.-C. Yang, W. Hwang and C.-T. Chuang, "Impacts of NBTI/PBTI on Timing Control Circuits and Degradation Tolerant Design in Nanoscale CMOS SRAM," *IEEE Transaction on Circuit Syst.*, Vol.58, No.6, June 2011, pp. 1239-1251.
- [8] K.C. Wu and D. Marculescu, "Aging-aware Timing Analysis and Opti-Mization Considering Path Sensitization", in *Proc. DATE*, 2011, pp. 1-6.

A Bloom Filter Based Data Management With Error Detection And Correction

V. K. Juvilna¹, S. Amalorpava Mary Rajee² and R.Ganesan³

¹PG Scholar, ²Assistant Professor, ³PG Program head,

Department of Electronics and Communication Engineering, VLSI Design,
Sethu Institute of Technology, Kariapatti - 626 115, Virudhunagar District, Tamil Nadu
E-mail: juvilna@gmail.com,maryrajee@yahoo.com,ganesanhod@gmail.com

Abstract

The rapid growth of memories in electronic devices, it is becoming a critical issue to save memory from being storing the existing data. Hence a new technology known as Bloom filters (BFs) provide a simple and effective way to check whether an element belongs to a set. BFs are implemented using electronic circuits. The contents of a BF are commonly stored in a high speed memory and required processing is done in a processor or in dedicated circuitry. some cases, the performance of those systems is affect by multiple cell upset(MCU). The stored data may change due to MCU. In order to improve the error in BF's Error Correction Code known as Decimal Matrix Code (DMC) is used to detect and correct errors. The results show that the proposed scheme can effectively perform error detection and correction in BF's.

Keywords: Bloom Filters (BFs), Decimal Matrix Code (DMC), Error Correction Code(ECC), Multiple Cell Upset(MCU)

1. INTRODUCTION

Bloom filters are compact data structures for probabilistic representation of a set in order to support membership queries (i.e. queries that ask: "Is element X in set Y?"). This compact representation is the payoff for allowing a small rate of *false positives* in membership queries; that is, queries might incorrectly recognize an element as member of the set. It will check whether the input is present in the set are not. It will reject if it is existing data and adds to memory when it is new input.

Filters can be built incrementally: as new elements are added to a set the corresponding positions are computed through the hash functions and bits are set in the filter. Moreover, the filter expressing the reunion of two sets is simply computed as the bit-wise OR applied over the two corresponding Bloom filters.

Bloom filters are compact data structures for probabilistic representation of a set in order to support membership queries. The main design tradeoffs are the number of hash functions used (driving the computational overhead), the size of the filter and the error (collision) rate.

2. PROPOSED SCHEME

Transient multiple cell upsets (MCUs) are becoming major issues in the reliability of memories exposed to radiation environment. To prevent MCUs from causing data corruption, more complex error correction codes (ECCs) are widely used to protect memory, but the main problem is that they would require higher delay overhead.

Recently, matrix codes (MCs) based on Hamming codes have been proposed for memory protection. The main issue is that they are double error correction codes and the error correction capabilities are not improved in all cases.

The proposed DMC utilizes decimal algorithm to obtain the maximum error detection capability. Moreover, the encoder-reuse technique (ERT) is proposed to minimize the area overhead of extra circuits without disturbing the whole encoding and decoding processes.

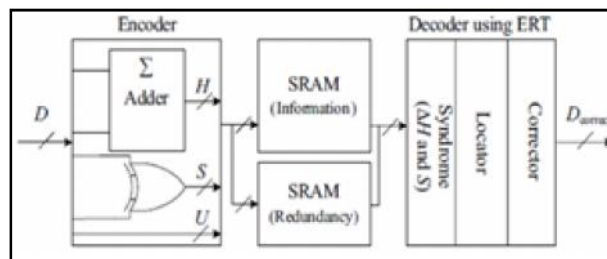


Fig.1 Decimal matrix codes

The ERT uses DMC encoder itself to be part of the decoder. The proposed DMC is compared to well-

known codes such as the existing Hamming, MCs, and punctured difference set (PDS) codes.

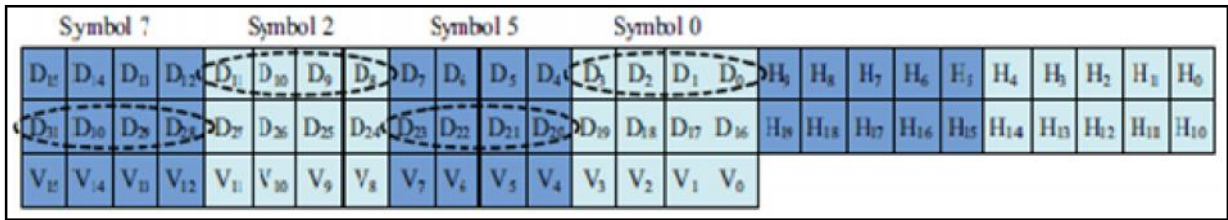


Fig.2 32 bit DMC

The proposed schematic of fault-tolerant memory is depicted in Figure 4.1. First, during the encoding (write) process, information bits D are fed to the DMC encoder, and then the horizontal redundant bits H and vertical redundant bits V are obtained from the DMC encoder. When the encoding process is completed, the obtained DMC code word is stored in the memory. If MCUs occur in the memory, these errors can be corrected in the decoding (read) process. Due to the advantage of decimal algorithm, the proposed DMC has higher fault-tolerant capability with lower performance overheads.

In the fault-tolerant memory, the ERT technique is proposed to reduce the area overhead of extra circuits and will be introduced in the following sections.

2.1 PROPOSED DMC ENCODER:

In the proposed DMC, first, the divide-symbol and arrange-matrix ideas are performed, i.e., the N -bit word is divided into k symbols of m bits ($N = k \times m$), and these symbols are arranged in a $k1 \times k2$ 2-D matrix $k = k1 \times k2$, where the values of $k1$ and $k2$ represent the numbers of rows and columns in the logical matrix respectively). Second, the horizontal redundant bits H are produced by performing decimal integer addition of selected symbols per row. Here, each symbol is regarded as a decimal integer. Third, the vertical redundant bits V are obtained by binary operation among the bits per column. It should be noted that both divide- symbol and arrange-matrix are implemented in logical instead of in physical.

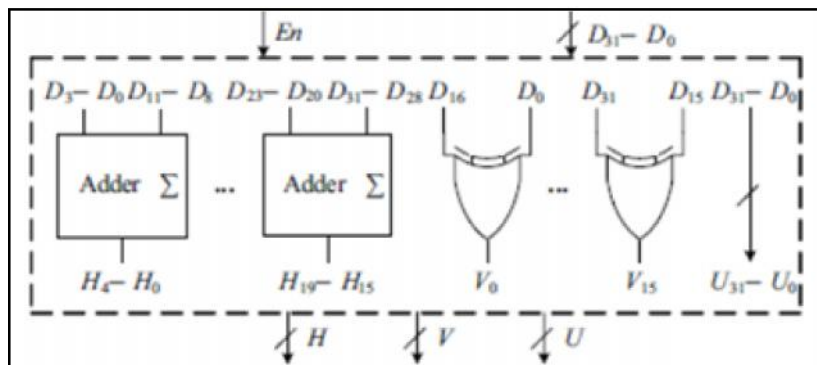


Fig.3 32 bit DMC Encoder structure

Therefore, the proposed DMC does not require changing the physical structure of the memory. To explain the proposed DMC scheme, we take a 32-bit word as an example. The cells from $D0$ to $D31$ are information bits. This 32-bit word has been divided into eight symbols of 4-bit. $k1 = 2$ and $k2 = 4$ have been chosen simultaneously. $H0-H19$ are horizontal check bits $V0$ through $V15$ are vertical check bits.

However, it should be mentioned that the maximum correction capability (i.e., the maximum size of MCUs can be corrected) and the number of

redundant bits are different when the different values for k and m are chosen. Therefore, k and m should be carefully adjusted to maximize the correction capability and minimize the number of redundant bits. For example, in this case, when $k = 2 \times 2$ and $m = 8$, only 1-bit error can be corrected and the number of redundant bits is 40. When $k = 4 \times 4$ and $m = 2$, 3-bit errors can be corrected and the number of redundant bits is reduced to 32. However, when $k = 2 \times 4$ and $m = 4$, the maximum correction capability is up to 5 bits and the number of redundant bits is 36. In this paper, in order to enhance the reliability of memory, the error correction capability

is first considered, so $k = 2 \times 4$ and $m = 4$ are utilized to construct DMC.

The horizontal redundant bits H can be obtained by decimal integer addition as follows:

$$H4H3H2H1H0 = D3D2D1D0 + D11D10D9D8 \quad (\text{Eq.1})$$

$$H9H8H7H6H5 = D7D6D5D4 + D15D14D13D12 \quad (\text{Eq.2})$$

The symbol “+” represents decimal integer addition.

For the vertical redundant bits V , we have

$$V0 = D0 \oplus D16 \quad (\text{Eq.3})$$

$$V1 = D1D17$$

(Eq.4)

2.2 PROPOSED DMC DECODER:

To obtain a word being corrected, the decoding process is required. For example, first, the received redundant bits $H4H3H2H1H0$.

$$\Delta H4H3H2H1H0 = H4H3H2H1H0' - H4H3H2H1H0 \quad (\text{Eq.5})$$

$$S0 = V0 + V0 \quad (\text{Eq.6})$$

When $\Delta H4H3H2H1H0$ and $S3$ “ $S0$ ” are equal to zero, the stored codeword has original information bits in symbol 0 where no errors occur. When $\Delta H4H3H2H1H0$ and $S3$ “ $S0$ ” are nonzero, the induced errors (the number of errors is 4 in this case) are detected and located in symbol 0, and then these errors can be corrected by

$$D0_{\text{correct}} = D0 + S0 \quad (\text{Eq.7})$$

The proposed DMC decoder which is made up of the following sub modules, and each executes a specific task in the decoding process: syndrome calculator, error locator, and error corrector. It can be observed from this figure 4 that the redundant bits must be recomputed from the received information bits D and compared to the original set of redundant bits in order to obtain the syndrome bits ΔH and S . Then error locator uses ΔH and S to detect and locate which bits some errors occur in. Finally, in the error corrector, these errors can be corrected by inverting the values of error bits.

In the proposed scheme, the circuit area of DMC is minimized by reusing its encoder. This is called the ERT. The ERT can reduce the area overhead of DMC without disturbing the whole encoding and decoding processes. It can be observed that the DMC encoder is also reused for obtaining the syndrome bits in DMC decoder.

Therefore, the whole circuit area of DMC can be minimized as a result of using the existent circuits of encoder. Besides, this figure also shows the proposed decoder with an enable signal En for deciding whether the encoder needs to be a part of the decoder. In other words, the En signal is used for distinguishing the encoder from the decoder, and it is under the control of the write and read signals in memory. Therefore, in the encoding (write) process, the DMC encoder is only an encoder to execute the encoding operations. However, in the decoding (read) process, this encoder is employed for computing the syndrome bits in the decoder. These clearly show how the area overhead of extra circuits can be substantially reduced.

3. SIMULATION RESULTS

3.1 Passing New Input to Bloom Filter

The simulation result of the bloom filter is shown in the following figures. The inputs are fed into the bloom filter. The encoding part of DMC will check whether the input data is present or not.

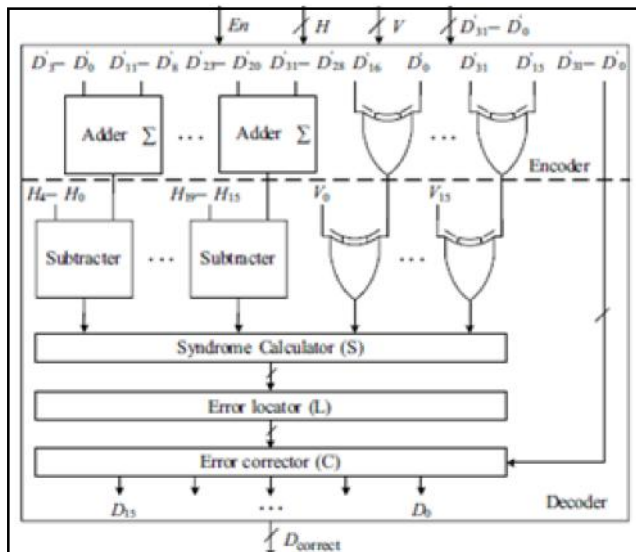


Fig.4 32 bit DMC Decoder structure

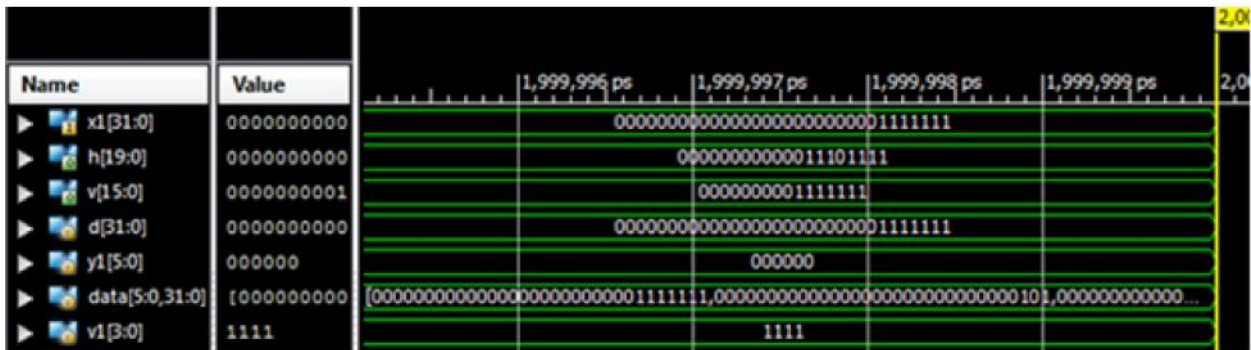


Fig. 5 Passing input to bloom filter

The figure 6 shows that the input data is new input hence the value is added into the memory. The added value is displayed as a message.

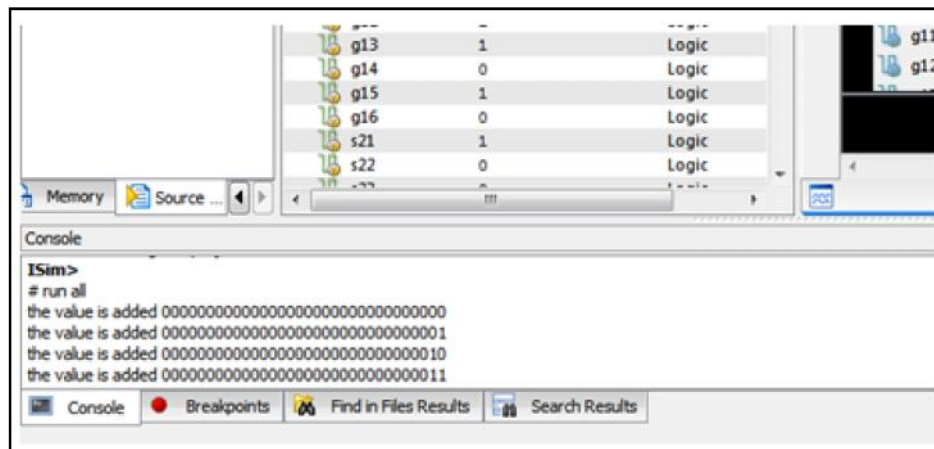


Fig. 6 Simulation result of data insertion

3.2 Passing Existing Input to Bloom

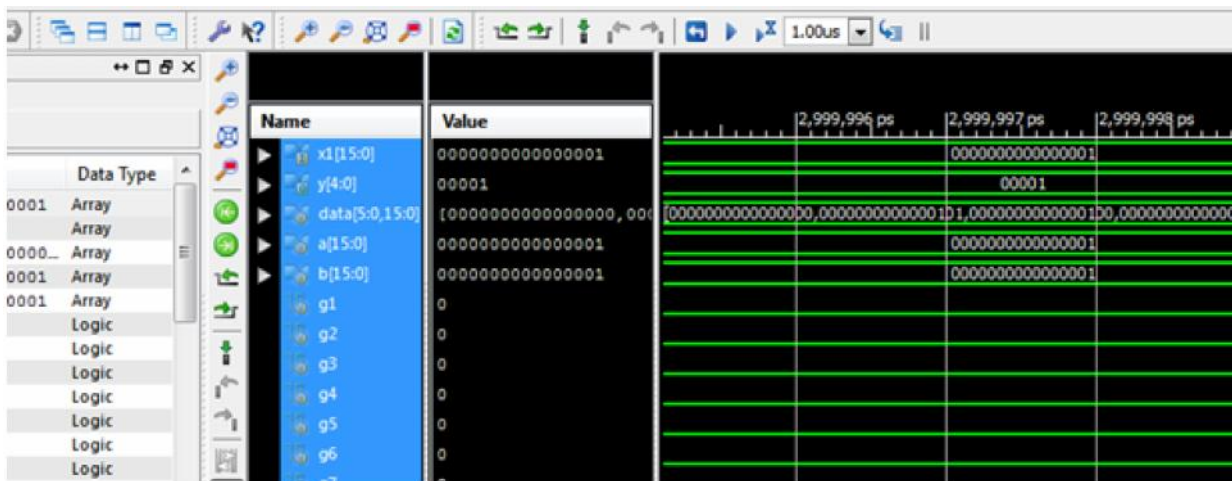


Fig.7 Passing input to bloom filter

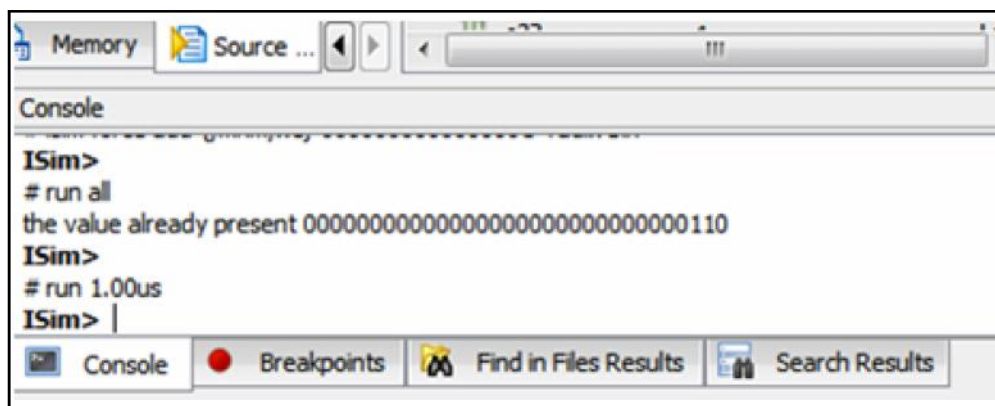


Fig. 8 Simulation result of data rejection

The figure 8 shows that the input data is already exist. Hence the value is rejected.

3.3 Decoder Output

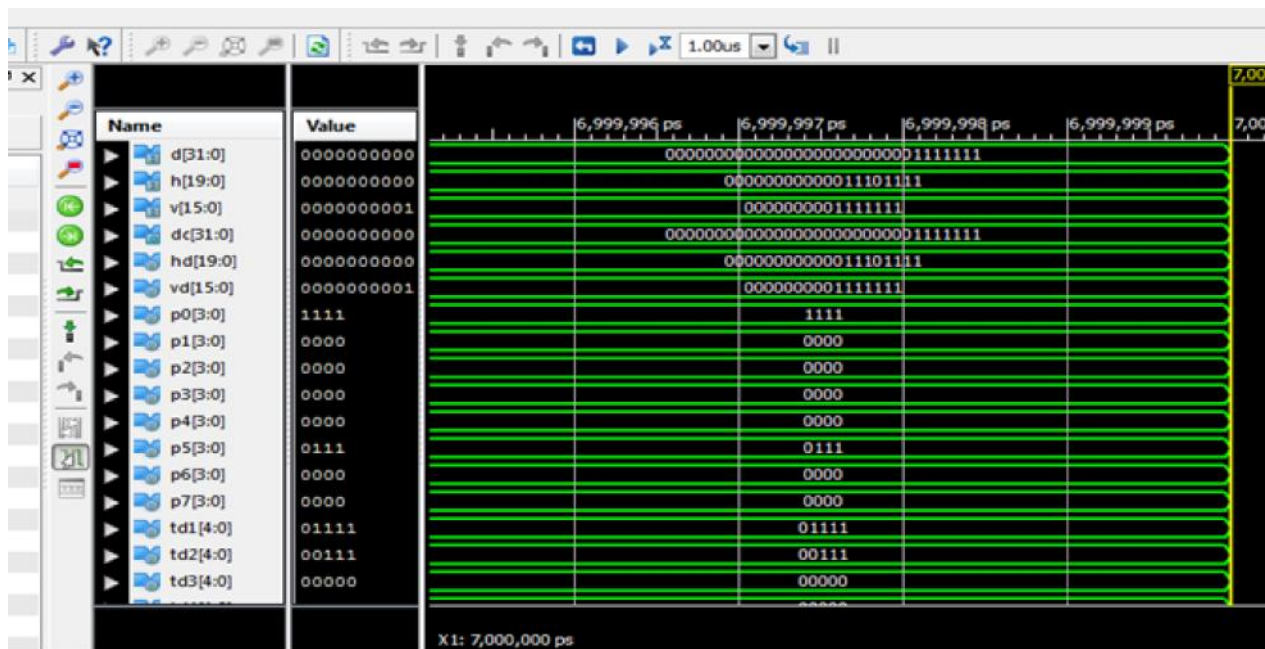


Fig.9 Decoder output

The proposed has been simulated and the synthesis report can be obtained by using Xilinx ISE 12.1i. The various parameters used for computing existing and proposed systems with Spartan-3 processor are given in the table 1.

Table 1 Result Analysis of Existing and Proposed Scheme

Sl.No.	Parameter	Existing	Proposed
1	SLICES	129	50
2	LUT	237	84

4. CONCLUSION AND FUTURE WORK

In this brief, a new application of BFs has been proposed. The idea is to use an efficient error correction code in BF to prevent the data inside the memory. Novel per-word DMC was proposed to assure the reliability of memory. The proposed protection code utilized decimal algorithm to detect errors, so that more errors were detected and corrected. The obtained results showed that the proposed scheme has a superior protection level against large MCUs in bloom filter memory. Simulation results shows our proposed bloom filter has improved performance in terms of memory protection.

In future the comparison time of the comparator will be improved hence the bloom filter is enhanced in both memory protection and comparison time.

REFERENCES

- [1] B. Bloom, "Space/time Tradeoffs in Hash Coding with Allowable Errors", *Commun. ACM*, Vol.13, No. 7, 1970, pp. 422-426.
- [2] C. L.Chen and M. Y. Hsiao, "Error-correcting Codes for Semiconductor Memory Applications: A State-Of-The-Art Review", *IBM J. Res. Develop.*, Vol. 28, No.2, 1984, pp.124-134.
- [3] D. Bhavsar, "An Algorithm for Row-Column Self-Repair of RAMs and its Implementation in The Alpha 21264", in *Proc. Int. Test Conf.*, (1999), pp.311-318.
- [4] A. Moshovos, G. Memik, B. Falsafi and A. Choudhary, "Jetty: Filtering Snoops for Reduced Energy Consumption in SMP Servers", in *Proc. Annu. Int. Conf. High-Perform. Comput. Archit.*, 2001, pp.85-96.
- [5] M. Mitzenmacher, "Compressed Bloom Filters", in *Proc. 12th Annu. ACM Symp. PODC*, 2001, pp.144-150.
- [6] A. Broder and M. Mitzenmacher, "Network Applications of Bloom Filters: A Survey", in *Proc.40th Annu. Allerton Conf.*, 2002, pp.636-646.
- [7] S. Dharmapurikar, H. Song, J. Turner, and J. W. Lockwood, "Fast Hash Table Lookup Using Extended Bloom Filter: An Aid to Network Processing", in *Proc. ACM/SIGCOMM*, 2005, pp. 181-192.
- [8] M. Nicolaidis, "Design for Soft Error Mitigation," *IEEE Trans. Device Mater. Rel.*, Vol.5, No.3, 2005, pp.405-418.
- [9] F. Bonomi, M. Mitzenmacher, R. Panigrahy, S.Singh and G.Varghese, "An Improved Construction for Counting Bloom Filters", in *Proc. 14th Annu. ESA*, 2006, pp.1-12.
- [10] T. Kocak and I. Kaya, "Low-power Bloom Filter Architecture for Deep Packet Inspection", *IEEE Commun. Lett.*, Vol. 10, No. 3, 2006, pp. 210-212.
- [11] G. Wang, W. Gong, and R. Kastner, "On the Use of Bloom Filters for Defect Maps in Nanocomputing", in *Proc. IEEE/ACM ICCAD*, 2006, pp.743-746.
- [12] C. Fay *et al.*, "Bigtable: A Distributed Storage System for Structured Data", *ACM TOCS*, Vol.26, No. 2, 2008, pp. 1-4.
- [13] S. Elham, A. Moshovos and A. Veneris, "L-CBF: A low-Power, Fast Counting Bloom Filter Architecture", *IEEE Trans. Very Large Scale Integr. (VLSI) Syst.*, Vol.16, No.6, 2008, pp.628-638.
- [14] N. Kanekawa, E. H. Ibe, T. Suga and Y. Uematsu, "Dependability in Electronic Systems: Mitigation of Hardware Failures, Soft Errors, and Electro-Magnetic Disturbances", New York, NY, USA: Springer-Verlag, 2010.
- [15] M. Mitzenmacher and G. Varghese, "Biff (Bloom Filter) Codes: Fast Error Correction for Large Data Sets", in *Proc. IEEE ISIT*, 2012, pp. 1-32.
- [16] S. Pontarelli and M. Ottavi, "Error Detection and Correction in Content Addressable Memories by Using Bloom Filters", *IEEE Trans. Comput.*, Vol. 62, No.6, 2013, pp.1111-1126.

Comparative Analysis of Different Wheeling Charge Methodologies

N. Selvam¹ and P.L. Somasundaram²

¹PG Student, ²Senior Asst.Professor, Department of Electrical and Electronics Engineering,
E M. Kumarasamy College of Engineering, Karur - 639 113, Tamil Nadu
E-mail:selvamkrr@gmail.com,somasundarampl.eee@mkce.ac.in

Abstract

In the restructured power system need to develop the transmission cost scheme that can provide the useful economic information to power markets, such as generation, transmission companies and customers. In this paper proposes an analytical approach for comparative analysis of MW-MILE, MVA-MILE, POSTAGE-STAMP methods. Wheeling cost is the most important parameter for recovering the invested cost. All these wheeling methods allocate the charges based on transmission capacity and wheeling distance. The approach based on applying different wheeling charge methods on IEEE-14 bus system.

Keywords: POSTAGE- STAMP method, Restructured power system, Wheeling charge, MW-MILE, MVA-MILE.

1. INTRODUCTION

Electrical energy playing a fundamental part in our life. In today's modern society, electrical energy can be found everywhere. For providing energy in household appliances such as lighting, air-conditioners, televisions sets to office equipment such as computers, fax machines and also providing energy for the industrial. Machineries, electrical energy has become sheer necessity in our life. That's why electric power industry is probably the largest and the most complex industry in the world. Generation, transmission and distribution of Electricity must be accomplished at minimum cost but at maximum efficiency. For many years in the past, the electric power industries in the world are operating in regulated, monopolistic market.

Large power companies often dominate the overall authority over all activities in generation, transmission and distribution. These companies often have owned the assets and operations of these three activities and are referred as vertically integrated utilities. Now, these vertically integrated utilities are owned and run by governments in many parts of the world.

2. DEREGULATION

In deregulation environment, generation, transmission and distribution are independent activities; there is a competition among generators for customers. Main benefits from the deregulation are, cheaper electricity, efficient capacity expansion planning, cost minimization, more choice and better service. Since the

electrical power supply industry around the world has experienced a period of rapid and irreversible change. The need for more efficiency in power production and delivery has led to a restructuring of the power sectors in several countries traditionally under control of federal and state governments.

3. OPEN ACCESS TRANSMISSION SYSTEM

The Open Access Same-Time Information System (OASIS) is an Internet-based system for obtaining services related to electric power transmission in North America. It is the primary means by which high-voltage transmission lines are reserved for moving wholesale quantities of electricity. OASIS permits posting, viewing, uploading, and downloading of transmission transfer capability in standardized Protocols. The data posted on OASIS should clearly identify what service is available, which requests were accepted, denied, interrupted or curtailed, permitting business decisions to be made solely from the OASIS-derived information.

4. WHEELING

The term "wheeling" has a number of definitions. Wheeling is the use of transmission or distribution facilities of a system to transmit power of and for another entity. The figure1 shows the general wheeling diagram.

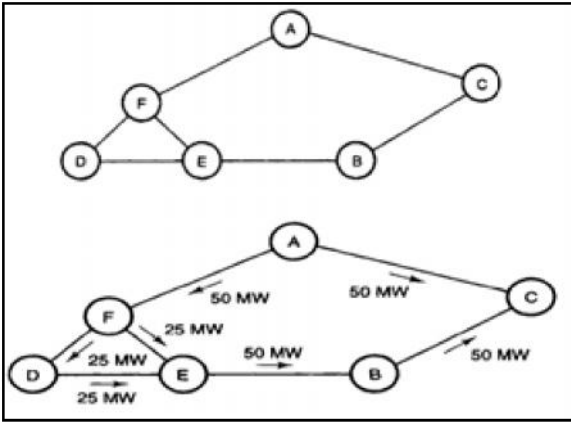


Fig.1 General wheeling diagram. Fig.2 Six interconnected wheeling diagram

Wheeling occurs on an AC interconnection that contains more than two utilities whenever transaction takes place. Consider the six interconnected control areas shown in Figure 2. Consider the six interconnected control areas. Areas A and C negotiate the sale of 100 MW by A to C. A to F transferring some amount of power and F area power is transfer to C area through the areas D & E. remaining power is transferring areas A to C.

5. BILATERAL TRANSACTIONS

A bilateral transaction involves a trade negotiated between two participants, with price, quantity and other trade data known only by the parties involved. In the power market one buyer and seller are involved in the bilateral transactions. Since bilateral transactions do not occur on regulated exchanges, such transactions are referred to as “off exchange” or “over the counter” (OTC) transactions. Over-the-counter or off-exchange trading is done directly between two parties, without any supervision of an exchange. It is contrasted with exchange trading, which occurs via these facilities. An exchange has the benefit of facilitating liquidity, mitigates all credit risk concerning the default of one party in the transaction, provides transparency, and maintains the current market price. In an OTC trade, the price is not necessarily made public information.

6. MULTILATERAL TRANSACTIONS

Multilateral means that multiple parties can input their selling and buying intentions into the system and a transaction is established between these parties when intentions match. The multilateral transactions based on bilateral transactions among market participants.

7. WHEELING CHARGE CALCULATION

7.1 Mw-Mile Method

The MW-Mile method is also known as Line-by-line method. The change in the magnitude of power flow on the system caused by wheeling transaction is taken into consideration in order to assist in the allocation of the wheeling costs of each of the wheeling transaction. One distinct feature is the length of the transmission lines used in the transaction is also taken into consideration when determining the wheeling costs. This attempts to solve the flaws in the rolled-in-embedded method where the distance between the point of supply and the point of the recipient has no effect in determining the usage of the transmission system by the wheeling transaction. MW-mile method attempts to allocate the wheeling costs based on the actual system usage as close as possible. Therefore, Two power flow executions are needed with one having native loads only and the only with the wheeling transaction comes into play. The power flow-mile on each transmission line of the system due to a particular wheeling transaction is calculated by obtaining the product of the transmission line length and the change in the magnitude of the power flow caused by the transaction. The power flow-miles of each transmission line are totalled up to represent the amount of the transmission resources used by the corresponding transaction. The total system capacity is obtained by totalling up the product of each transmission line length and some measures of the contribution made by the transmission facility towards the capacity of the system. This contribution can be measures by several alternatives such as measuring the temperature based rating, surge impedance loading, actual power flows.

In the original MW-Mile methodology DC power flow formulation was used to estimate the usage of firm transmission services by wheeling transactions, and the procedure for multi- transaction assessment may be outlined as follows.

STEP 1: For a transactions t , the transactions related flows on all network lines MW_t, k (kEK) are first calculated using optimal power flow model considering the nodal power injections only involved in that transactions.

STEP 2: The magnitude of MW flow on every line is multiplied by its length L_k (in miles) and the cost per MW per unit length of line C_k (in \$/MW-MILE), and summed over the all network lines as:

$$MWMILE_t = \sum_{k \in K} C_k L_k MW_{t,k}$$

The above process is repeated for each transaction $t \in T$, including one comprised of the utility's native generators and loads. Finally, the responsibility of transaction t to the total transmission capacity cost is determined by:

$$TC_t = Total_cost \frac{MWMILE_t}{\sum_{t \in T} MWMILE_t}$$

The MW MILE method recovers the fixed transmission cost in the restructured power system.

7.2 Mva-Mile Method

In the above method i.e. in MW mile method reactive power changes in the facilities caused by the transmission have not been considered. Reactive power flow can effect line losses and voltage magnitude when customer loading is heavy, reactive power flow can push bus voltages, top change transformer settings or circuit loading to their limits, or when oppositely oriented can bring them off limits. The MVA mile method, reflect the actual customer loading condition. In MVA mile method both are real power flow and reactive power flow is taken into consideration. According to MVA mile method, the costs are allocated proportional to the charge in the line MW flows and line MVAR flows caused by transmission transaction and length of the line in miles. Two power flows executed successfully, with and without the wheeling transaction T , yield $(\Delta MVA_f)_T$ the changes in MVA flows in all transmission line facilities. The transaction cost CT in \$/hr for a transaction T is given by the following equation.

$$C_{WT} = \frac{C * \sum_f ((\Delta MVA_f)_T * L_f)}{\sum_T ((\sum_f \Delta MVA_f)_T * L_f)}$$

Where,

L_f = Length of transmission line f .

$(MVA)_f_T$ = MVA power flow in facility f due to transaction T

$(\Delta MVA)_f_T$ = Change in power flow in facility f due to transaction T due to transaction T .

7.3 Postage-Stamp Method

Postage stamp rate method is traditionally used by electric utilities to allocate the fixed transmission cost among the users of firm transmission service. This method is an embedded cost method, which is also called the rolled in embedded method. This method does not require power flow calculations and is independent of the transmission distance and network configuration. The magnitude of the transacted power for a particular power transaction is usually measured at the time of system peak load condition:

$$RT = TC * (Pt / P_{peak})$$

Where R_t is the transmission price for transaction t , TC is the total transmission charges and P_t and P_{peak} are transaction t load and the entire system load at the time of system peak load condition. The main purpose of using this methodology is the entire system is considered as a centrally operated integrated system. This method is simpler. Since this method ignores the actual system operation, it is likely to send incorrect economic signal to transmission customers.

8. OPTIMAL POWER FLOW

The optimal power flow is a very large and very difficult mathematical programming problem. Almost every mathematical programming approach that can be applied to this problem has been attempted and it has taken developers many decades to develop computer codes that will solve the OPF problem reliably. The main objective of optimal power flow is to minimize the generation cost in the power system. There are two constraints in the optimal power flow. In the equality constraints generation balances the load. In the inequality constraints generations mismatches the load. The IEEE-14 bus system is solved using mat lab software in Optimal Power Flow method using the Interior Point algorithm. Traditionally, classical optimization methods were used to effectively solve OPF. But more recently due to incorporation of FACTS devices and deregulation of a power sector, the traditional concepts and practices of power systems are superimposed by an economic market management. So OPF have become complex. In recent years, Artificial Intelligence (AI) methods have been emerged which can solve highly complex OPF problems.

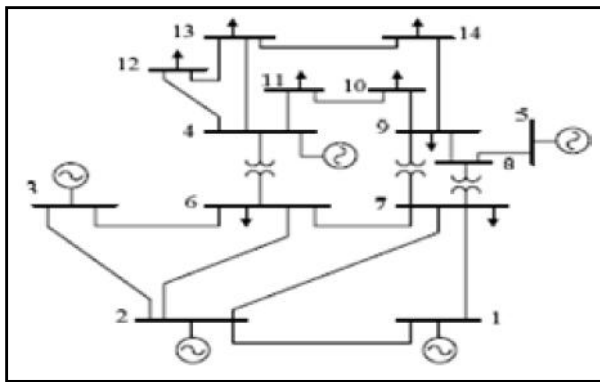


Fig.3 IEEE-14 Bus System

9. RESULT & DISCUSSION

Table 1 Bilateral Transactions

Transactions	From Bus	To Bus	Magnitude Transaction
1	4	10	10MW

Table 2 Results of Bilateral Transactions

Branch		From Bus Power Injection		To Bus Power Injection		Loss	
From bus	To bus	P(MW)	Q(MVAR)	P(MW)	Q(MVAR)	P(MW)	Q(MVAR)
1	2	129.4	-6.5	-126.5	9.5	2.8	8.8
1	5	64.7	6.5	-62.7	-3.3	2.0	8.5
2	3	55.5	0.5	-54.2	0.4	1.3	5.6
2	4	48.4	-0.1	-47.2	0.4	1.2	3.8
2	5	37.5	1.8	-36.7	-3.2	0.7	2.2
3	4	-11.6	4.8	11.7	-5.5	0.1	0.2
4	5	-46.3	11.2	46.6	-10.2	0.2	0.9
4	7	26.8	-3.4	-26.8	4.8	0.0	1.4
4	9	17.2	1.6	17.2	-0.08	0.0	1.5
5	6	45.2	15.2	-45.2	-10.4	0.0	4.8
6	11	8.7	4.4	-8.6	-4.3	0.08	0.1
6	12	7.7	2.6	-7.6	-2.4	0.07	0.1
6	13	17.5	7.7	-17.3	-7.2	0.2	0.4
7	8	-9.0	-8.5	9.0	8.8	0.0	0.2
7	9	35.8	3.7	-35.8	-2.3	0.0	1.3
9	10	13.9	3.5	-13.8	-3.3	0.06	0.1
9	14	9.6	3.0	-9.5	-2.7	0.1	0.2
10	11	-5.1	-2.4	5.1	2.5	0.02	0.06
12	13	1.5	0.8	-1.5	0.8	0.007	0.0
13	14	5.4	2.3	-5.3	-2.2	0.05	0.1

Table 3 Comparison of Wheeling Charges for Bilateral Transactions

Line	Wheeling Cost of MVA-MILE Method	Wheeling Cost of MW-MILE Method	Wheeling Cost of POSTAGE-STAMP Method
2-4	-1.9	-1.8	44
3-4	3.2	2.57	-10.66
4-5	-18.81	14.06	-42.58
4-7	32.91	32.62	24.63
4-9	31.08	29.49	15.82
9-10	61.13	61.31	12.78
10-11	11.39	-14.06	-4.73

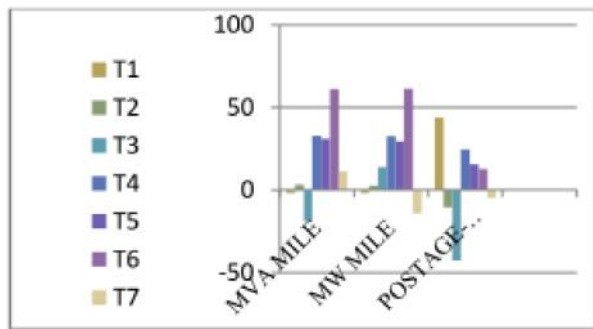


Fig.4 Bilateral transaction

Table 4 Multilateral Transactions

Transaction	From Bus	To Bus	Magnitude of Transaction
1	9,13,14,10	7,11,12	50MW

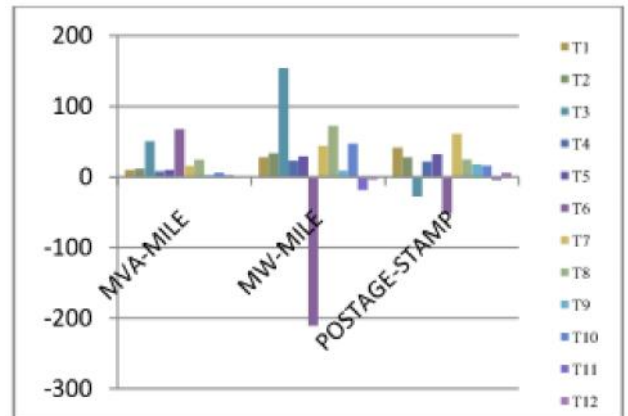


Figure 5 Multilateral Transactions

Table 5 Result of Multilateral Transactions

Branch		From Bus Power Injection		To Bus Power Injection		Loss	
From bus	To bus	P(MW)	Q(MVAR)	P(MW)	Q(MVAR)	P(MW)	Q(MVAR)
1	2	130.8	-7.0	-127.8	10.2	2.9	9.02
1	5	67.29	7.01	-65.07	-3.1	2.2	9.1
2	3	52.0	-0.01	-50.87	0.3	1.1	4.9
2	4	51.3	0.1	-49.8	0.5	1.4	4.2
2	5	40.2	2.1	-39.2	-3.1	0.8	2.6
3	4	-4.9	4.3	5.0	-5.5	0.03	0.08
4	5	-46.8	11.2	47.1	-10.2	0.3	0.9
4	7	26.3	-3.7	-26.3	5.1	0.0	1.3
4	9	17.5	1.4	-17.5	0.17	0.0	1.5
5	6	49.6	14.9	-49.6	-9.2	0.0	5.7
6	11	17.3	5.3	-17.1	-4.7	0.2	0.5
6	12	13.6	3.7	-13.4	-3.2	0.2	0.4
6	13	20.3	7.6	-20.0	-7.1	0.2	0.5
7	8	-32.3	-8.4	32.3	10.2	0.0	1.8
7	9	38.6	3.2	-38.6	-1.7	0.0	1.5
9	10	15.5	3.1	-15.4	-2.9	0.07	0.20
9	14	11.2	2.4	-11.0	-2.1	0.1	0.3
10	11	6.4	-2.8	-6.4	2.9	0.03	0.09
12	13	-2.6	1.6	2.6	-1.6	0.02	0.02
13	14	3.8	2.9	-3.8	-2.8	0.03	0.08

Table 6 Comparison of Wheeling Charges for Multilateral Transactions

Line	Wheeling Cost of MVA-MILE Method	Wheeling cost of MW-MILE Method	Wheeling cost of POSTAGE-STAMP Method
4-7	9.6	27.9	41.8
4-9	11.7	33.2	27.9
6-11	50.7	154	-27.6
6-12	8.1	23.0	21.7
6-13	9.7	29.47	32.3
7-8	67.5	-211	-51.3
7-9	15.54	44	61.4
9-10	24.4	72.7	24.6
9-14	2.7	9.0	17.8
10-11	6.2	47	16.2
12-13	2.13	-18.2	-4.1
13-14	-0.7	-4.0	6.1

10. CONCLUSION

The wheeling charges are calculated in IEEE-14 Bus system using the MW-MILE, MVA-MILE, POSTAGE-STAMP methods under the open access transmission system. In future the wheeling charges can be calculated for real time system using different wheeling charge methods.

REFERENCES

- [1] H. H. Happ, "Cost of Wheeling Methodologies", IEEE Trans. on Power Systems, Vol. 9, No.1, 1994, pp.147-156.
- [2] W.J. Lee, C.H. Lin and L.D. Swift, "Wheeling Charge Under a Deregulated Environment", IEEE Trans. Ind. Appl., Vol. 37, No.1, 2001, pp.178-183.
- [3] J. Park, J. Lim and J. Won, "An Analytical Approach for Transmission Costs Allocation in Transmission System", IEEE Trans. on Power Systems, Vol.13, No.4, 1998, pp. 1407- 1412.
- [4] J. Bialek, "Allocation of Transmission Supplementary Charge to Real and Reactive Power Loads", IEEE Trans. On Power Systems, Vol.13, No.3, August 1998, pp.749-754.
- [5] J. W. Marangon Lima, "Allocation of Transmission Fixed Charges: An Overview", IEEE Trans. on Power Systems, Vol.11, No.3, August 1996, pp.1409-1418.
- [6] H. Happ, "Cost of Wheeling Methodologies", IEEE Trans. on Power Systems, Vol.9, No.1, February 1994, pp.147-156.
- [7] A. J. Wood and B. F. Wollenberg, "Power Generation, Operation and Control", New York: Wiley, 1996.

Analysis on Various Optimization Techniques for Selecting Gain Parameters in FOC of an E-Drive

Meher Anusha Vanapalli¹, Raja Sekhar Kammala² and Sathish Laxmanan³

¹Department of Industrial Power and Automation, NIT Calicut (Intern at RBEI) - India

^{2&3}Senior Engineer, Robert Bosch Engineering and Business Solutions Ltd, Coimbatore - 641 035, Tamil Nadu

Abstract

Field Oriented Control (FOC) is commonly used for controlling electrical machines like PMSM (Permanent Magnet Synchronous Motor) and Induction machines etc., which are majorly used in Electric and Hybrid Vehicles. For optimal performance of the algorithm (FOC) or any PID based controller it is required that the controller is tuned to its best parameters over the entire operating range of the electrical machine. Several conventional methods (Ziegler-Nichols) to optimize the current control parameters in FOC, (or tuning any PID controller) were highly unsatisfactory in terms of large overshoot and steady state error, because of manual involvement in selecting the initial points and tuning them. Based on the literature survey, it is observed that optimization techniques like pattern search can provide a better solution for tuning of current control parameters in FOC. In few zones (Speed > Base Speed) of operating region, parameters obtained through pattern search are not satisfactory.

This paper compares different optimization techniques like Pattern Search, Genetic Algorithm and Simulated Annealing algorithms, where the error criteria is considered as the summation of Integral of Time-weighted Absolute Error (ITAE) and Integral Square Error (ISE) between desired and actual response and the best possible results are presented. The above analysis is thus useful in identifying the best optimization technique for tuning of PID parameters in FOC of an E-Drive used in various hybrid vehicles.

Keywords: *Controller Tuning, Field Oriented Control (FOC), Genetic Algorithm, Integral of Time-weighted Absolute Error (ITAE), Integral Square Error (ISE), Pattern Search, Simulated Annealing.*

1. INTRODUCTION

Several advanced controller designs have been developed in the past two decades. In spite of these, We do see the use of PI controller in most of the closed loop control systems (automatic process control applications), because of its robustness and simple structure. PI controllers are used as current controllers in closed loop control of E-drive. Tuning of this PI controller plays major role in Field Oriented Control (FOC) of PMSM machine. Many tuning techniques have been developed based on the objective as ITAE. Ziegler and Nichols proposed simple tuning rules for PID controller [Rohit G, 2012]⁹. But these tuning rules are having following disadvantages (a) consumes more time for computation as it involves trial and error (b) not applicable for processes which are unstable in open loop, (c) forces the system into marginal stability, which may leads system to unstable for small external disturbances [Mohammad Shahrokhi]⁶. Because of these

disadvantages in classical tuning method (Ziegler and Nichols), three optimization techniques (Pattern Search, Genetic Algorithm, Simulated Annealing) are analyzed in this paper.

2. FIELD ORIENTED CONTROL

In FOC[R. Krishnan, 2010]⁷, motor currents are transformed from u-v-w (stationary) reference frame into d-q (rotating) reference frame by using Clarks and Park transformations, so that ideally the current space vector is fixed in magnitude and quadrature in direction with respect to the rotor. Because the current space vector in the d-q reference frame is static, the P-I controllers operate on dc signals, rather than sinusoidal signals. This isolates the controllers from the time variant winding currents and voltages, and therefore it eliminates the limitation of controller frequency response and phase shift on motor torque. This is the major advantage of FOC [Copley Controls Corp]³.

Figure.1 represents the control strategy in FOC. Here two PI controllers are used. One for direct current component and other for quadrature current component. The reference input commands for I_d and I_q are derived from desired torque command. The outputs from the

two PI controllers represent voltage space vector with respect to rotor, which can be transformed into three phase voltages by using inverse Clarks and Park transformations. These control signals are given to Space Vector PWM inverter, which will drive the motor.

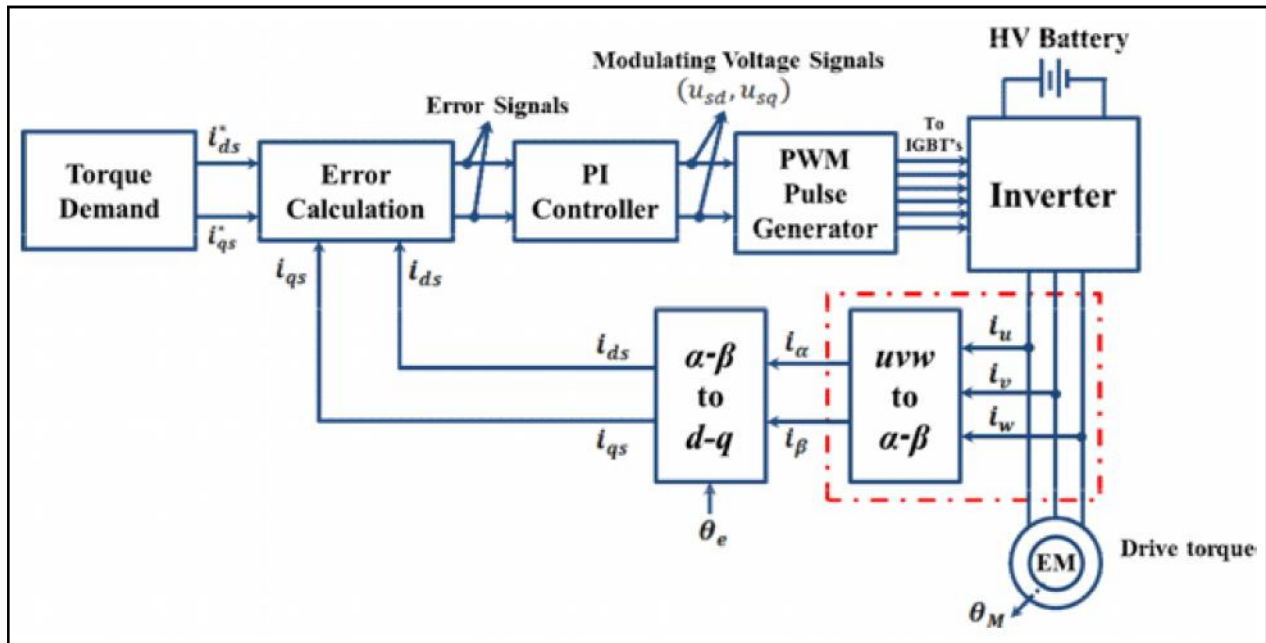


Fig.1 Field oriented control of PMSM machine

3. OPTIMIZATION ALGORITHMS

As mentioned earlier optimization algorithms Pattern Search, Genetic Algorithm and simulated annealing are discussed in this section.

3.1 Pattern Search

Hooke and Jeeves proposed pattern search algorithm in 1961. It is a direct search algorithm. This is larger search in the improving direction. Larger moves are made as long as the improvement continuous. A pattern is a set of vectors $\{x_i\}$, which points to search at each iteration [John W, 2014]⁴. The set $\{x_i\}$ is defined by the number of independent variables in the objective function $f(x)$. It varies one parameter of the set at a time by steps of the same magnitude and derives the next point $\{x_{i+1}\}$. If there is decrease (for minimization) in the objective function value ($f(x_{i+1}) < f(x_i)$), then it expands the step size. When there is increase in the objective function value ($f(x_{i+1}) > f(x_i)$), then it compress the step size and repeat the process until the steps were reached sufficiently small. It gives faster convergence but sometimes results local optimum point [MathWorks]⁵. Selection initial point plays major role.

3.2 Genetic Algorithm

GA, first introduced by John Holland in the early 1970's, to mimic processes observed in natural selection. This is powerful stochastic algorithm based on Darwin's theory "survival of the fittest". Initially GA maintains a population of individuals (also called chromosomes) and modifies the population probabilistically by some genetic operators such as selection, crossover and mutation. Efficiency of GA is based on Population size, mutation rate and cross over frequency [Vikrant Vishal, 2014]¹¹. It has main drawback as premature and slow convergence.

3.3 Simulated Annealing

This method was introduced by Scott Kirkpatrick, C. Daniel Gelatt and Mario P.Vecchi in 1983. This is adopted from Metropolis-Hastings algorithm. It models the physical process of heating a material and then slowly lowering the temperature to decrease defects, thus minimizing the system energy. A new point is randomly generated at each iteration based on probability distribution with a scale proportional to the temperature. It not only accept points whose objective function value

is less than that of the current point but also accept points whose objective function value is more than that of the current point, with certain probability. By accepting points that raise the objective function, the algorithm avoids being trapped in local minima in early iterations and is able to explore globally for better solutions. Temperature cooling schedule plays major role [MathWorks]⁵.

4. OBJECTIVE FUNCTION

The performance indices taken for optimization are ITAE (Integral Time Absolute Error):

$$ITAE = \int t e(t) dt \tag{1}$$

ISE (Integral Square Error):

$$ISE = \int e^2(t) dt \tag{2}$$

The ITAE index has major advantages as producing smaller overshoot and oscillations, so that settling time is less. It has best selectivity compared other indices Integral Square Error (ISE) and Integral Absolute Error (IAE) [R. N. Patel, 2007]¹. In ISE and IAE error alone is considered but in ITAE time span of the error is also considered hence settling time can be reduced.

5. RESULTS

Optimization of controller parameters (Kp, Ki) is performed by considering three operating points in speed torque characteristics of PMSM motor. Those are at (a) below base speed (b) base speed and (c) above base speed.

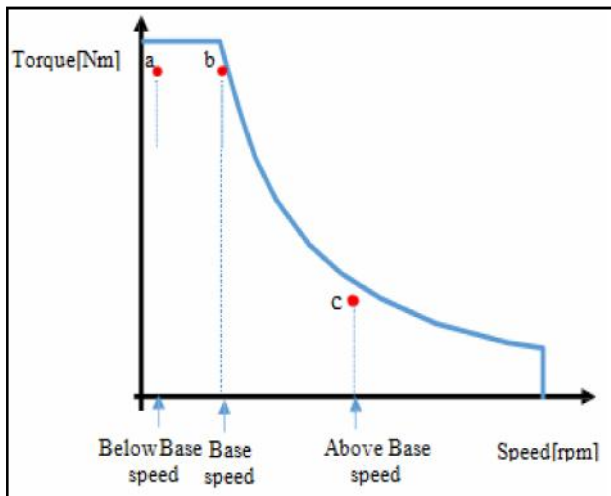


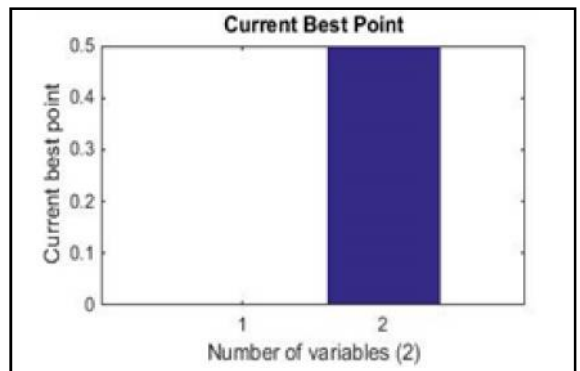
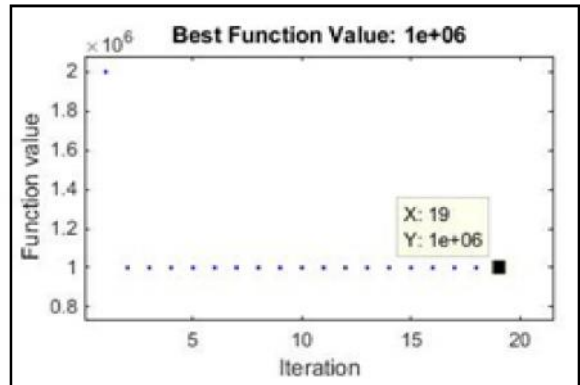
Fig.2 Speed torque characteristics of PMSM

5.1 PMSM Machine Parameters

Table 1 PMSM Machine Parameters

Parameter	Value
Armature resistance (m ohm)	13.5
D- axis inductance Ld (mH)	10.022
Q axis inductance Lq (mH)	15.1
Flux linkages (V s)	0.026
Number of pole pairs	6

5.2 Results at speed: 0.5P.U and torque: 0.578P.U with PS, GA and SA



(a) Pattern search failed to converge as limitation in 'tolerance function' reached. Objective function value = 1e6.

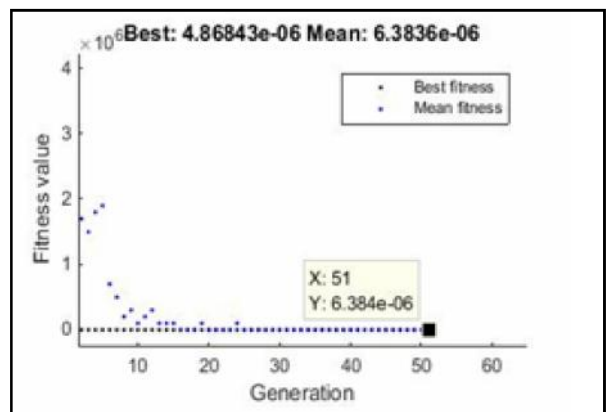
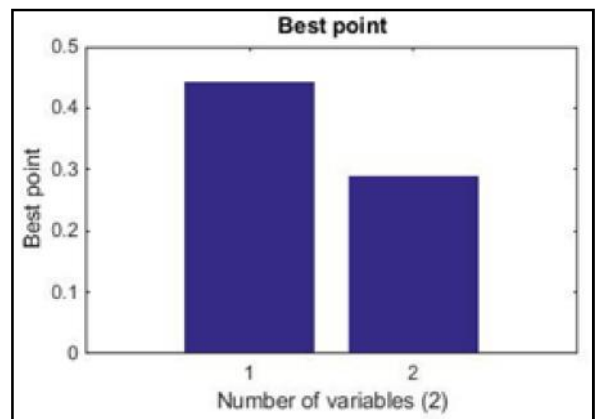
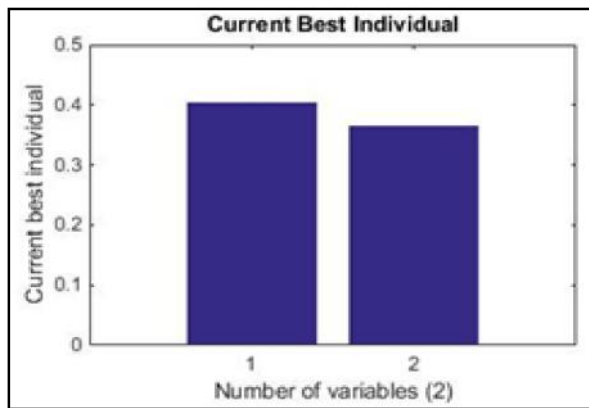


Table 2 Comparison of Pattern Search, Genetic Algorithm and Simulated Annealing

	Kp	Ki	Peak Overshoot (%)	Ripple (%)	Settling time (Secs)	Convergence time (Secs)
Working Point 'a' : Speed 0.19P.U and Torque 0.9P.U (Below Base Speed)						
PS	1.5624	329.2	2.22	2.58	0.55	4.0781e+03
GA	1.8156	399	0.56	1.78	0.04	1.544e+04
SA	1.4596	588.4	1.24	1.42	0.02	1.55e+05
Working Point 'b' : Speed 0.38P.U and Torque 0.9P.U (Base Speed)						
PS	Not converged	Not converged				
GA	1.784	387	1.78	1.96	0.05	2.3773e+04
SA	1.9912	201	1.24	2.04	0.08	1.67e+05
Working Point 'c' : Speed 0.5P.U and Torque 0.578P.U (Above Base Speed)						
PS	Not converged	Not converged				
GA	2.6148	730.4	1.38	3.32	0.035	2.2509e+04
SA	2.7732	579.8	1.04	3.46	0.04	1.5375e+05



(b) Objective function output reaches to $6.3e-6$. Thus the output obtained are optimized. $K_p = 0.4P.U$ and $K_i = 0.36P.U$.

(c) Objective function output reaches to $6.3e-6$. Thus the output obtained are optimized. $K_p = 0.44P.U$ and $K_i = 0.29P.U$.

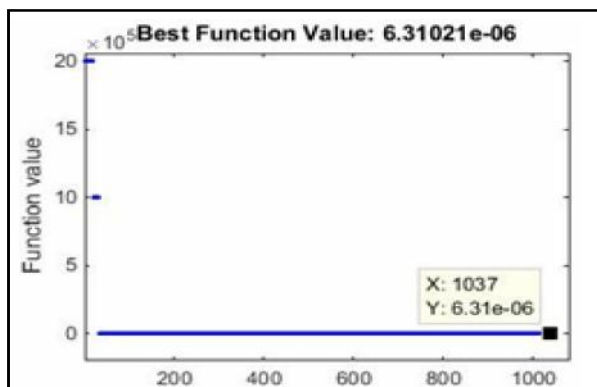


Fig.3 Results for (a) Pattern search (b) Genetic Algorithm (c) Simulated Annealing

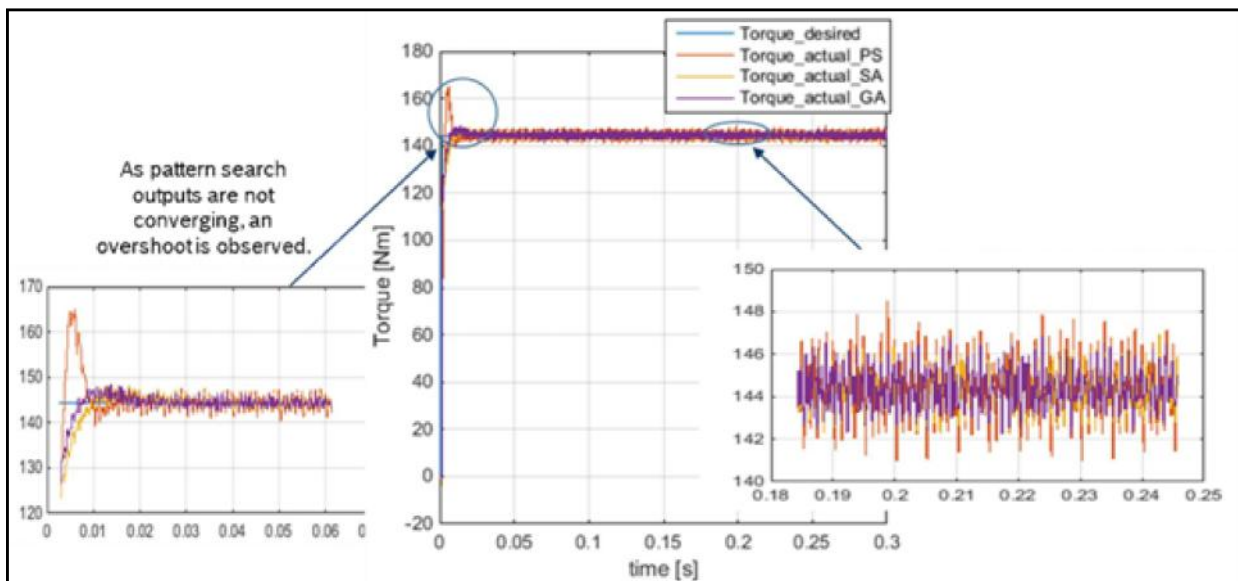


Fig.4 Torque waveform at speed: 0.5P.U and torque: 0.578P.U

6. CONCLUSIONS

In this paper, three optimization algorithms PS, GA and SA are analyzed. Simulation is performed using MATLAB Simulink. Initial point selection plays a vital role in pattern search output convergence. If a better initial point is chosen, Pattern Search converges fast. At working point greater than base speed, GA and SA are giving good results compared to PS, where SA takes more time to give a converged result. Merging of two algorithms like PS and GA gives good performance. For example if we use GA to find out initial point selection and that is fed as an input to PS then this hybrid algorithm results improved performance in time consumption. This can be taken as future work.

REFERENCES

[1] R. N. Patel, "Application of Artificial Intelligence for Tuning the Parameters of an AGC International Journal of Electrical, Computer", Energetic, Electronic and Communication Engineering Vol.1, No.2, 2007.

[2] R. Krishnan, "Permanent Magnet Synchronous and Brushless DC Motor Drives", 2010 (Conference Proceedings)

[3] Deepyaman Maiti, Ayan Acharya, Mithun Chakraborty, Amit Konar and Ramadoss Janarthanan, "Tuning PID and $PI/\lambda D^\delta$ Controllers Using the Integral Time Absolute Error Criterion", 4th International conference on

Information and Automation for Sustainability, 2008.

[4] Rohit G. Kanojiya, P. M. Meshram, "Optimal Tuning of PI Controller for Speed Control of DC motor drive using Particle Swarm Optimization", International Conference Advances in Power Conversion and Energy Technologies (APCET), 2012.

[5] Tomy Sebastian, Gordon R. Slemon and M.A. Rcahman, "Modelling of Permanent Magnet Synchronous Motors IEEE Transactions on Magnetics, Vol.22, No. 5, September 1986.

[6] Vikrant Vishal, Vipin Kumar, K. P. S. Rana and Prabhat Mishra, "Comparative Study of Some Optimization Techniques Applied to DC Motor Control", IEEE International Conference on Advance Computing (IACC), 2014.

Automated Gesture Recognition System Using Raspberry Pi

N. Geraldine Shirley¹ and Neethu Krishna²

¹Assistant Professor, Department of Electronics and Communication Engineering,
Sri Ramakrishna Engineering College, Coimbatore - 641 022, Tamil Nadu

²Assistant Professor, Department of Electronics and Communication Engineering,
VSB College of Engineering Technical campus, Coimbatore 642 109, Tamil Nadu

Abstract

Hand gesture recognition embedded system can be used as an interfacing medium between the computer and human using different hand gestures in order to control the computer. In this proposed system, a real time vision based hand gesture interaction prototype which depends upon finger gestures using color markers is designed. The objective is to develop an embedded system by which one can communicate with any digital device with less hardware requirements and using an external camera to capture the gestures. Identifies different color markers on the fingers and when the mouse emulation is started, the software tracks those markers using the camera. The main aim is to create a low cost and energy efficient gesture interpretation system which uses computer vision to analyze different sets of gestures or actions done using the human fingers and automatically goes to sleep mode when there is no gestures detected.

Keywords: Computer vision, Energy efficient, Embedded system, Hand gesture recognition, Raspberry Pi.

1. INTRODUCTION

Gesture recognition is the process of recognizing and interpreting a stream of continuous sequential gesture from the given set of input data. Gestures are non-verbal information which is used to make computers understand human language and develop a user friendly human computer interface. Human gestures are perceived through vision and this paper aims to use computer vision to analyze different sets of gestures using human fingers and interpret them in order to control the system.

Most of the recognition systems are based on PC but the portability of PC is limited by its weight, size and power consumption. The way to avoid the disadvantages in PC is by using an embedded system which is low cost, power efficient. The approach proposed here is simple and cost effective as it requires less hardware to implement and no sensors are required. The system is developed to interpret set of gestures into mouse control instructions.

FingerMouse is a free computer pointing interface which is used as an alternative to the mouse. A vision system constantly monitors the hand and tracks the color markers placed in the fingertips of each finger and the screen cursor is moved using different gestures.

Double click (left click) and right click is performed using different color markers on the fingers. Raspberry Pi is a Linux based platform which uses Python as the main programming language and software development on Linux is easy as it is an open source code development environment. The system consist of a Raspbian camera which continuously monitors and tracks the gestures.

2. RELATED WORKS

Many researchers have proposed numerous methods for hand gesture recognition system. Abhinav has proposed a wearable gestural interface which lets the user to use natural hand gestures to interact with the information [1]. The main advantage in this is it integrates digital information into the physical world and its objects and uses hand gestures to interact with digital information, supports multi-touch and multi-user interaction. Some drawbacks are the use of color markers and it is not used in 3D gesture tracking. Saikat et al has proposed a gesture interpretation system capable of controlling the computer mouse using thermal camera [2]. The efficiency of the system is minimized and can be dramatically improved by background subtraction but it is designed only with two hand gestures which is a limited input systems. Shiguo et al has proposed an automatic user state recognition model to control the TV system [3]. Reduced power consumption and computational cost and its limitations are ultrasonic sensor is used for

detection Experimental results has shown that it is an effective method to use Raspberry Pi board to actualize embedded image capturing system [5]. Dynamic gestures which are performed in complex background [4] can be identified by hand gesture recognition system. Thermal cameras [6] can be integrated along with web camera to identify the hand gestures but in addition to it calibration of thermal camera has to be done periodically. A framework is designed which is a low cost yet effective gesture interpretation system. By using a camera and a tiny projector the system can be controlled using hand gestures during presentations.

The gesture recognition system is an embedded system with less power consumption and efficient image capturing system. This system is more advantageous than PC based systems in terms of cost and portability. Raspberry Pi which is a mini computer is an embedded system which is more efficient in controlling a system through gestures. Linux operating system provides many software choices in order to do a specific task which adds additional functionality in choosing Raspberry Pi.

3. GESTURE RECOGNITION EMBEDDED SYSTEM

3.1 System Componentes

The system is composed of the Raspberry Pi board and the Raspbian camera to capture the video. The Raspberry Pi board is the central module of the whole embedded image capturing and processing system with Broadcom BCM2835 system-on-chip multimedia processor at 700MHz in which CPU core is a 32 bit ARM1176JZF-S RISC processor. Even though the Raspberry Pi is a computer it does not have a hard drive like traditional computers, instead it relies on the SD card for starting up and storing of information. A 16GB SD card is used in this system. The Raspbian camera module is a 5MP CMOS camera with a fixed focus lens that is capable of capturing still images as well as high definition video. The power supply to the board is 5V and is connected via a micro USB connector. The Raspberry Pi board is connected to the Raspbian camera through the dedicated CSI interface. The system block diagram is shown in Figure 1.

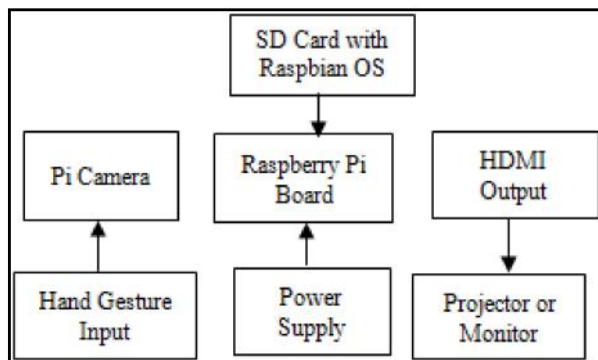


Fig.1 Block diagram of the proposed system

3.2 Raspberry PI

Hardware is a physical device that can be touched or held, like a hard drive or a mobile phone. Software can be thought of as a program or a collection of programs that instruct a computer on what to do and how to do it. Below is an image of the Raspberry Pi which describes some of the components that make up the hardware.

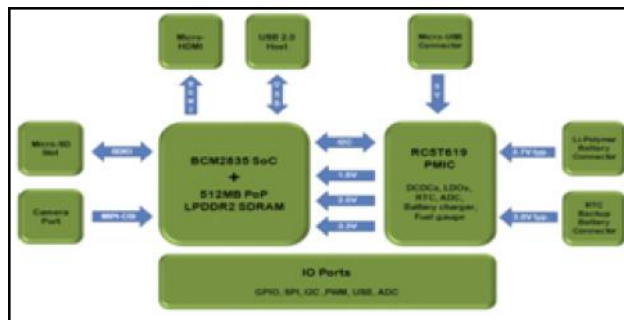


Fig.2. Hardware components of raspberry Pi

The hardware description of Raspberry Pi which is shown in Figure 2 consists of the GPIO pin, SD slot, USB port and Micro USB connector. The GPIO pins are used for serial communication for interfacing GSM and GPS etc. It uses 16GB SD for installing the Raspbian OS and for storage. The USB port is used for connecting keyboard, mouse, dongle and pen drive. The power supply is given through USB connector.

3.3 Gesture Detection

The system begins by analyzing the captured video frame from the Raspbian camera. Normally the video has to be cut in different images to identify the hand gestures using different color markers. The image obtained is often in theBGR format and it has to be first converted into HSV color space. There are several steps for gesture recognition which is shown in Figure 3.

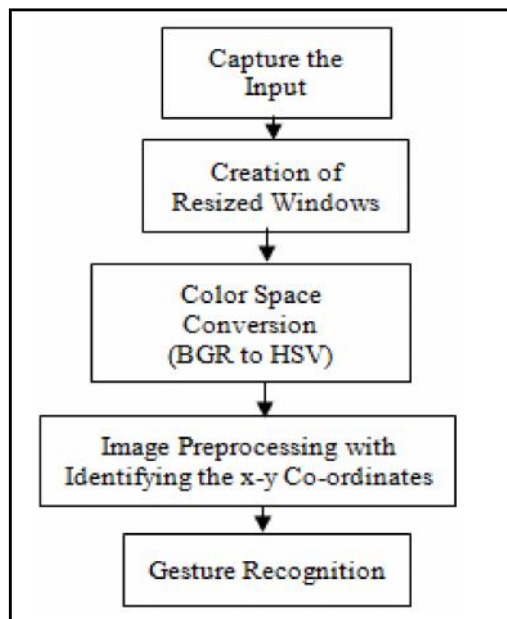


Fig.3 Framework of the system

3.3.1 Capture the Input: The first step is to capture the live video stream from the Raspbian camera. In reference [5], this camera has no infrared filter thus making it perfect to capture images which even during low light conditions.

The color markers are identified and the video is converted into picture frames for gesture recognition.

Image Acquisition: The next step is to create windows for different color markers which are detected. Resize the frames in order to reduce the resolution which will in turn reduce the computation time. In references [2][8] noise reduction is done by using the antialiasing filters.

3.3.2 Color Space Conversion: A proper color model is needed to perform classification. The captured image which is in the BGR color space is converted to HSV (Hue Saturation Value). HSV color space is the most suitable one for color based image segmentation. Hue value represents the shades of the color, S describes how pure the hue color is and V provides the intensity of the color. Different HSV values for different colors are provided to represent the gray image of that particular color. The gesture recognition system is processed dynamically for computation and to reduce the complexity color markers are used for detection instead of skin tone detection which is used in reference [4]. The resized window which shows the original image detecting the yellow color marker and the converted gray image is shown in Figure 4.

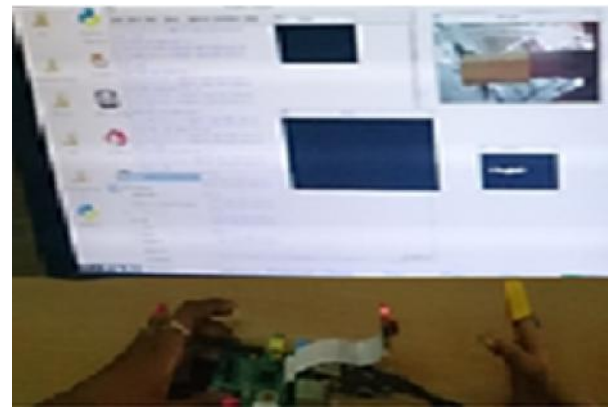


Fig.4 Detection of yellow color marker with the converted gray image

3.3.3 Image Preprocessing: In this phase the color markers are detected and the x-y co-ordinates are identified for the detected image. To identify the x-y co-ordinates of the color markers the size of the monitor is known and the x-y co-ordinates are calculated using pixel co-ordinate system where the position is identified by $px=0$ and $py=0$ corresponding to the top-left corner of the window. For each frame the system recognizes the color markers and the corresponding x-y co-ordinates are displayed. Reference [6] uses background modeling and calibration of the which makes the system more efficient in computation.

3.3.4 Gesture Recognition: To recognize the gestures the gesture can be either one finger or two finger gestures with different color markers. In one finger gesture analysis red color marker is placed in the index finger and it is used to control the cursor movements in the screen. In two finger gesture analysis along with index finger the thumb and middle finger is used for left click and right click. Thus the system is controlled by finger gestures using different color markers. In reference [7] it uses two approaches that are used for cursor movement control which is using resolution mapping and weighted speed cursor control. Using pixel co-ordinate system the resolution size of the window is calculated and mapping is done for cursor movement.

The pseudo code for cursor movement identifying red color marker is shown in Figure 5. It uses the pixel co-ordinate system and the resized window size of the red color marker identification window is used where the HSV value of red color is given and the (mx, my) pixel co-ordinates are calculated. The `getpixel` function is used to identify the red color detected within the resized

window and the move function is used for cursor movement with respect to the (mx,my) co-ordinates.

```

for x in range(1,299):
for y in range(1,162):
    r,g,b=picture.getpixel((x,y))
    if rdetect == 0:
        if r >= 125 and g <= 60 and b <= 60:
            mx=x*4
            my=y*3.5
            m.move(mx,my)
            rdetect = 1
    
```

Fig.5 Pseudo code for cursor movement

The pseudo code for mouse left click identifying yellow color marker is shown in Figure 6. Similarly, the same condition is done for identifying the left click where the HSV value changes for yellow color marker. The click function is used to perform the action with respect to the pixel co-ordinates of the window. It has three subordinates where the first one represents the maximum size of the x co-ordinate of the window, second represents the maximum size of the y co-ordinate of the window.

```

for x in range(1,167):
for y in range(1,93):
    r,g,b=picture.getpixel((x,y))
    if ydetect == 0:
        if r >= 130 and g <=70 and b >= 130:
            m.click(400,695,1)
            m.click(400,695,1)
            ydetect = 1
    
```

Fig.6 Pseudo code for mouse left click

The pseudo code for mouse right click identifying blue color marker is shown in Figure 7. This is similar to left click where the HSV value for blue color is given and click function takes the pixel co-ordinates as its parameter and performs the right click.

```

for x in range(1,167):
for y in range(1,93):
    r,g,b=picture.getpixel((x,y))
    if bdetect == 0:
        if r <= 60 and g <= 60 and b >= 90:
            m.click(mx,my,2)
            bdetect = 1
    
```

Fig.7 Pseudo code for mouse right click

Using resolution mapping the resolution size of different window screens can be calculated. During presentations the projector screen resolution is mapped with the resized windows of different color markers. These finger gestures can be used to control the next and previous slide buttons during presentation. A smart TV can also be controlled using hand gestures during net access.

3.4 State Recognition

For the mouse actions carried out different states are assigned. Absent state is assigned when the finger is idle. The four states are: *Right Click, Left Click, Double Click, Absent*. The action detection is sensed by the camera and the mouse clicks are performed. When the user's finger is idle without any change in the gestures then the system goes to power off (sleep) mode. This is implemented in the algorithm by assigning the wait time for each action detected. The wait time is compared and accordingly the system goes to sleep mode. This saves the energy consumption and it can be used as a portable device.

4. SOFTWARE IMPLEMENTATION

The Raspberry Pi is a Linux based operating system environment with python as the main programming language. The development environment used here is the IDLE (Integrated Development Environment) which is the basic platform for python. Along with IDLE OpenCV library version 2.4.8 is used for solving computer vision problems. OpenCV-Python is the library of Python bindings designed to solve computer vision problems and it provides all the functions to develop the gesture movements. Python allows programmers to define their own types using classes, which are most often used for object-oriented programming. Python has a large standard library, commonly cited as one of Python's greatest strengths, providing tools suited for many tasks.



Fig.8 Python shell window

The Python Shell window shown in Figure 8 is used for running the code and viewing the results of the code. In the menu bar Debug option provides the run module which will debug the code and will show the execution results.

5. EXPERIMENTAL RESULTS

The system consist of Raspberry Pi interfaced with Raspbian camera where the color markers placed in the fingers are used to control the system. The Raspberry Pi interfaced with Raspbian camera along with the monitor window is shown in Figure 9.



Fig.9 Raspberry Pi interfaced with Raspbian camera with the monitor window

The software running in the background in the Python IDE along with the resized windows for each color detected is shown in Figure 10. Its shows the (x,y) co-ordinates for the red color detected which can be used to recognize the cursor movement.

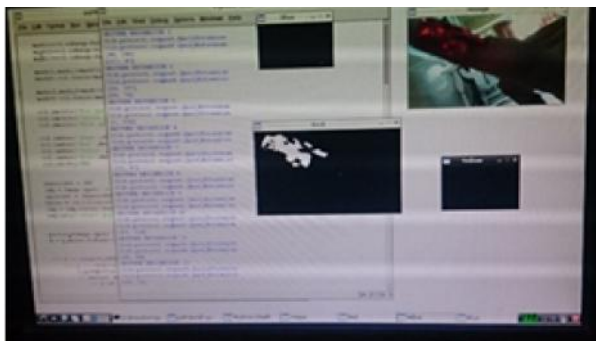


Fig.10 Software running in the background in Python IDE

The red color marker placed on the index finger is used for cursor movement which is placed on a Desktop icon is shown in Figure 11. The software running at the background is used to identify the red color and the functions are used for cursor movement.



Fig.11 Detection of red color marker for cursor movement

The blue color marker is used to perform the right click. In Figure 12, the right click is performed showing a pop up menu for the Desktop icon selected using the cursor movement. Once the blue color is detected the software running at the background will perform the right click function on the specified area in the monitor screen.



Fig.12 Detection of blue color marker for right click

The yellow color marker placed on the finger is used for doubleclick (left click). In Figure 13, the left click is performed showing a pop up menu for the Desktop icon selected. When the yellow color is detected the software running at the background will perform the double click at the pointed area in the monitor.



Fig 13. Detection of yellow color marker for left click

Thus the system is controlled by finger gestures using the Raspberry Pi which is an efficient and effective embedded system.

6. CONCLUSION

This paper provides a computer vision gesture interpretation embedded system which controls the mouse performing different operations for different gestures. Designing an embedded system with Raspberry Pi which is smaller, low cost with less power consumption is more convenient than the traditional PC-based gesture recognition system. The development environment using python language makes it easier to detect the gestures using color markers. In future more gestures can be introduced with different color markers for some functions like scroll, zoom in, zoom out etc. This can be applied in other applications like robotics, interactive video games.

REFERENCES

- [1] Abhinav Sharma, Mukesh Agarwal, Anima Sharma, Sachin Gupta, "Sixth sense Technology", in Proc. International Journal on Recent and Innovation Trends in Computing and Communication, Vol.1, April 2013, pp. 277-282.
- [2] Saikat Basak, Arundhuti Chowdhury, "A Vision Interface Framework for Intuitive Gesture Recognition using Color based Blob Detection", in Proc. International Journal of Computer Applications, Vol.90, No.15, March 2014.
- [3] Shiguo Lian, Wei Hu, Kai Wang, "Automatic User State Recognition for Hand Gesture Based Low-Cost Television Control System", IEEE Transactions on Consumer Electronics, Vol. 60, No. 1, February 2014, pp.107-115.
- [4] Mohamed Alsheakhali, Ahmed Skaik, Mohammed Aldahdouh, Mahmoud Alhelou, "Hand Gesture Recognition System", in Computer Engg Department, The University of Gaza, 2011.
- [5] G.Senthilkumar, K.Gopalakrishnan, V.Sathish Kumar, "Embedded Image Capturing System Using Raspberry Pi System", in Proc. International Journal of Emerging Trends & Technology in Computer Science, Vol.3, April 2014, pp. 213-215.
- [6] Bobo Zeng, Guijin Wang, Xinggang Lin, "A Hand Gesture Based Interactive Presentation System Utilizing Heterogeneous Cameras", in Tsinghua Science and Technology, Vol.17, No.3, June 2012, pp.329-336.
- [7] Kamran Niyazi, Vikram Kumar, Swapnil Mahe and Swapnil Vyawahare, "Mouse Simulation Using Two Coloured Tapes", in Proc. International Journal of Information Sciences and Techniques, Vol.2, No.2, March 2012, pp.57-63.
- [8] Raspberry Pi [Online]. Available: <http://www.raspberrypi.org>.

Assessment and Enhancement of Transient Stability in Power System Using ETAP Software

A. Maria Sindhuja and D. Raj Kumar

Assistant Professor, Department of Electrical and Electronics Engineering,

M.Kumarasamy College of Engineering, Karur - , Tamil Nadu

E-mail: mariasindhuja@gmail.com, rajkumard.eee@mkce.ac.in

Abstract

The main objective of this work is to perform effective transient stability analysis of a particular power system. The purpose of performing transient stability on the power system is to study the stability of a system under various disturbances. The stability of power system is the ability of generators to remain synchronism even when subjected to disturbances. For giving referred response system, we have taken IEEE 9 bus system, where it is subjected to various disturbances. The swing curves for the various generators of various bus systems is plotted to comment the stability of system. The factors affecting the stability are analysed and methods for obtaining a better stability of the system under the fault conditions are also studied. From the study, the prediction of effective response of the system is modelled and estimated. Prediction progress is not involved with the non-deterministic way, instead of that we proposed a statistical based regressive model. In this work, we have taken Partial Least Square Regression (PLSR) analysis to extract the relationship among the variable. From that effective response is feed through the system and observed the behaviour of the system. The work exhibited the effective response of the system when it is affected by the fault at various location. Effectiveness of the system is portrayed in terms of transient stability of Generators, where it gives the margin for the system to produce good response.

Keywords: Transient stability, Synchronism, Swing curves, Prediction, Regressive, Partial least square regression

1. INTRODUCTION

Day by day demand of electrical power is increasing due to expansion of industrial, residential and commercial sectors. In this regard, electric utility companies are being asked to run their machines very close to their maximum output. To meet this demand, the size of the interconnected power system is increasing, which in turn is resulting in an increase in the modification cost of these power systems. The utility companies are planning and adopting wide range of design options to reduce the higher modification cost. In this circumstance, detail studies related to transient stability analysis are carried out by considering different assumptions. Transient stability analysis requires huge amount of computational efforts due to large size of interconnected power system. Due to network complexity, power system stability is divided into smaller areas including rotor angles, frequency and voltage stabilities. Rotor angle stability refers to the ability of synchronous machines of an interconnected power systems to remain in synchronism after being subjected to a fault [1-2]. N. Amjady and S. F. Majedi [2] have proposed a new hybrid intelligent system for prediction of transient stability.

In their paper, the intelligent system is composed of a processor, an array of neural networks (NN) and an interpreter. In [3], the authors have demonstrated that the study of transient stability of a system is important not only for design and coordination of protection scheme at the planning stage but also for security control during system operation. A. M. Mihirig and M. D. Wvong [4] have proposed a catastrophe theory to determine the transient stability regions of multimachine power systems. They have calculated transient stability limits from the bifurcation set and the critical clearing time from the catastrophe manifold equation. Distributed approach for real time transient analysis have already been mentioned by some authors (e.g., see [5]) describing stability analysis for large number of machines and busbars. A direct method of Lyapunov functions has been used to recognize the fault location as a critical factor for the determining the boundary of the stability region [6]. A new method has been developed for economic dispatch together with nodal price calculations which included transient stability constraints and, at the same time, optimized the reference inputs to the flexible AC transmission system (FACTS) devices for enhancing system stability and reducing nodal prices [7, 8].

The accuracy of using static (nonlinear) load models with suitably identified parameters for transient stability analysis has been examined in [9]. Here, numerical studies have been conducted using on-line measurement data for modelling real power behaviours during disturbances and hence were deemed adequate for transient stability analysis. In [10], the authors have carried out Transient stability analysis in different cases such as peak and off-peak loads, connection and disconnection of busbar, with and without current limit reactor (CLR). In this case, the transient stability in peak load condition was more stable than that in off-peak load condition; the transient stability with bus-bar disconnected was more stable than that with bus-bar connected; the transient stability with CLR was more stable than that without CLR. Transient stability analysis in terms of machines rotor angle, electrical power, machines speed and terminal voltage has been done for Sarawak grid system using power system simulation for engineers in [11]. A power system analysis toolbox (PSAT) was used to study transient stability analysis for the IEEE 14-bus system with wind connected generator in [12]. Systematic investigations of transient stability analysis have been conducted by the combination of step-by-step integration and direct methods in [13]. In this case, more time was required to calculate potential and kinetic energies of all machines before and after the faults. Carlo Cecati and Hamed Latafat [14] have studied transient stability of a two-machine infinite bus by time-domain versus transient energy function when affected by large disturbances. Here, they have used the Lyapunov function and decentralized nonlinear controller to study transient stability.

2. PROPOSED METHOD

The proposed method is developed is based on the regression analysis. The purpose of this note is to try and lay out some of the techniques that are used to take data and deduce a response (y) or responses in terms of input variables (x values). This is a collection of topics and is meant to be a refresher not a complete text on the subject for which there is many. See the references section. These techniques fall into the broad category of regression analysis and that regression analysis divides up into linear regression and nonlinear regression. This first note will deal with linear regression and a follow-on note will look at nonlinear regression. Regression analysis is used when you want to predict a continuous dependent variable or response from a number of independent or input variables. If the dependent variable is dichotomous, then logistic regression should be used.

The independent variables used in regression can be either continuous or dichotomous (i.e. take on a value of 0 or 1). Categorical independent variables with more than two values can also be used in regression analyses, but they first must be converted into variables that have only two levels. This is called dummy coding or indicator variables. Usually, regression analysis is used with naturally-occurring variables, as opposed to experimentally manipulated variables, although you can use regression with experimentally manipulated variables.

One point to keep in mind with regression analysis is that causal relationships among the variables cannot be determined. The areas I want to explore are 1) simple linear regression (SLR) on one variable including polynomial regression e.g. $y = b_0 + b_1x + b_2x^2 + \dots + b_px^p$, and 2) multiple linear regression (MLR) or multivariate regression that uses vectors and matrices to represent the equations of interest. Included in my discussions are the techniques for determining the coefficients (e.g. b_0, b_1, \dots, b_p) that multiply the variants (e.g. least squares, weighted least squares, maximum likelihood estimators, etc.).

Under multivariate regression one has a number of techniques for determining equations for the response in terms of the variants: 1) design of experiments (DOE), and 2) point estimation method (PEM), are useful if data does not already exist, 3) stepwise regression either forward or backward, 4) principal components analysis (PCA), 5) canonical correlation analysis (CCA), 6) Generalized Orthogonal Solutions (GOS), and 7) partial least squares (PLS) analysis are useful when data already exists and further experiments are either not possible or not affordable.

Types of Regression analysis can be classified as A) Ordinary least square regression analysis B) Partial least square regression analysis C) Partial least square regression analysis. Partial least squares regression is an extension of the multiple linear regression models (see, e.g., Multiple Regression or General Stepwise Regression). In its simplest form, a linear model specifies the (linear) relationship between a dependent (response) variable Y, and a set of predictor variables, the X's, so that

$$Y = b_0 + b_1X_1 + b_2X_2 + \dots + b_pX_p \quad (1)$$

In this equation b_0 is the regression coefficient for the intercept and the b_i values are the regression coefficients (for variables 1 through p) computed from

the data. So for example, you could estimate (i.e., predict) a person's weight as a function of the person's height and gender. You could use linear regression to estimate the respective regression coefficients from a sample of data, measuring height, weight, and observing the subjects' gender. For many data analysis problems, estimates of the linear relationships between variables are adequate to describe the observed data, and to make reasonable predictions for new observations (see Multiple Regression or General Stepwise Regression for additional details).

The multiple linear regression models have been extended in a number of ways to address more sophisticated data analysis problems. The multiple linear regression model serves as the basis for a number of multivariate methods such as discriminate analysis (i.e., the prediction of group membership from the levels of continuous predictor variables), principal components regression (i.e., the prediction of responses on the dependent variables from factors underlying the levels of the predictor variables), and canonical correlation (i.e., the prediction of factors underlying responses on the dependent variables from factors underlying the levels of the predictor variables).

These multivariate methods all have two important properties in common. These methods impose restrictions such that (1) factors underlying the Y and X variables are extracted from the $Y'Y$ and $X'X$ matrices, respectively, and never from cross-product matrices involving both the Y and X variables, and (2) the number of prediction functions can never exceed the minimum of the number of Y variables and X variables.

Partial least squares regression extends multiple linear regression without imposing the restrictions employed by discriminate analysis, principal components regression, and canonical correlation. In partial least squares regression, prediction functions are represented by factors extracted from the $Y'XX'Y$ matrix. The number of such prediction functions that can be extracted typically will exceed the maximum of the number of Y and X variables.

In short, partial least squares regression is probably the least restrictive of the various multivariate extensions of the multiple linear regression models. This flexibility allows it to be used in situations where the use of traditional multivariate methods is severely limited, such as when there are fewer observations than predictor

variables. Furthermore, partial least squares regression can be used as an exploratory analysis tool to select suitable predictor variables and to identify outliers before classical linear regression.

3.RESULTS AND DISCUSSION

The ETAP software is used to study the transient stability analysis of the IEEE three-machine, nine-bus bar power system network. The base MVA and system frequency are considered to be 100 MVA and 50 Hz, respectively. The single-line diagram of the three-machine power system is shown in Figure 1.

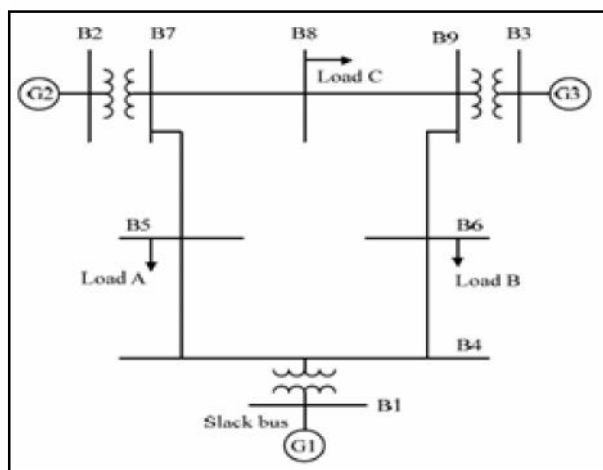


Fig.1 IEEE 9 bus system

Here, generator G1 is connected to slack bus 1, whereas generators 2 (G2) and 3 (G3) are connected to bus bars 2 and 3, respectively. Loads A, B and C are connected in bus bars 5, 6 and 8 respectively. Initially, fast decoupled method is used for load flow analysis. Then transient stability analysis has been carried out by monitoring the performance of the generators (G1, G2 and G3). The first case has been dealt with a three-phase fault occurring near bus 5 of the line 5-4.

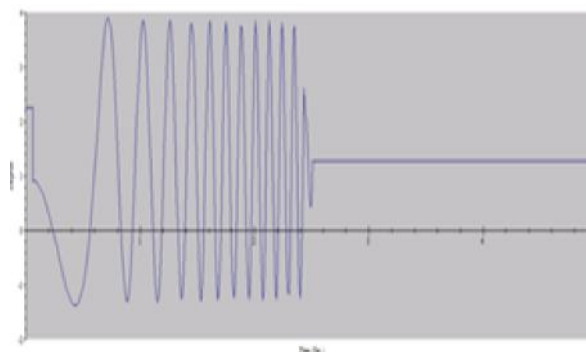


Fig.2 Absolute Power Angle of Generator 1 when fault at line 1

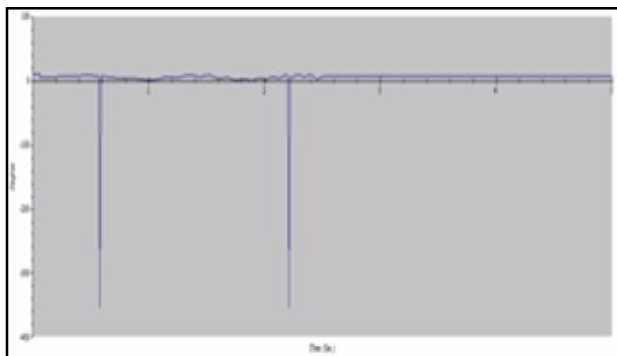


Fig.3 Absolute Power Angle of Generator 2 when fault at line 1

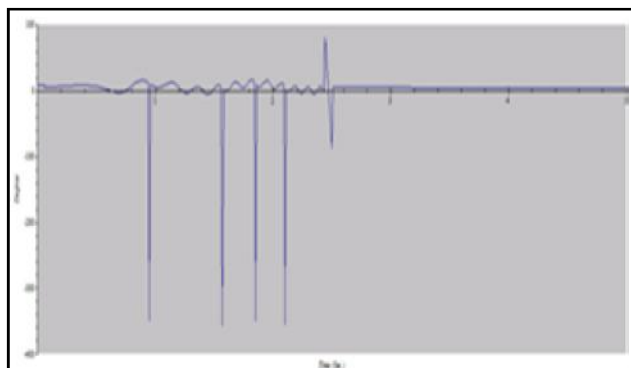


Fig.4 Absolute Power Angle of Generator 3 when fault at line 1

The fault is cleared by connecting the over current relay across the faulted line. The swing angles of the generators G2 and G3 have been calculated by subtracting the swing angles of the generator G1. The swing angles of generators G2 and G3 are plotted in the t plane, which are shown in Figure 5. An inspection of Figures 5,6,7 shows that the three-machine system is stable.

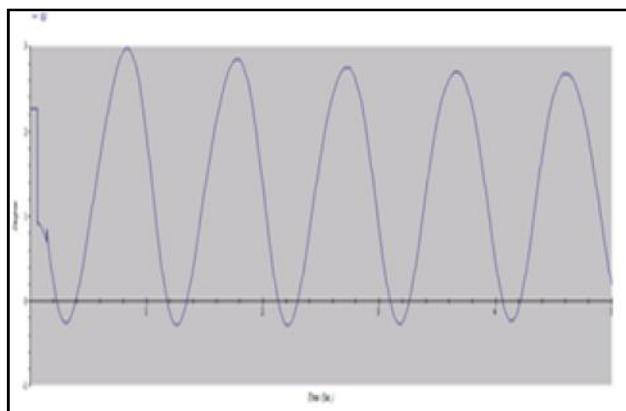


Fig.5 Absolute Power Angle of Generator 1

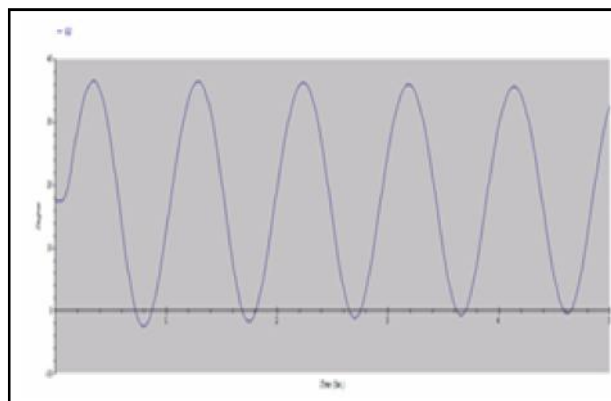


Fig.6 Absolute Power Angle of Generator 2

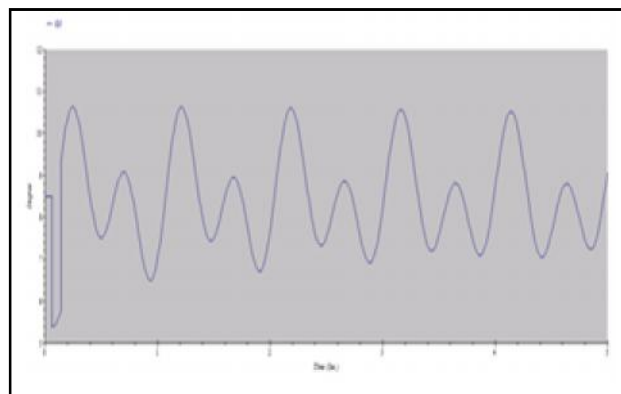


Fig.7 Absolute Power Angle of Generator 3

The coefficient partial least square regression model has been constructed by usage of MINITAB platform. As a result of this constructed model, it is fitted with the validated model that portrays the exact progress of transient stability progress.

By the observed variable results through ETAP, PLS regression coefficient model has been constructed and the validation of the model is analyzed. Cross validation results are shown in figure 8.

Table 1 Coefficient Model of Relay Timing

#	C1	C2	C3	C4	C5	C6	C7	C8	C9	C10	C11	C12	C13	C14	C15	C16	C17
	relay11	relay10	relay6	relay7	optimerelay11	Coef3	Fit3	Resid3	SResid3	Coef4	Fit4	Resid4	SResid4				
1	1.950	1.950	0.262	0.262	59.7	-243.126	-57.50	117.202	0.46738	-243.126	-57.50	117.202	0.46738				
2	1.220	1.950	0.262	0.262	146.0	-208.873	119.98	26.020	0.09770	-208.873	119.98	26.020	0.09770				
3	0.851	0.851	0.806	5.420	292.0	403.190	299.99	-417.987	-1.53560	403.190	709.99	-417.987	-1.53560				
4	0.258	0.258	1.180	1.850	1368.0	9.966	1393.24	274.765	1.15373	9.966	1093.24	274.765	1.15373				
5	1.950	1.950	0.262	0.262	59.7		-57.50	117.202	0.46738		-57.50	117.202	0.46738				
6	1.220	1.950	0.262	0.262	146.0		119.98	26.020	0.09770		119.98	26.020	0.09770				
7	0.851	0.851	0.806	5.420	292.0		299.99	-417.987	-1.53560		709.99	-417.987	-1.53560				
8	0.258	0.258	1.180	1.850	1368.0		1393.24	274.765	1.15373		1093.24	274.765	1.15373				

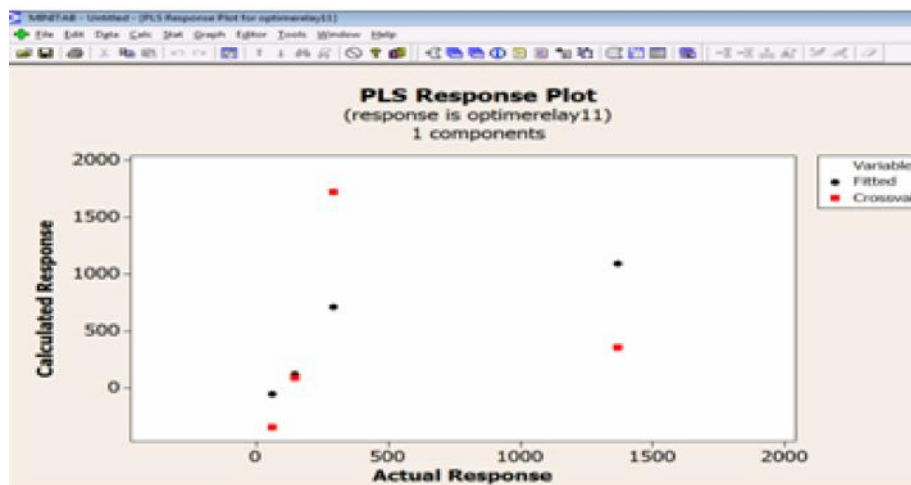


Fig.8 PLS Response Plot

4. CONCLUSION

Transient analysis of a system has been improved by the way of coordinating the relays in efficient and effective model. Predictive model has been done through exquisite time delays in order to assure the transient response within the stable region. Predicting the effective model has done through Partial least square model where it gives the fitness value of 89 percent to assure the effective prediction. Extraction of features and predicting the transient stability response is to be done through hybrid intelligence system.

REFERENCES

- [1] P. Kundur, J. Paserba, V. Ajjarapu, A. Bose, C. Canizares, N. Hatziargyriou, D. Hill, A. Tankovic, C. Taylor, T. Van Cutsem, and V. Vittal, "Definition and Classification of Power System Stability-IEEE/CIGRE Joint Task Force on Stability Terms and Definition", IEEE Transactions on Power Systems, PWS Vol. 19, No. 3, 2004, pp. 1387-1401.
- [2] N. Amjadi, S. F. Majedi, "Transient Stability Prediction by a Hybrid Intelligent System", IEEE Transactions on Power System, PWS Vol. 22, No. 3, 2007, pp. 1275-1283.
- [3] M. L. Scala, G. Lorusso, R. Sbrizzai and M. Trovato, "A Qualitative Approach to the Transient Stability Analysis", IEEE Transaction on Power Systems, PWS Vol. 11, No. 4, 1996, pp. 1996-2002.

- [4] A. M. Mihirig and M. D. Wvong, "Transient Stability Analysis of Multimachine Power Systems by Catastrophe Theory", IEEE Proceedings C: Generation, Transmission and Distribution, Vol. 136, No. 4, 1989, pp. 254-258.
- [5] G. Aloisio, M. A. Bochicchio, M. La Scala, R. Sbrizzai, "A Distributed Computing Approach for Real Time Transient Stability Analysis", IEEE Transactions on Power Systems, Vol. 12, No. 2, 1997, pp. 981-987.
- [6] A. M. Eskicioglu, O. Sevaioglu, "Feasibility of Lyapunov Functions for Power System Transient Stability Analysis by the Controlling UEP Method", IEE Proceedings C: Generation, Transmission and Distribution, Vol. 139, No. 2, 1992, pp. 152-156.
- [7] T. T. Nguyen, A. Karimishad, "Transient Stability-constrained Optimal Power Flow for Online Dispatch and Nodal Price Evaluation in Power Systems with Flexible AC Transmission System Devices", IET Generation, Transmission and Distribution, Vol. 5, No. 3, 2011, pp. 332-346.
- [8] H. D. Chiang, B. K. Choi, Y. T. Chen, D. H. Huang, M. G. Lauby, "Representative Static Load Models for Transient Stability Analysis: Development and Examination", IET Generation, Transmission and Distribution, Vol. 1, No. 3, 2007, pp. 422-431.
- [9] O. Zhu, B. Kim, K. Kim, "Transient Stability Analysis on the Offsite Power System of Korean Nuclear Power Plants", The 46th Universities Power Engineering Conference, 2011, pp. 1-4, 5-8.
- [10] A. M. Mohamad, N. Hashim, N. Hamzah, N. F. N. Ismail, M. F. A. Latip, "Transient Stability Analysis on Sarawak's Grid using Power System Simulator for Engineers", IEEE Symposium on Industrial Electronics and Applications, 2011, pp. 521-526, 25-28.
- [11] A. G. Pillai, P. C. Thomas, K. Sreeranjini, S. Baby, T. Joseph, S. Srecdharan "Transient Stability Analysis of Wind Integrated Power Systems with Storage using Central Area Controller", IEEE International Conference on Microelectronics, Communications and Renewable Energy, 2013, pp. 1-5.
- [12] H. H. Al-Marhoon, I. Leevongwat, P. Rastgoufard, "A Practical Method for Power System Transient Stability and Security Analysis" IEEE PES Transmission and Distribution Conference and Exposition, 2012, pp. 1-6.
- [13] Carlo Cecati and Hamed Latafat, "Time Domain Approach Compared with Direct Method of Lyapunov for Transient Stability Analysis of Controlled Power System", IEEE International Symposium on Power Electronics, Electrical Drives, Automation and Motion, 2012, pp. 695-699.

Antioxidant Activities of A Few Common Seaweeds from the Gulf of Mannar and the Effect of Drying As the Method of Preservation

R.Charu Deepika¹, J.Madhusudhanan² and T.Charles John Bhaskar³

^{1&2}Department of Biotechnology, Shri Andal Alagar College of Engineering, Mamandur-603 111, Tamil Nadu

³Scientist & Managing Director, GeoMarine Biotechnologies Pvt Ltd

Abstract

The pharmaceutical, food and several other industries have experienced great expansion in the demand for seaweeds due to their significant applications as ingredients in functional foods and richness in antioxidant ingredients. The three selected seaweeds found in the coastal areas of Gulf of Mannar, Tamil Nadu are Sargassum wightii, Gracilaria corticata and Kappaphycus alvarezii. The collected samples were stored under 4°C until used. These samples were investigated for antioxidant activity due to the presence of phytochemicals like tannins and polyphenols. Commercially, many marine algae are used as various nutritional products including antioxidant for use or as nutraceutical supplement. In such case, the formulation of products from algae involves drying as a major step in preservation. Thus, the effect of different drying temperatures on the phytochemical constituents in seaweed after harvest is evaluated. The potential difference between the fresh and dried seaweeds as possible food supplement is discussed with the data. Further, the antioxidant activity after extraction of essential products like carrageen, agar and alginate is studied and the impact of drying on the same.

Keywords: Antioxidant activity, *Gracilaria corticata*, *Kappaphycus alvarezii*, Polyphenols, *Sargassum wightii*

1. INTRODUCTION

Bio-stimulant properties of seaweeds are explored for use in agriculture and the antimicrobial activities for the development of novel antibiotics. Seaweeds have some valuable medicinal components such as antibiotics, laxatives, anticoagulants and suspending agents in radiological preparations. Seaweeds have recently received significant attention for their potential as natural antioxidants. Fresh and dried seaweeds are utilized as human food (K. Nisizawa et al., 2002) especially in coastal areas; the consumption of seaweed is high when compared to other areas (N. Kaliaperumal et al., 1995). Dietary seaweeds include marine algae from brown, green and red taxonomies such as the Laminariales, Ulvales and Porphyridiales, respectively (Anggadiredja et al., 1997; Yan et al., 1998).. Lipid peroxidation leads to deterioration of biological systems due to ROS. BHT and BHA have been suspected of being responsible for liver damage and carcinogenesis (Grice, 1986; Wichi, 1988; Hettiarachchy et al., 1996). Antioxidant activity of marine algae may arise from carotenoids, tocopherols and polyphenols. These compounds directly or indirectly contribute to inhibition or suppression of free radical generation (Y. Athukorala et al., 2003). Air drying is the most frequently used dehydration operation in the food

and chemical industry (Ibrahim et al., 2009; Saeed et al., 2008). The wide variety of seaweeds, available to the consumers and the interesting concern for meeting quality specifications and energy conservation, emphasize the need for a thorough understanding of the drying process. Hence, the present study focus upon antioxidant activity of selected three seaweeds in fresh and dry conditions. Further, the antioxidant activity after extraction of essential products like carrageen, agar and alginate is studied and the impact of drying on the same.

2. MATERIALS AND METHODS

2.1 Collection and Extraction of Seaweeds

The selected seaweeds - *Sargassum wightii*, *Gracilaria corticata* and *Kappaphycus alvarezii* were collected from Gulf of Mannar, Tamil Nadu. The samples were washed thoroughly in seawater followed by tap water and finally in distilled water to remove unwanted salts and other materials. Then 10g of each seaweed were weighed in which 5 g was shade dried and other 5 g was sun dried. Aqueous extractions of all the three seaweeds were performed by adding 1 g of seaweed to 6 mL of phosphate buffer and incubated for 24 hours. The supernatant was carefully separated and kept in airtight amber bottle and stored for conducting different assays.

2.2 Extraction of Carrageenan and Alginate

Kappaphycus alvarezii a carragenophyte was used in the extraction. Carrageenan extraction was performed as described previously (Ohno et al., 1994) with slight modifications. The alginate extraction was performed using *Sargassum wightii* according to Nishigawa (1985).

2.3 Determination of Total Phenolic Content

Total phenolic content assay in each extracts were measured using Folin-Ciocalteu method (Kahkonen *et al.*, 1999). 5 mL of Folin-Ciocalteu phenol reagent and 4 mL of 7.5% (w/v) sodium carbonate were added to 1 mL of seaweed extracts which were incubated for 2 hours in a dark place at room temperature for the reaction to take place. The absorbance of the reaction mixtures were measured at 765 nm wavelength using spectrophotometer. Gallic acid standard was used for comparative study.

2.4 Nitric Oxide Scavenging Assay

Phenolic compounds are considered to exhibit radical scavenging properties (Umayaparvathi S et al., 2012). The nitric oxide scavenging assay was performed by adding 1.5 mL of each extract to separate test tubes (1.5 mL distilled water was added to control instead of extract) to which 1.5 mL of 10 mM sodium nitrite was added and incubated for 2 hours 30 minutes, after which 1 mL of these incubated samples were added with 2 mL of 0.33% sulphanic acid and left for another incubation period of 5 minutes in room temperature. Freshly prepared 300 μ l of 0.1% naphthol was added and the absorbance was measured at 540 nm after incubation period.

2.5 Assay for Inhibition of Lipid Peroxidation

An oleic acid emulsion was prepared by adding 0.25 mL of oleic acid with 9.75 mL of isopropanol. 0.5 mL of extract was added with 0.5 mL of isopropanol and 1 mL of 0.05M phosphate buffer and stored in dark place. At regular intervals of time (0 and 24 hours), 0.1 mL of incubated sample was taken for the measurement of degree of oxidation by ferric thiocyanate method. The absorbance was recorded at 500 nm after 3 minutes incubation.

2.6 Beta-carotene Bleaching(BCB) Assay

β -carotene bleaching assay was performed as earlier described (T. Juntachote and E. Berghofer, 2005). 3 mL aliquot of the β -carotene emulsion was added to 40 mg of linoleic acid and 400 mg of Tween 40. After the chloroform has evaporated, 100 mL of distilled water was added to the mixture and mixed vigorously. The initial absorbance values were recorded at 470 nm and 700 nm immediately. From which 3 mL of β -carotene/linoleic acid emulsion were mixed with 100 μ L of each seaweed extract. The tubes were incubated at 50°C for 60minutes and absorbance was recorded at 470 nm and 700 nm.

Degradation rate (DR) of β -carotene = $[\ln (A_{\text{initial}} / A_{\text{sample}})]/60$

Antioxidant activity (%) = $[(DR_{\text{control}} - DR_{\text{sample}}) / DR_{\text{control}}] \times 100$

2.7 Ferrous ion Chelating (FIC) Activity

The ferric ion chelating assay was conducted using ferrous sulphate and ferrozine (N. Singh and P.S. Rajini, 2004). 0.1 mL of extract solution was added to 1.0 ml of 0.1mM FeSO₄ and 1.0 ml of 0.25mM ferrozine. The tubes were shaken well and left undisturbed for 10 min. The absorbance was measured at 562 nm after incubation of 10 minutes. Blank was prepared by replacing ferrozine with water whereas the control consisted of water in place of the extract.

Chelating effect (%) = $(A_{\text{control}} - A_{\text{sample}}) / A_{\text{control}} \times 100$

2.8 Ferric ion Reducing Antioxidant Power (FRAP) Assay

The FRAP assay was performed with slight modifications from that followed earlier (HowYee Lai and YauYan Lim, 2011). 1 mL of each extract was added to 2.5 mL of 0.2M phosphate buffer (pH 6) and 2.5 mL of potassium ferricyanide (1% w/v) and incubated for 20 min at 50°C, after which 2.5 mL of 10% trichloroacetic acid was added. An aliquot of 2.5 mL of each mixture was diluted, before adding 0.5 mL of (0.1% w/v) ferric chloride and incubated for about 30 minutes. Absorbance was measured at 700 nm. A calibration curve was constructed using gallic acid.

3. RESULTS AND DISCUSSION

3.1 Total Phenolic Content

A number of studies have focussed on the biological activities of phenolic compounds, which are potential

antioxidants and free radical-scavengers (Sugihara et al., 1999). The phenol content of *Kappaphycus alvarezii* was found higher than others. *Sargassum wightii* had quite lower than *Kappaphycus* but much higher than *Gracilaria corticata*.

Table 1 Total Phenolic Content of Seaweed Extracts

Seaweed Extracts	Absorbance 765nm	Total Phenolic Content (mg (GAE)/100gdw Seaweed)
<i>Kappaphycus alvarezii</i>	0.96	0.92
<i>K. alvarezii</i> (after carrageen extraction)	0.63	0.58
<i>Sargassum wightii</i>	0.77	0.61
<i>S. wightii</i> (after alginate extraction)	0.61	0.54
<i>Gracilaria corticata</i> (fresh)	0.34	0.27
<i>G. corticata</i> (shade dried)	0.27	0.20
<i>G. corticata</i> (sun dried)	0.19	0.15

3.2 Nitric Oxide Scavenging Assay

The scavenging effect of the seaweeds measured by this assay resulted in proving that *Gracilaria* has the

largest scavenging activity compared to others, but *Kappaphycus* was quite high whereas *Sargassum* showed lowest scavenging activity.

Table 2 Nitric Oxide Scavenging Effect of Seaweed Extracts

Seaweed Extracts	Absorbance 540nm	Scavenging Activity (%)
<i>Kappaphycus alvarezii</i>	0.14	63.15
<i>K. alvarezii</i> (after carrageen extraction)	0.17	55.26
<i>Sargassum wightii</i>	0.23	39.47
<i>S. wightii</i> (after alginate extraction)	0.19	50.00
<i>Gracilaria corticata</i> (fresh)	0.11	71.05
<i>G. corticata</i> (shade dried)	0.11	45.54
<i>G. corticata</i> (sun dried)	0.06	71.05
Control	0.38	

3.3 Assay for Inhibition of Lipid Peroxidation

Inhibition activity of *Gracilaria corticata* was found to be higher than other two extracts in both cases- before

and after incubation. Further, this activity was increased on incubation in *Gracilaria* and *Kappaphycus* whereas in *Sargassum* the inhibition was reduced after 24 hours of incubation.

Table 3 Lipid Peroxidation - Inhibition Assay

Seaweed Extracts	Absorbance		Inhibiting activity (%)	
	0 hr	24 hrs	Before incubation (0 hrs)	After (24 hrs)
<i>K. alvarezii</i>	0.19	0.14	57.77	61.11
<i>S. wightii</i>	0.27	0.31	40.00	13.88
<i>G. corticata</i> (fresh)	0.16	0.12	64.44	66.66
Control	0.45	0.36		

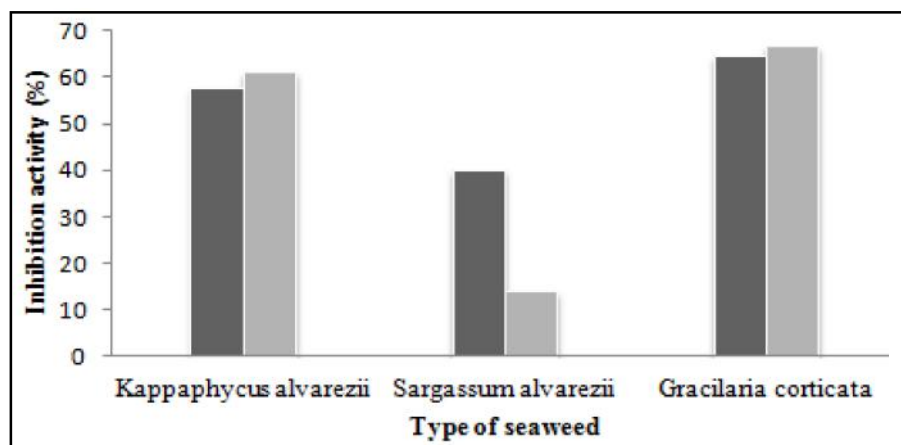


Fig.3 Lipid peroxidation inhibition assay – The reducing activity in percent vs three different types of seaweeds (Kappaphycus alvarezii, Sargassum wightii & Gracilaria corticata) at two different incubation periods.

*series 1 & 2 refers to value calculated from readings taken at 0 hour & 24 hours respectively.

3.4 Beta-carotene Bleaching Assay

BCB method measured the ability of an antioxidant to inhibit lipid peroxidation. In the BCB method, a model

system made of β -carotene and linoleic acid undergoes a rapid discoloration in the absence of an antioxidant. The antioxidant activity was expressed as percent inhibition relative to the control.

Table 4 Beta Carotene Bleaching - Inhibition Assay

Seaweed Extracts	Absorbance (470 & 700nm)				Antioxidation Activity (%) (Calculated with A470 & A700)	
	Initial		Sample			
K. alvarezii	0.18	0.27	0.17	0.25	91.30	86.30
S. wightii	0.22	0.31	0.16	0.23	51.80	79.60
G. corticata (fresh)	0.20	0.24	0.17	0.27	75.40	91.90
Control	0.15	0.20	0.30	0.39		

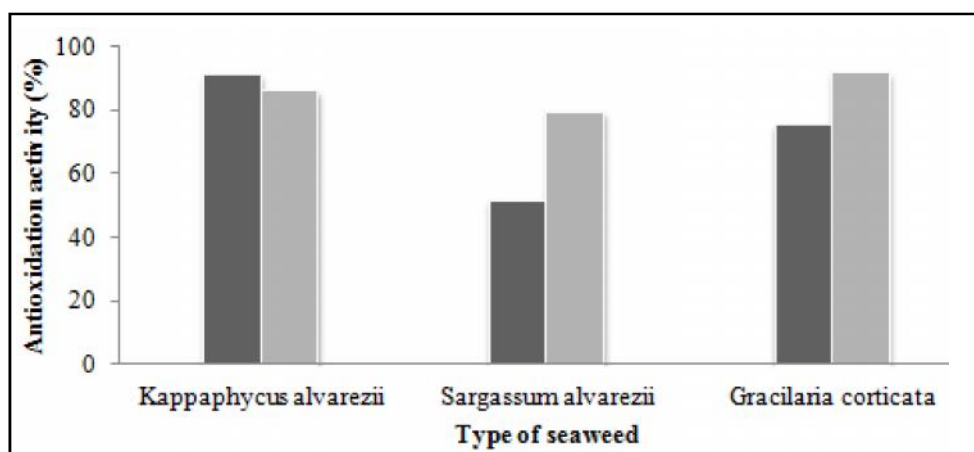


Fig.4 Beta carotene bleaching inhibition assay - antioxidant activity in percent vs three different types of seaweeds (Kappaphycus alvarezii, Sargassum wightii & Gracilaria corticata) at two different wavelengths (470 & 700 nm)

*series 1 & 2 refers to value calculated from readings taken at 470nm & 700nm respectively.

3.5 Ferrous Ion Chelating (FIC) activity

Fe²⁺ has been known to accelerate formation of hydroxyl radicals via the Fenton reaction, leading to occurrence of many diseases (B. Halliwell., 1996). It is reported that chelating agents that form -bonds with a

metal ion, are effective secondary antioxidants since they reduce the redox potential, thereby stabilizing the oxidized form of the metal ion (K.S. Kumar et al., 2008). Ferrozine can quantitatively chelate with Fe²⁺ and form a red coloured complex.

Table 5 Ferrous ion Chelating Activity

Seaweed Extracts	Absorbance at 562nm	Chelating Activity (%)
Kappaphycus alvarezii	0.39	41.79
K. alvarezii (after carrageenan extraction)	0.52	22.38
Sargassum wightii	0.56	16.41
S. wightii (after alginate extraction)	0.48	28.35
Gracilaria corticata (fresh)	0.38	43.28
G. corticata (shade dried)	0.26	61.19
G. corticata (sun dried)	0.34	49.25
Control	0.67	

3.6 Ferric ion Reducing Antioxidant Power (FRAP) Assay

In this assay, the ferric ions are reduced to ferrous, which is a redox reaction involving single electron transfer

by the action of antioxidants in the seaweed extracts which directly signifies the reducing power. Our present study has shown that Sargassum wightii has got lowest reducing activity compared to Kappaphycus alvarezii and Gracilaria corticata.

Table 6 Ferric Ion Reducing Activity

Seaweed Extracts	Absorbance (700nm)	Reducing Activity (mg GAE/100gdw)
Kappaphycus alvarezii	0.27	12.0
Sargassum wightii	0.13	6.0
Gracilaria corticata (fresh)	0.23	11.4
Control	0.47	

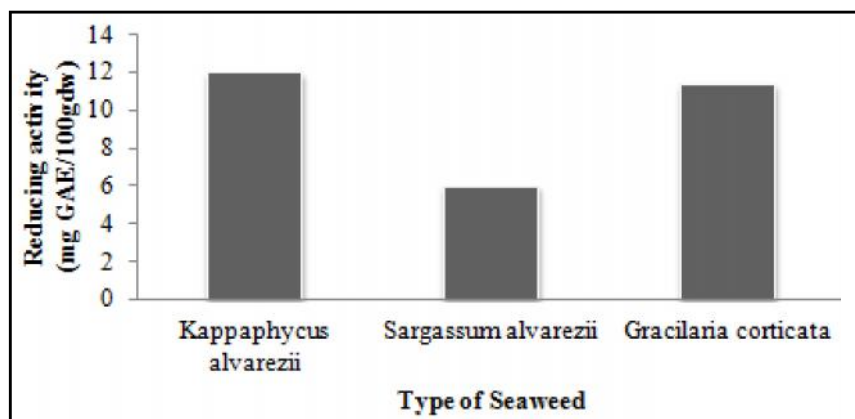


Fig.6 Ferric ion reducing activity – plot of reducing activity in percent vs three different types of seaweeds (Kappaphycus alvarezii, Sargassum wightii & Gracilaria corticata)

4. CONCLUSION

The difference in the correlations between TPC and antioxidant assays indicates the versatility of the group of phenolic compounds in the seaweeds and their different responses to different methods for the determination of the antioxidant activity, this difference is due to the fact that Folin-Ciocalteu method determined the sum of phenolic compounds, whereas individual phenolic compounds have very different responses on the Folin Ciocalteu reagent and antioxidant activity (B.Matthaus, 2005). Sun drying which is widely used for processing is found to increase the chelating activity and phenolic content but shade drying does not produce much effect on the phytochemicals. In general there is some reduction in the quantity of total phenolic content after carrageenan extraction which also reflects in its antioxidant and free radical scavenging activity but in the case of alginic acid extraction from *Sargassum wightii*, there is some increase in the total phenolic activity as well as antioxidant and free radical scavenging activity. It could be due to the fact the process involved in carrageenan production might remove part of the polyphenols and in the alginate process, they might get concentrated or the active molecules involved could be contributed by substances other than polyphenols as we can see that in fact there is some reduction in polyphenols after alginate extraction. Retention of activity to a greater extent gives a hope of using the waste from seaweed industry for obtaining value added compounds from seaweeds.

REFERENCES

- [1] Y. Athukorala, K.W. Lee, S. Choonbok, B.A. Chang, S.S. Tai, "Potential Antioxidant Activity of Marine Red Algae", (*Grateloupia filicina*), *Journal of Food Lipid*, Vol.10, 2003, pp.251-265.
- [2] J. Anggadiredja, R. Andyani and M. Hayati, "Antioxidant Activity of *Sargassum Polycystum* (Phaeophyta) and *Laurencia Obtusa* (Rhodophyta) from Seribu islands", *Journal of Applied Phycology*, Vol.9, 1997, pp.477-479.
- [3] H.C.Grice, "Safety Evaluation of Butylated Hydroxytoluene (BHT) in the Liver, Lung and Gastrointestinal Tract", *Food and Chemical Toxicology*, Vol.24, 1986,pp.1127-1130.
- [4] B. Halliwell, "Antioxidants in Human Health and Disease", *Annual.Review of Nutrition*, Vol. 6, 1996, pp.33-50.
- [5] N.S.Hettiarachchy,K.C.Glenn, R.Gnanasambandam and M.G. Johnson, "Natural Antioxidant Extract from Fenugreek (*Trigonella Foenumgraecum*) for Ground Beef Patties", *Journal Food Science*, Vol.61, 1996, pp.516-519.
- [6] HowYee Lai and YauYan Lim, "Evaluation of Antioxidant Activities of the Methanolic Extracts of Selected Ferns in Malaysia," *International Journal of Environmental Science and Development*, Vol. 2, No. 6, December 2011.
- [7] M. Ibrahim, K. Sopian and W.R.W. Daud, "Study of the Drying Kinetics of Lemon Grass", *American Journal Of Applied Sciences*, Vol.6, No.6, 2009, pp.1070-1075.
- [8] Je JY, *et al.*, "Antioxidant Activity of Enzymatic Extracts from the Brown Seaweed *Undaria Pinnatifida* by Electron Spin Resonance Spectroscopy", *LWT-Food Sci Technology*, Vol.42, 2009, pp.874-878.
- [9] T. Juntachote and E. Berghofer, "Antioxidative, Properties and Stability of Ethanolic Extracts of Holy Basil and Galangal", *Food Chemistry*, Vol.92, Sept. 2005, pp. 193-202.
- [10] N. Kaliaperumal, S. Kalimuthu, J.R. Ramalingam, "Economically Important Seaweeds, CMFRI-Special Publication, Cochin", 1995, pp.40-62.
- [11] K.S. Kumar, K. Ganesan, P.V.S. Rao, "Antioxidant Potential of Solvent Extracts of *Kappaphycus alvarezii* (Doty) – An Edible Seaweed", *Food Chemistry*, Vol.107, March 2008, pp.289-295.
- [12] B.Matthaus, "Antioxidant Activity of Extracts Obtained From Residues of Different Oilseed", *Journal of Agricultural and Food Chemistry*, Vol.50, May 2002, pp.3444-3452.
- [13] K. Nisizawa, Kaiso, "Bountiful Harvest from the Sea's Sustenance for Health and Well Being by Preventing Common Life Style Diseases", *Japan Seaweed Association, Japan*, 2002, pp. 59-6.
- [14] K. Nishigawa, "Fr.xtract Method of Alginic Acid", In, *Research nethod of algae*, edited by K. Nishigawa and M. Chthara, 1985, pp. 624-626.
- [15] M. Ohno, D.B. LARGo and T.IKuMo'ro, "Growth rate, Carrageenan Yield and Gel Properties of Cultured Kappa Carrageenan Producing Red Alga *KaPPmphyeus Alvarezii* CDoty) Doty in the Subtropical Waters of Shikoku, Japan, *Journal of Applied Psychology*", Vol.6, No.1, 1994, pp.1-5.
- [16] N. Singh, P.S. Rajini, "Free Scavenging Activity of an Aqueous Extract of Potato Peel", *Food Chemistry*, Vol.85, May 2004, pp. 611-616.

- [17] N. Sugihara, T. Arakawa, M. Ohnishi and K. Furuno, "Anti And Pro-Oxidative Effects of Flavonoids on Metal Induced Lipid Hydroperoxide- Dependent Lipid Peroxidation In Cultured Hepatocytes Located With /-Linolenic Acid", *Free Radical Biology and Medicine*, Vol.27, 1999, pp.1313-1323.
- [18] S.Umayaparvathi, M. Arumuga, T. Balasubramanian and S. Meenakshi, "In Vitro Antioxidant Properties and FTIR Analysis of Two Seaweeds of Gulf of Mannar", *Asian Pac J Trop Biomed.* 2012;1 (Suppl 1):S66-S70.
- [19] H.P. Wichi, "Enhanced Tumor Development by Butylated Hydroxyanisole (BHA) from The Prospective of Effect on Forestomach and Oesophageal Aquamous Epithelium", *Food and Chemical Toxicology*, Vol.26, 1988, pp.717-723.
- [20] X. Yan, T. Nagata and X. Fan, "Antioxidative Activities in Some Common Seaweeds", *Plant Foods for Human Nutrition*, Vol.52, 1998, pp.253-262.

Optimization, Standardization of Extraction and Characterization of Lutein (Xanthophyll) Extracted from Halotolerant Microalgae *Chlorella Salina*

S. Gayathri¹, S.R. Radhika Rajasree², L. Aranganathan¹ and T.Y. Suman¹

¹Research Scholars, ²Scientist & Head, Centre for Ocean Research,
Sathyabama University - 600 119, Chennai, Tamil Nadu
E:mail:radhiin@gmail.com

Abstract

Carotenoid extraction from algae is currently under intensive research due to the increased demand for naturally occurring compounds, which are especially rich in biologically active isomers. This study aimed to improve the commercial viability of microalgae-based Lutein production using an isolated microalga Chlorella, as it is a promising alternative source of Lutein, and can be cultivated heterotrophically with high efficiency. In this study, a whole process of Lutein production by heterotrophic Chlorella salina, including cultivation, reference extraction and determination of Lutein, was provided. The effects of solvents and pretreatments on Lutein content were examined. An optimized protocol for the extraction of microalgal Lutein has been developed. The extracted Lutein was spectroscopically characterized using UV-Vis and Fluorescence spectroscopy and chromatographically using HPLC. The effects of pretreatment conditions were examined in terms of yield and activity of the extracts. Hexane was shown to be the best solvent in the extraction of microalgal Lutein. Thus, the extraction yield achieved with this process was higher than 30% of dry weight. The HPLC result coincides apparently with the HPLC chromatogram of the previous studies of Lutein. EEM analysis revealed that the fluorescence intensity peak appeared at an Ex/Em of 450/518nm. Thus, the protocol developed in this study allows efficient extraction of Lutein from C. salina and could be exploited commercially for large scale production.

Keywords: *C.salina, Fluorescence Spectroscopy, HPLC, Lutein, Microalgae.*

1. INTRODUCTION

Carotenoids are colored lipid-soluble compounds that can be found in higher plants and algae, as well as in non-photosynthetic organisms like animals (although they are not able to synthesize carotenoids), fungi, and bacteria. Carotenoids are responsible for the red, orange and, yellow colors of plant leaves, fruits, and flowers, as well as for the color of feathers, crustacean shells, fish flesh and skin, etc. (Gudin 2003; Johnson and Schroeder 1995; Negro and Garrido-Fernandez 2000). In algae and higher plants, carotenoids play multiple and essential roles in photosynthesis. They contribute to light harvesting, maintain structure and function of photosynthetic complexes, quench chlorophyll triplet states, scavenge reactive oxygen species, and dissipate excess energy (Demming-Adams and Adams 2002). The pigmentation properties of carotenoids have granted to some of them extensive application in the food and feed industry (Borowitzka and Borowitzka 1988; Todd Lorenz and Cysewski 2000). The requirement in aquaculture and animal farming for these compounds also rests on their additional positive effects on adequate growth and reproduction of commercially valuable species.

Lutein is among the most important carotenoids in foods and human serum and, together with zeaxanthin, is the essential component of the pigment present in the macula lutea (or yellow spot) in the eye retina and in the eye lens (Alves-Rodrigues and Shao 2004; Whitehead et al. 2006). Lutein is used as food dyes and especially as feed additives in aquaculture and poultry farming (Todd Lorenz and Cysewski 2000). During the last few years, additional applications for lutein have received considerable interest, especially those related to human health. Mainly on the basis of epidemiological studies, lutein is currently considered as effective agent for the prevention of a variety of human diseases. Evidence supporting a protective role of lutein in delaying chronic disease is accumulating (Mares-Perlman et al. 2002; Alves- Rodrigues and Shao 2004; Whitehead et al. 2006).

Naturally occurring Lutein is produced mainly in higher plants and algae (12). Compared with higher plants, algae have an advantage since they can be cultivated in bioreactors and thus are a continuous and reliable source of the product (13). The main microalgal carotenoids are astaxanthin, β -carotene and lutein. The

carotenoid lutein can be produced by several micro-algae (Table 1) such as *Chlorella sp.* (Del Campo et al., 2004; Wei et al., 2008), *Muriellopsis sp.* (Del Campo et al., 2000), *Scenedesmus sp.* (Sanchez et al., 2008) and *Chlamydomonas sp.* (Garbayo et al., 2008). The lutein content, unlike astaxanthin and β -carotene, is fairly equivalent in the majority of the abovementioned microalgal-species. However, only *Muriellopsis sp.* and *Scenedesmus almeriensis* have been studied and tested in scaled-up systems under mass production conditions (Fernandez-Sevilla et al., 2010). Lutein is a primary Carotenoid and its role is to act in maintaining the structure and functioning of photosystems. Lutein is an important carotenoid for pigmentation in aquaculture and poultry farming, as well as for the coloration of drugs and cosmetics.

Chlorella sp. is a chlorophycean microalga, which shows high lutein content (up to 25 mg l⁻¹ culture) under specific culture conditions, as well as high growth rate and standing cell density. In this study, a whole process of Lutein production by heterotrophic *Chlorella salina*, including cultivation, reference extraction and determination of Lutein, was provided. Several important parameters for extraction were optimized and satisfactory extraction efficiency was achieved, which can be useful for exploitation in a large scale. The objective of this research was to optimize an analytical procedure for lutein extraction from microalgae. The focus was on solvent mixture, pretreatment, and cell disruption method. Not only the amount of extracted lutein was considered, but also the potential effect of the extraction procedure on degradation of the compound.

2. MATERIALS AND METHODS

2.1. Micro Algae Culturing and Harvesting

Chlorella salina was obtained from CIBA, Chennai, Tamilnadu, India, and cultivated heterotrophically in Microalgal laboratory at Sathyabama University using sterile f/2 medium (Guillard and Ryther, 1962) under 5000 lux illuminated with white fluorescent bulb for 12 : 12hr light and dark condition for 15 days. Growth was monitored by measuring the optical density at 550nm. When the culture reached stationary phase, the biomass was harvested by centrifugation at 8500rpm for 10min to get thick algal paste. Then the microalgal paste was rinsed with distilled water to remove residual salts and then dried in hot air oven at 60°C for 8 h.

2.2. Effect of Cell Disruption Methods

Various pretreatment methods were adopted to break microalgal cells for effective extraction of Lutein. The overall procedures of Lutein extraction from microalgae composed mainly of cell disruption, saponification, and solvent extraction steps have been reported in the literature. In this study, different methods like acid lysis, ultrasonication and thermal treatment using autoclave were used to break microalgal cells. In brief, 2-3g of biomass was used; processing time differs from 1hr-3hr to observe the efficiency of the cell disrupting methods. The autoclave was operated at 121°C, 15lbs pressure for 10min, 20min, and 30min; the ultrasonicator was operated at 70 aptitudes for 5min, 10min, and 15 min. A control experiment was carried out under optimum condition without any pretreatment. To validate the disruption success the absorption of centrifuged samples (3 min at 13400 rpm; dilution 1/10) were photometrically measured.

2.3 Effect of Solvent on Extraction

The investigation on the best solvent for efficient extraction of Lutein from microalgal cells was carried out. Freeze-dried microalgae were extracted using different organic solvents and their lutein contents were investigated using UV-Vis spectroscopy (Shimadzu Co., Ltd., Japan) at 450nm. The solvents often used in the literature such as Dichloromethane, Acetone, Methanol, hexane and Diethyl ether were tested. Lutein content extracted using different solvents were compared. The mixture was centrifuged at 1000 rpm for 2–3 min. The supernatant (organic phase) was then collected. Repeated extraction was carried out to recover lutein from the microalgal suspension.

Concentration of Lutein ($\mu\text{g/g}$ of sample) =

$$A \times V \text{ (ml)} \times \text{dilution factor}$$

$$\epsilon \times W \text{ (g)}$$

Where, A = Absorbance at 446 nm, V = Volume of extract in ml, ϵ = Absorption coefficient (2589), W = Dry weight of sample.

2.4. Extraction of Lutein

Cell slurries from acid treatment, ultrasonication, and autoclaving were subjected to Lutein extraction by Shi and Chen (12). In brief, 2ml of thoroughly mixed culture fluid was centrifuged at 3000 rpm for 10min, and the supernatant, and the supernatant was discarded. 1 ml of

a solution containing 2.5% ascorbic acid and 10 M KOH was added to the conical tube containing the cell pellets, and the mixture was incubated at 60°C for 10 min before cooled down to room temperature. Nineteen ml of methanol was subsequently added to mixture for the extraction of Lutein. The mixture was then centrifuged at 3000 rpm for 15 min at 4°C, and the supernatant was collected and lyophilized to obtain powdered lutein.

2.6 Chromatography Analysis and Purification of Lutein

The extracted carotenoids were determined by HPLC, using a C18 column (5µm, 150mmx46). The mobile phase consisted of methanol/acetonitrile (90:10 V/V) and flow rate was at 1.0 mL/min. Peaks were monitored at 450 nm, and absorption spectra of each peak were scanned from 190 to 800 nm using dual λ absorbance detector.

3. RESULTS AND DISCUSSION

3.1 Effect of Solvent

Another important consideration of extraction efficiency is the type of solvent used [31]. In literature, various solvents were used to evaluate the extraction efficiency for pigments, whereas no universal protocol was developed for this purpose since solvent selection seems to be greatly dependent on the type of microalgae species and target pigments [28, 30]. Therefore, it is still necessary to identify the best solvent for lutein recovery from *C. salina*. In this study, the solvents used were hexane, diethyl ether, acetone, dichloromethane, ethanol and methanol, with 4–6 extraction runs until the supernatant phase were colorless. Higher recovery of lutein was achieved with the use of Hexane (with lutein content 2.51 mg/g; nearly 100% recovery), Methanol (lutein content 2.00 mg/g or 90% recovery) and Acetone (lutein content 1.83 mg/g or 70% recovery).

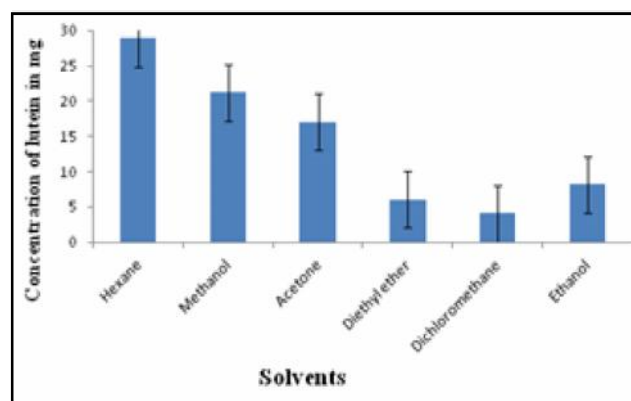


Fig.1 Effect of different solvents on lutein recovery

3.2 Effect of Cell Disruption Methods

The cell wall is a complex entity with unique characteristics related to the growth phase of a given microalga species: it differs in thickness, rigidity and its constituents. Production of algal lutein included cell cultivation, biomass harvesting, cell wall disruption, and subsequent extraction and purification steps. Owing to the presence of thick cell wall of the microalgae, the extent of cell wall breaking greatly influences the efficiency of the pigment extraction (Ming-Chang Chan et al., 2013). Several methods such as acid hydrolysis, ultrasonic treatment and thermal treatment were used in the work to disrupt the cell walls for recover intracellular lutein. The amount of Lutein extracted from *C. salina* was used as an indication of the efficiency of the cell-disruption method used. No significant differences could be detected between the different cell-disruption methods, which indicate that the cell wall is penetrated or dissolved by the solvents used, so it does not need to be destroyed for optimum extraction. The spectrophotometric analysis of the crude extract were analyzed from 300-700nm. Despite using a large volume of solvent for extraction complete decolourization of the algae were not observed. Chlorophyll was not completely removed from the sample. Spectrophotometer analysis showed a major peak at 444nm and a shoulder peak at 648nm corresponding to that of chlorophyll. Spectrum shows shift in the wavelength of Lutein after acidic treatment. The acid treatment resulted in oxidative decomposition or cis/trans transformation as shown by shift in absorption spectra. Similar observations were made with various concentrations of HCl on *Rhodotorula yeasts* (Peterson et al., 1954) and in spinach by Kachick et al., (1991).

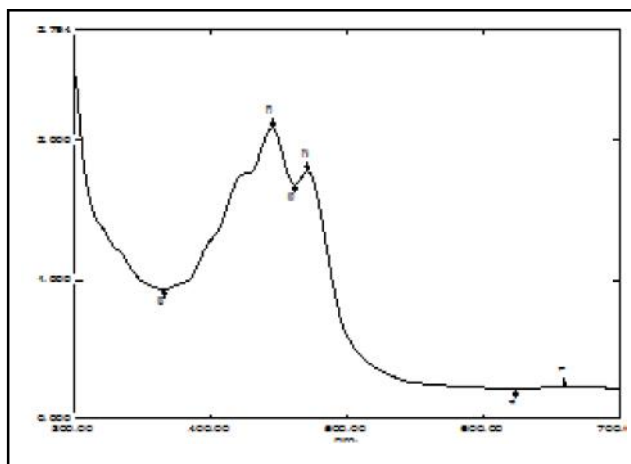


Fig.2 Spectrum of crude Lutein extracted without treatment

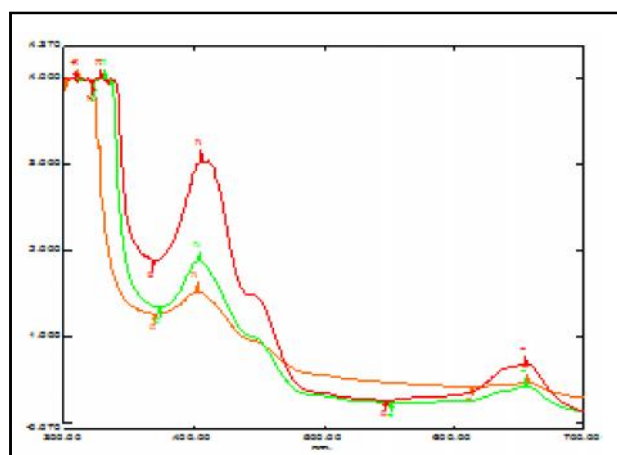


Fig.3 Spectrum of HCl assisted extraction of Lutein at various reaction periods (1hr, 2hr & 3hr)

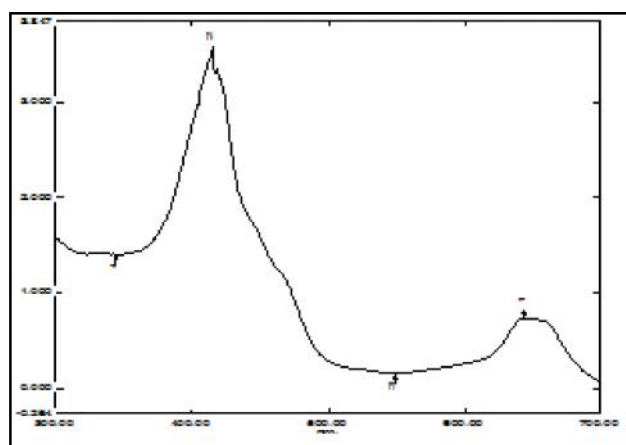


Fig. 4 Spectrum of ultrasound assisted extraction of Lutein at various reaction periods (10min & 15min)

3.3 Chromatographic analysis and Fluorescence Emission

The carotenoid profile was quantified by HPLC after a reference extraction procedure. The HPLC analysis

results indicate that the compound in the solution was detected at retention time of about 4.35 mins. The typical HPLC spectra of lutein extracted from *C. salina* was shown in Fig.5. Results are identified with the help of standards and of comparison with that of literature results (Hejazi et al., 2002). Fluorescence properties were investigated using fluorescence spectrometer (Shimadzu, RF-5301). EEM Fluorescence Spectrometer was used to identify the optimum excitation and emission of the species. To Date, reports on the observation of micro algal compounds using EEM fluorescence Spectrometer are quite limited. Upon excitation with 450 nm light, the emission spectra of Lutein show two peaks at 450 nm.

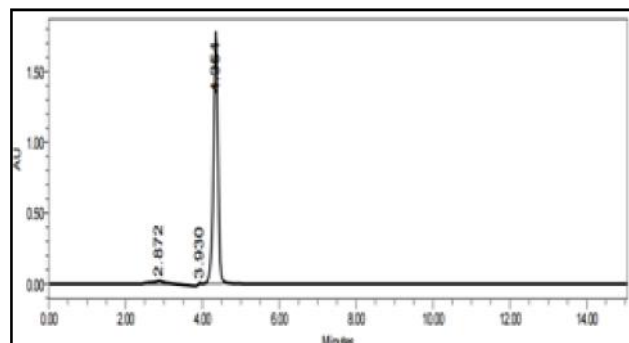


Fig.5 HPLC Chromatogram of purified Lutein (after saponification) at 450nm

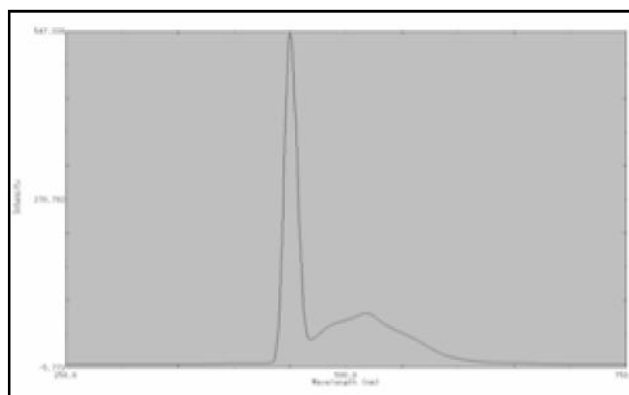


Fig.6 Excitation Emission maxima of Lutein at 450nm

4. CONCLUSION

An optimized analytical procedure was developed for lutein extraction from microalgae. The amount lutein extracted from microalgal biomass is highly dependent on the solvent used. Hexane gave the highest lutein content and is thus preferred most effective solvent. When performing this dried biomass seems to be good this makes weighing easier. No significant differences were observed between pigment amounts (from each pretreatment) analyzed by UV/visible light spectrometry. The differences in pigment composition between studies give reliable evidence that carotenoids respond

distinctively to growth conditions. Although it is widely known that these substances are quite sensitive to environmental changes, the methodological differences in the studies cited may actually be the principal reason behind the variable pigment composition reported therein.

REFERENCE

- [1] A. Alves-Rodrigues and A. Shao, "The Science Behind Lutein", *Toxicol Lett*, 2004, Vol.150, No.1, pp.57-83.
- [2] MA. Borowitzka, LJ. Borowitzka, "Micro-Algal Biotechnology", Cambridge University Press, Cambridge, UK, 1988, pp.27-58
- [3] JA. Del Campo, H. Rodríguez, J. Moreno, MA. Vargas, J. Rivas and MG. Guerrero, "Accumulation of Astaxanthin and Lutein in *Chlorella Zofingiensis* (Chlorophyta)", *Appl Microbiol Biotechnology*, Vol.64, 2004, pp.848-854.
- [4] JA. Del Campo, J. Moreno, H. Rodríguez, MA. Vargas, J. Rivas and MG. Guerrero, "Carotenoid Content of Chlorophycean Microalgae", Factors Determining Lutein Accumulation in *Muriellopsis* sp. (Chlorophyta). *J Biotechnol*, Vol.76, 2000, pp.51-59.
- [5] Demming-Adams B, Adams WW III 2002. Antioxidants in Photosynthesis and Human Nutrition", *Science*, 2153, pp.298-2149.
- [6] Fernandez-Sevilla JM, Fernandez FGA, Grima EM 2010. Biotechnological production of lutein and its applications. *Appl. Microbiol Biotechnol*; 86:27-40.
- [7] I. Garbayo, M. Cuaresma, C. Vílchez, J.M. Vega, "Effect of abiotic stress on the production of lutein and b-carotene by *Chlamydomonas acidophila*", *Process Biochem.*, 2008, Vol.43, pp.1158-1161.
- [8] Gudin C 2003. Une histoire naturelle de la séduction. Éditions du Seuil, Paris, France.
- [9] M.A. Hejazi, C. de Lamarliere., J.M.S.Rocha, M. Vermue, J. Tramper and R.H. Wijffels, "Selective Extraction of Carotenoids from the Microalgae *Dunaliella Salina* with Retention to Viability", *Biotechnol. Bioeng.*, Vol.79, 2002, pp.29-36.
- [10] EA. Johnson and WA. Schroeder, "Microbial Carotenoids", *Adv Biochem Eng Biotechnol*, Vol.53, 1995, pp.119-178.
- [11] F. Khachik, GR. Beecher, MB. Goli and WR. Lusby "Separation, Identification & Quantification of Carotenoids in Fruits, Vegetables & Human Plasma by High Performance Liquid Chromatography", *Pure & Appl. Chem*, Vol.63, No.1, 1991, pp.71-80.
- [12] JA. Mares-Perlman, AE. Millen, TL. Ficek and SE. Hankinson, "The Body of Evidence to Support a Protective Role for Lutein and Zeaxanthin in Delaying Chronic Disease", *Overview. J Nutr*, Vol.132, 2002, pp.5185-5245.
- [13] JJ. Negro, J. Garrido-Fernández, Astaxanthin is the Major Carotenoid in Tissues of White Storks (*Ciconia ciconia*) Feeding on Introduced Crayfish (*Procambarus clarkii*), *Comp Biochem Physiol Part B Biochem Mol Biol*, Vol.126, pp.347-352.
- [14] WJ. Peterson, TA. Bell, JL. EtcHELLS and JR. Smart, "A Procedure for Demonstrating the Presence of Carotenoid Pigments in Yeasts", *J. Bacteriol.*, Vol.67, No.6, 1954, pp.708-713
- [15] J.F. Sanchez, J.M. Fernandez, F.G. Acien, A. Rueda, J. Perez-Parra and E. Molina, "Influence of Culture Conditions on the Productivity and Lutein Content of the New Strain *Scenedesmus Almeriensis*", *Proc. Biochem.* Vol.43, 2008, pp.398-405.
- [16] R. Todd Lorenz, GR. Cyswski, "Commercial Potential for *Haematococcus* Microalgae as a Natural Source of Astaxanthin", *Trends Biotechnol* Vol.18, 2000, pp.160-167.
- [17] AJ Whitehead, JA. Mares and RP. Danis, "Macular Pigment: A Review of Current Knowledge", *Arch Ophthalmol*, Vol.124, 2006, pp.1038-1045.

Biopharmaceuticals and Nutraceuticals from Marine Species and Marine Waste

T. Charles John Bhaskar

Scientist & Managing Director, Geomarine Biotechnologies (P) Ltd

Abstract

McKinsky puts the Global turnover of \$163 Billion in 2014 for Biopharmaceuticals. Annual growth of about 8% is double compared to the conventional pharma growth. The manufacturing facilities right now require \$200 to 500 million. Nutraceuticals form another important class of molecules gaining popularity due to less stringent regulations by FDA and increasing awareness among the common public on Antioxidants, probiotics, Free Radical Scavengers, etc., The paper will deal with the scenario in different countries with special reference to the Indian scenario. The diversity of such molecules spread across several marine plants and animals and their biopharmacological properties, such as antiviral, antineoplastic, novel anticoagulants, antiinflammatory, antibacterial and the nutraceutical molecules which have much potential from the sea will be dealt with. A review of opportunities for exploitation of such biopharmaceuticals and nutraceuticals from even marine waste would be made opening up to new avenues for research and exploitation considering the vast coastal areas of India. How an Institutional – Industrial Collaboration could open up a new win-win for both and how it could help the country at large especially in the days of Made-in India campaigns would be discussed.

1. INTRODUCTION

McKinsky report states the Global turnover to be of \$163 Billion in 2014 for Biopharmaceuticals. Biopharma's current annual growth is about 8% which is more than double as compared to the conventional pharma companies' growth and is expected to grow with a CAGR (Compound Annual Growth Rate) of 9.6% during the period 2015 – 2020.

The Biopharma industry is much different from the conventional pharma industries. The differences between

a conventional pharmaceutical compounds and biopharma compounds will make one understand why this industry is unique and important. For example if you take the molecule aspirin, it consists of just about 21 atoms with a molecular weight of 180.187 Daltons whereas a monoclonal antibody has a molecular weight of 150,000 Daltons.

Table 1 brings out the essential differences between the two products in terms of the process, cost and ease production.

Table 1 Process and Cost of Production

	Pharma Products	Bio pharma Products
Process of Production	Relatively Simple	More Complicated
Process Timings	Relatively Short	Longer Durations
Cost of Production	\$30 to 100 million	\$200 to 500 million
Yields	Good	Low Yields
Skill Requirement	Relatively Less	High Skills Required

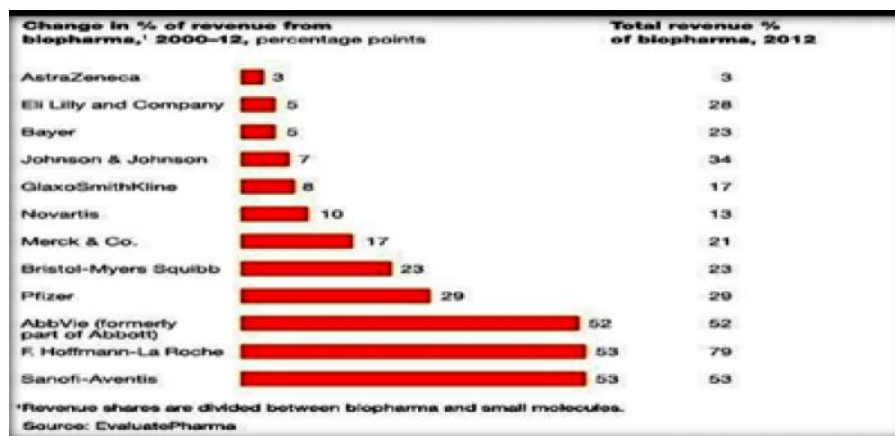
It could be seen from the Graph 1, how the major biopharma giants around the globe are shifting their production towards more of biopharmaceuticals. Indian Biopharma revenue is about \$3 Billion in 2014 which is 64 % of the all Biotech industries.

2. MARINE BIOPHARMACEUTICALS AND ITS EXPECTED GROWTH

About 20,000 Marine Bioactive compounds have been isolated in the last 50 years (Mayer A.M.S. and Glaser

K.B. 2013). The global market for marine-derived pharmaceuticals was valued at nearly \$4.8 billion in 2011, \$5.3 billion in 2012, and is projected to be worth nearly \$8.6 billion by 2016, a compound annual growth rate (CAGR) of 12.5% between 2011 and 2016 (Ref.3).

According to the author as quoted by Biospectrum, Marine Biotechnology should account for around 20 to 25 percent share in the total biotech industry. Marine biotechnology will play a major role in various sectors such as biopharma, bioagri, bioindustries and bioenergy.



Graph.1 Change in revenue of the major biopharma companies

This will include both biopharmaceuticals and nutraceuticals.

Some of the biopharmaceutical molecules, their origin, species from which they are obtained and their broad classification and their activity are given in the Table 2. The biodiversity of their occurrence is interesting as they occur in cyanobacteria to algae to lower animals such as sponges and even higher animals such as shark. Their complexity could be seen from the example of Pectinotoxin from Dinoflagellate, *Dinophysis caudata* (Figure 1) and Didedemins from Tunicate, *Trididemnum solidum* (Figure 2).

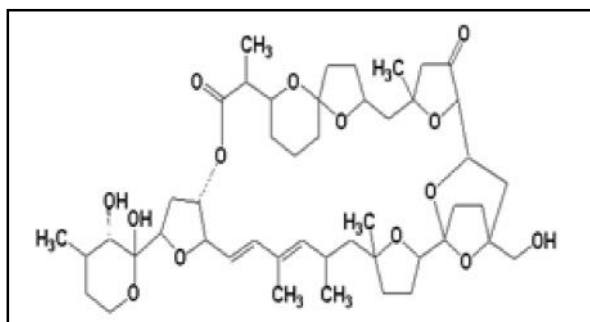


Fig.1 Pectinotoxin from Dinoflagellate, *Dinophysis caudata*

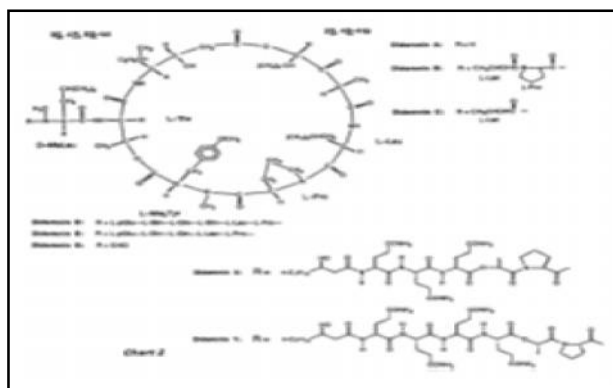


Fig.2 Didedemins from Tunicate, *Trididemnum solidum*

3. NUTRACEUTICALS FROM MARINE ORGANISMS

Dr Stephen DeFelice coined the term “Nutraceutical” from “Nutrition” and “Pharmaceutical” in 1989. According to Manisha Pandey et al (2010), nutraceuticals can be classified as:

1. Antioxidants
2. Prebiotics
3. Probiotics
4. Omega 3 fatty acids
5. Dietary fibers

According to the present author it can include a wide range of substances and microbes and can be classified as:

- 1) Prebiotics
- 2) Probiotics
- 3) Additives that are involved in the metabolism such as vitamins and minerals,
- 4) Essential Fatty acids including the omega 3 fatty acids
- 5) Antioxidants & Free radical scavengers
- 6) Dietary fibers
- 7) Immunostimulants
- 8) Molecules preventing diseases or modifying diseases like arthritis, diabetes but are not synthetic.
- 9) Antimicrobials of plant origin that are not antibiotics
- 10) Detoxifiers and others

According to a recent study published by Transparency Market Research, the global nutraceuticals market stood at US\$182.60 bn as of 2015, and will rise to US\$278.96 bn by 2021, exhibiting a CAGR of 7.3% from 2015 through 2021. Indian nutraceutical industry according to Assochem in partnership with RNCOS

Table 2 Some Biopharmaceutical Substances from Sea

Species / Classification	Organism	Compound	Action
Cyanobacteria	Lyngbia majuscula	Curacin A	Antitumour
Porifera	Cryptothesia crypta	Spongothymidine, Spongouidine,	Antiviral, Antitumour
Phytoplankton	Dinophysis acuta	DTX2	Anti inflammatory
Tunicate	Eudistoma olivaceum,	Eudistomins	Antiviral, antibacterial, anti tumour
Marine Algae	Ulva	Carrageenans	Anticoagulant, Antiviral
Actinomycete	Salinospora	Salinosporamide A	Antimicrobial, anticancerous
Bryozoans	Bucula neritina	Bryostatin I	Anti neoplastic, anti viral, anti inflammatory
Echinodermata	Holothuroidea	Holothurin	Anti microbial, anti tumour, nerve blocking, healing agent.

Business Consultancy Services is \$2.8 Billion and is bound to grow to 6\$.1 Billion in 2020 (Graph.2).

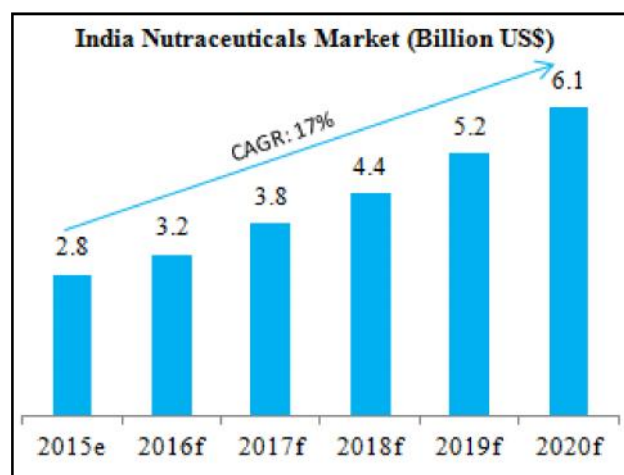


Fig.2 Indian nutraceuticals market trend

Nutraceuticals from marine sources is bound to increase with time. Some of the Food and nutraceuticals obtained from the marine sources are listed below:

1. Fish breads, fish oils, shark fin soup, etc
2. Seaweeds

3. Micro algae
4. Fodders
5. Chitosan
6. Astaxanthine
7. Bio Available Calcium from cuttlebone

Seaweeds are used in the manufacture of alginic acid, agar, floridean starch, carrageenan, ulvans and xylans to name a few. Many types of seaweed have shown high antioxidant and free radical scavenger activities in our laboratories studies and they provide good opportunity for production of nutraceuticals for use in human and veterinary products.

4. MARINE WASTES AS A SOURCE OF NUTRACEUTICALS

According to CMFRI report 3.59 million tons was the fish landing in India during 2014. About 80 % of it is from finfish. About 30% of this is discarded as waste. Shrimp production according to Times of India during 2014-15 was 4,34,558 MT. From fish waste protein hydrolysate or collagen from fish scale can be obtained.

The discards from the processing plants amount to 20 million tonnes which is equivalent to 25% of the world's total production from marine capture fisheries [4]. These wastes can be used to produce fish protein concentrate, fish oils and enzymes (such as pepsin and chymotrypsin) as well as other value added products. The fish oil is used for products such as margarine, omega-3 fatty acids (Ghaly AE, 2013).

Another waste is fish scale which could be used for production of pure and good quality collagen that be used by pharma industries. Many of the fish industries which export finished products produce huge wastes which mostly go as fertilizers or fodders. For example after the production of alginic acid or agar or carageenan the waste goes for fertilizer use or are burnt. Studies by our company indicate that, there is an appreciable amount of antioxidant and nutraceutical activity still left in these wastes. Many pigments could be still extracted from these wastes.

Shrimp shell and head forms about 40% the shrimp. From shrimp shell one can manufacture Chitosan which is implicated in cholesterol reducing activity as well as useful in age related problems in humans (Garry Kerch. 2015) Chitosan is a linear polysaccharide consisting of (1-4)-linked 2-amino-2-deoxy-b-D-glucopyranose (Roberts GAF.,1992). Another derivative from shrimp shell N-Acetyl Glucosamine is used in osteoarthritis (Garry Kerch 2015). The process of manufacturing chitin for example is simple involving demineralization by an acid followed by deproteinization by an alkali and then decolorization with hydrogen peroxide. If this product is further deacylated chitosan is obtained.

5. INDUSTRY-INSTITUTION COLLABORATION FOR RESEARCH AND COMMERCIALIZATION

Industry-Institution collaboration could take place at various levels. In simple case students' project could be provided by the industries which are industry specific. Though a new product may not emerge in 3 to 6 months, many steps leading to better product or help industry in standardising processes or optimize the processes in their industries. The collaboration could also work where in first 4 months of the project duration could be spent in industry and the next 2 months along with the Technology Business Incubators in the colleges / Universities leading to entrepreneurship spirit among the students and commercialization of a few products.

Industry-Academia -Research/Government Interface (IARGI) from CSIR, ICAR and many Industrial Associations are of immense importance in this direction. Though listing out the entire array of opportunities and Government initiatives in the Industry –Academia is possible here, certain schemes such as Industry Institute Partnership Cell (IIPC), Small Business Innovation Research Initiative(SBIRI),and Biotechnology Ignition Grant Scheme (BIG) are worth mentioning.

REFERENCES

- [1] Ralf Otto, Alberto Santagostino and Ulf Schrader “Rapid Growth in Biopharma: Challenges and Opportunities”, December 2014 McKinsey & Company.
- [2] A.M.S.Mayer and K.B.Glaser, “Marine Pharmacology and the Marine Pharmaceuticals Pipeline”, FASEB J. Vol. 27, 2013, pp.1167.7
- [3] [http://www.bccresearch.com/pressroom/phm/global-market-marine-derived-drugs-reach-nearly-\\$8.6-billion-2016](http://www.bccresearch.com/pressroom/phm/global-market-marine-derived-drugs-reach-nearly-$8.6-billion-2016).
- [4] <http://www.biospectrumindia.com/biospecindia/news/158167/marine-biotech-sector-shot-arm>
- [5] Manisha Pande, *et al.*, “Nutraceuticals: New Era of Medicine and Health”, Asian Journal of Pharmaceutical and Clinical Research. Vol.3, No.1, 2010, pp 11-15.
- [6] AE. Ghaly, VV. Ramakrishnan, MS. Brooks, SM. Budge and D. Dave, “Fish Processing Wastes as a Potential Source of Proteins, Amino Acids and Oils: A Critical Review”, J Microb. Biochem. Technology, Vol.5, 2013, pp. 107-129.
- [7] Roberts GAF, “Preparation of Chitin and Chitosan”, The Macmillan UK: London Press, 1992.
- [8] Garry Kerch, “The Potential of Chitosan and its Derivatives in Prevention and Treatment of Age-Related Diseases”, Mar. Drugs, Vol.13, 2015, pp.2158-2182.
- [8] AR. Shikhman, *et al.*, “Differential Metabolic Effects of Glucosamine and N-acetylglucosamine in Human Articular Chondrocytes”, Osteoarthritis and Cartilage, Vol.17, No.8, August 2009, pp.1022-1028.

Analysis and Comparison of Mechanical Properties of Alloy Steel gr.22 Material Welded by GMAW Process with Conventional SMAW Process

K. Karthikeyan¹, V. Anandakrishnan² and R. Alagesan³

^{1&3}Bharat Heavy Electricals Ltd, Tiruchirapalli - 620 014, Tamil Nadu

²Department of Production Engineering, NIT Tiruchirapalli - 620 014, Tamil Nadu

Abstract

Pressure part pipe headers in thermal power plants are being mostly manufactured using high strength alloy steel materials. Conventional method of welding the pipe header joints has been carried out by using Gas Tungsten Arc Welding (GTAW) root pass followed subsequent passes by Shielded Metal Arc Welding (SMAW) processes. In order to develop an alternate welding process with improved the weld quality, a full Gas Metal Arc Welding (GMAW) technology (Modified short arc process as Surface Tension Transfer (STT) root pass followed subsequent passes by pulsed current GMAW process) for header weld joints have been established. This paper deals with the analysis of mechanical properties of the alloy steel weld joints welded by modified GMAW process and comparison with respect to conventional Shielded Metal Arc weld joint properties of alloy steel grade 22 material.

Keywords: Alloy steel Gr.22 material, Mechanical testing, Pulsed GMAW Process, Surface Tension Transfer, SMAW Process.

1. INTRODUCTION

Alloy steel is steel containing specified quantities of elements (other than carbon and commonly accepted amounts of manganese, copper, silicon, sulphur and phosphorus) within the limits recognized for constructional alloy steels added to effect changes in mechanical or physical properties. As a guideline, alloying elements are added in lower percentages (less than 5%) to increase strength or harden ability, or in larger percentages (over 5%) to achieve special properties, such as corrosion resistance or extreme temperature stability. The pipe headers in thermal power plant boilers are predominantly of the alloy steel material based on the high pressure application used for the circulation of steam and water in the boiler and play a vital role in the fluid transfer required for the performance of the boiler. Mostly the headers are provided with a hand hole covered by dish end for maintenance purpose. Conventional welding of dish end to the hand hole is done using a GTAW process for root pass and SMAW process for filler pass which involves more time for the completion of one number of hand hole to the dish end butt joint. Hence to reduce this cycle time and improve the welding performance, an alternative method of welding using STT welding followed by Pulsed GMAW process is planned. Also, it is ensured that the quality of welding will be equivalent to the conventional welding process with reduced welding defects such as lack of fusion, incomplete penetration problem and etc.

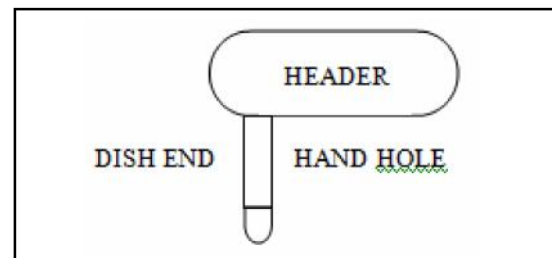


Fig.1 Typical hand hole pipe and dish end of the pipe headers

2. STT WELDING PROCESS

STT (Surface Tension Transfer) welding process is modern, high efficient and high quality welding process for thin wall materials joining and joining at root passes of thick materials. STT welding power source provide stable main welding parameters during welding process which enable welding by “short circuit arc”. The material transfer in electric arc is founded on surface tension force between weld pool and melted bead in electric arc. STT unit frequently and precisely controls welding current during welding. It sets an optimal welding parameters (which are stable) by significant changing of arc length and “stick out”. Principally, it is welding unit with possibility of welding parameters changing in milliseconds in order to obtain an optimal quality of welded joint. It is designed as a semiautomatic welding process for application where welding speed and “stick out” are variable. At STT

welding process it is possible to use different shielding gases and gases mixtures depending on application.

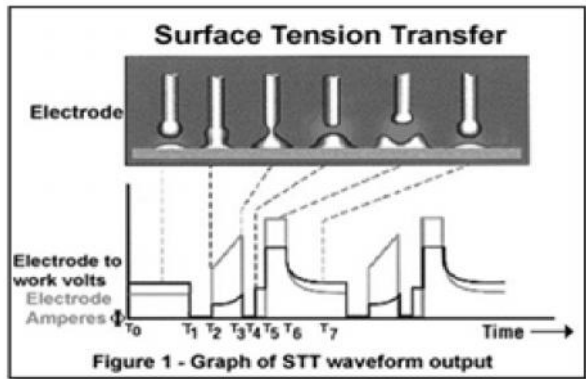


Fig. 2 Distribution of welding parameters in STT welding process

Conventional method welding of alloy steel pipes is either by manual or automatic TIG welding process (Tungsten Inert Gas) as a single bead or multi bead process. For joining higher diameter pipes combination of welding processes TIG + SMAW (Shielding Metal Arc Welding) or TIG + SMAW + SAW (Submerged Arc Welding) is usually used, depending on available equipment. Manual TIG welding process is used for root passes which is the most important and the most complex from the standpoint of weld ability (welding in non-accessible areas, denivelation in that joint area is the most evident, gap in weld joint root must be in rigid tolerance, preheating and gas shielding from root joint pipe side aggravate welding). STT welding process is process which will replace manual TIG welding process in described situation. STT welding process has some differences regarding to other fusion arc welding processes such as performing of welding process is in cycles, valid welding parameters set up on power source display assure stability of electric arc and the whole welding process as a repeatability of welding process and welding current is changing in milliseconds, depending of process arc voltage sensing.

3. DESIGN METHODOLOGY

The advantage of using full Gas Metal Arc Welding (GMAW) process is producing comparatively faster, long, clean, continuous weld of thick wall alloy steel pipe with respect to conventionally used Shielded Metal Arc Welding (SMAW) process has been established. However, the necessity of applying the conventional GMAW process in short and spray modes of metal transfer in welding of root and filler passes respectively has led to high spatter, burn through and large amount of

metal deposition. Control of the adverse influence of conventional GMAW on required weld joint quality has been successfully addressed by application of surface tension transfer (STT) for root pass followed by pulsed current GMAW (P-GMAW) process for filler passes. In order to increase the productivity with desired weld joint quality, the semi- automatic welding positioner is used. Prior to its application the suitability and effectiveness of the positioner with respect to speed control and GMAW torch head manipulation in groove was tested. After that, by using the positioner full GMAW technology for hand-hole pipe butt welding were established. The quality of weld joints has been checked and analyzed by X-ray radiography. Further, to qualify the weld joint conventional mechanical properties have been studied.

4. DESIGN OF EXPERIMENT

For selecting the optimum parameter for welding of hand hole pipe, Taguchi orthogonal L4 array has been selected with three factors and 2 levels. The three factors are namely, welding current, welding voltage and travel speed. From the output, properties like bead width, bead height and penetration was calculated. Based on the necessary penetration, bead width and bead height the parameters were selected. The optimum parameters for the welding were around Current 220 A, Voltage 38 V and Travel speed 28 mm/min.

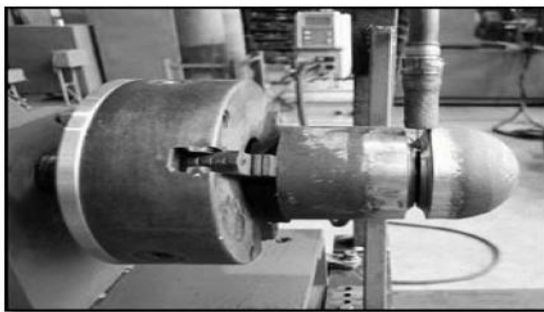
Table 1 Taguchi's L4 Orthogonal Array Method

Welding Current , A	Welding Voltage , V	Travel Speed , mm/min
200	36	24
200	38	26
220	36	26
220	38	28

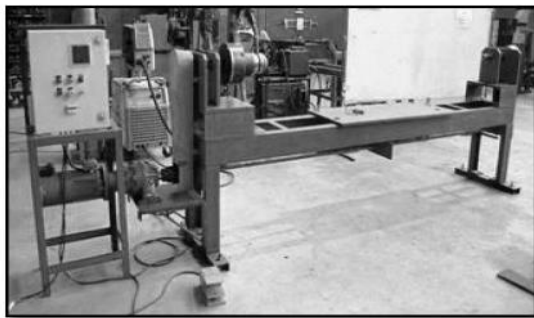
5. EXPERIMENTAL SETUP

A semi-automatic welding positioner along with torch head attachment is used for the welding process. The welding positioner consists of a three jaw chuck, electrical motor assembly, speed controller box with digital display and torch holding device. The positioner can operate with various welding speeds by controlling the knob fitted within speed controller box. Weld groove has been prepared as per conventional groove design for edge preparation. Prior to welding, the groove surface was checked visually followed by acetone cleaning to

ensure the clean groove wall. The welding was carried out by multi-pass gas metal arc welding process. During welding, the pipes were held horizontally with the help of three jaws clamping system in a rotating table and the welding was carried out in 1GR position. The root pass was carried out by wave form controlled GMAW, commonly referred as surface tension transfer (STT) process followed by pulsed current GMAW process. After each weld pass, appearance of the weld deposit has been visually checked. During welding all the parameters were recorded with the help of digital controlled meter fitted with the welding power source. The photographic view of the experimental setup is shown below.



(a)



(b)

Fig.3 (a) & (b) showing the photograph of welding positioner and welding process

6. MECHANICAL TESTING OF WELDING

After carrying out the welding, sectioning of the weld joints was made by power saw and the test specimens were prepared of various mechanical tests. The collection of differently oriented specimens for mechanical tests from different location of the weld in reference to the weld joint has been shown.

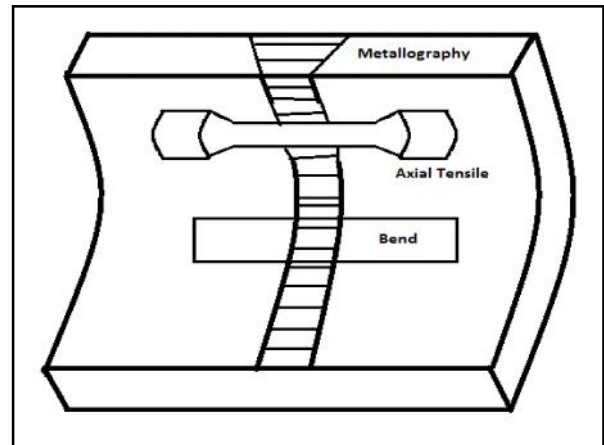


Fig.4 Schematic representation of test specimens collected for mechanical testing

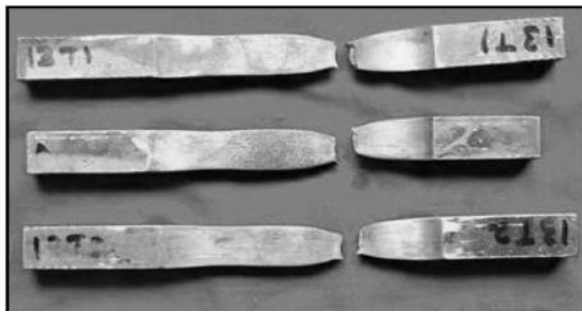
6.1 Studies on Tensile Test

As per AWS B4.0 standard, tensile testing of the axial weld joint having weld at its center has been carried out using flat tensile test specimens. Comparison of tensile strength of the weld joints (after PWHT) of the specimen welded by STT root pass followed by Pulsed GMAW process and specimen welded by conventional SMAW process have been tabulated below. The values depicts that weld joints of the modified GMAW process is better than the conventional method of welding.

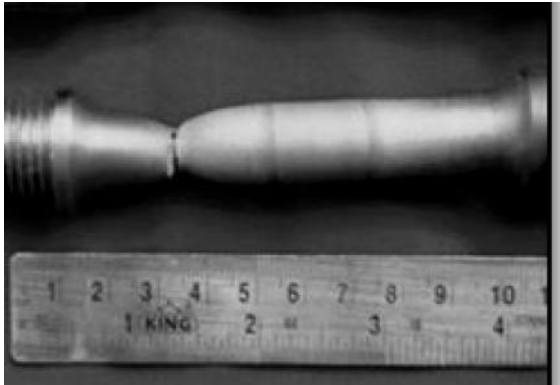
Table 2 Tensile Strength of Weld Joints

Sl. No	Tensile Strength in Mpa	
	Modified GMAW Process	Conventional SMAW Process
1	465	468
2	478	473
3	483	481

The axial tensile property of the weld joints weld by full GMAW process is done in Universal Testing Machine UTE-60. It is observed that, fracture occurred in base metal and not in the weld joints as shown below and it ensures that the weld joints meets the quality requirement.



(a)

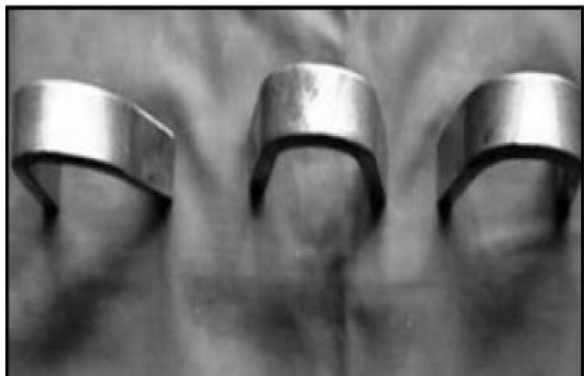


(b)

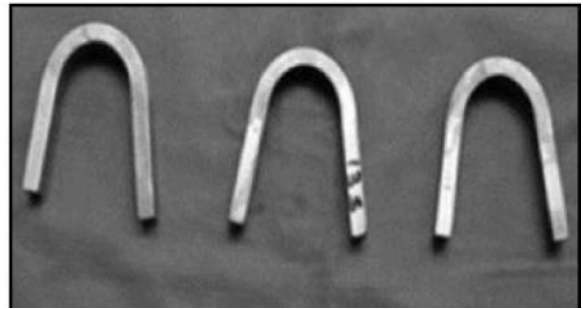
Fig. 5 (a) & (b) Fracture location of weld joints after tensile testing

6.2 Studies on Bend Test

The side faces and root bend tests of pipe weld joint has been carried out as per AWS B4.0 standard. The side root and face bend results of the weld joints prepared by full GMAW procedure are as also shown below in figure 6. It is observed that, after bending the specimens are not showing any open discontinuity or cracks. Thus, it infers that the weld joints prepared by full GMAW procedure showed good formability.



(a)



(b)

Fig.6 (a) & (b) showing the photograph of bend tested specimens

6.3 Studies on Hardness Test

Using Vickers's hardness testing machine, the distribution of hardness across the weld joint with reference to the HAZ adjacent to fusion line was studied at a load of 10 kg. The hardness test was performed according to the ASTM E92 standard. Hardness of the specimen by welded by STT root pass followed by Pulsed GMAW process and specimen welded by conventional SMAW process has been given below.

Table 3 Hardness of Weld Joint

Sl. No.	Hardness, HV (After PWHT)	
	Modified GMAW Process	Conventional SMAW Process
1	171	172
2	175	173
3	176	175

Comparison of hardness of the weld joints of the two specimens have been graphically represented below, which shows the hardness of the weld joints are better in the modified GMAW process compared to the conventional SMAW process.

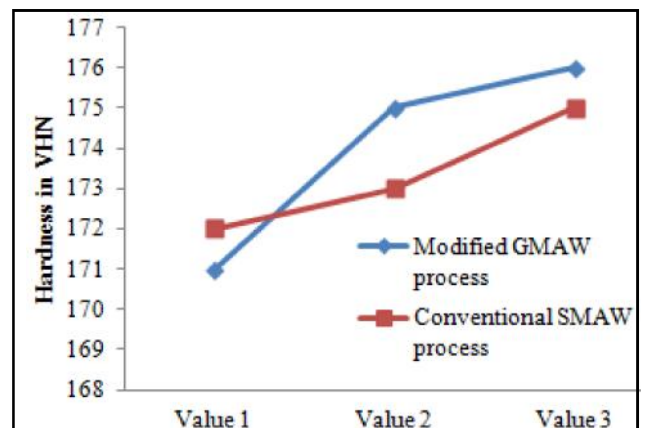


Fig.7 Graphical comparison of hardness of weld joints

6.4 Studies on Impact Toughness

Impact toughness of the weld joint (after PWHT) of the specimen welded by STT root pass followed by Pulsed GMAW process have been studied and it is compared to the specimen welded by conventional welding process is given below:

Table 4 Cv - Impact Toughness of Weld Joint

Sl. No.	CV, Impact Toughness, J/m ³ (After PWHT)	
	Modified GMAW Process	Conventional SMAW Process
1	235	236
2	233	234
3	230	232

Comparison of impact toughness of the weld joints of the two specimens have been graphically represented below, which shows the impact toughness of the weld joints are similar and meets the standard quality requirements.

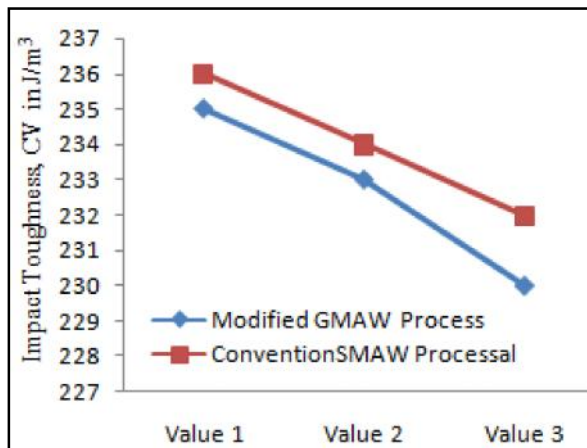


Fig. 8 Graphical comparison of impact toughness of weld joints

7. CONCLUSIONS

Thus, full Gas Metal Arc Welding (GMAW) technology (Modified short arc process as Surface Tension Transfer (STT) root pass followed subsequent passes by pulsed current GMAW process) have been established for weld joints of hand hole pipe and dish end of the alloy steel pipe headers. The weld joints prepared by full GMAW technology meets required radiography and mechanical properties. Thus it is equivalent and alternate welding process for the time consuming welding process of GTAW root pass followed by SMAW process. Also it is concluded that there is a significant

improvement in weld quality and productivity with reduced cycle time by using modified GMAW process.

REFERENCES

- [1] ASME, ASME Boiler and Pressure Vessel Code, Section VIII Div.1 2013 Edition, American Society of Mechanical Engineers - New York, 2013
- [2] ASTM E 92 Standard Test Method for Vickers Hardness of Metallic Materials published by American Society for Testing Material (ASTM),2003
- [3] AWS B4.0:2007 Standard Methods for Mechanical Testing of welds approved by the American National Standards Institute May 2, 2007
- [4] Bolboaca, D. Sorana and Lorentz Jantschi, “Design of Experiments: Useful Orthogonal Arrays for Number of Experiments from 4 to 16”, Entropy 9.4, 2007, pp.198-232.
- [5] Bruce D. De Runtz, “Accessing the Benefits of Surface Tension Transfer Welding to Industry”, Journal of Industrial Technology, Vol.19, No.4, 2003.
- [6] Dunder Marko, Ivan Samardzic and Stefanija Klaric, “Monitoring of Main Welding Parameters at STT Welding Process”, International Research / Expert Conference Trends in the Development of Machinery and Associated Technology, Vol.9, 2005.
- [7] D. Watkins, H. B. Smartt and C. J. Einerson, Proc. Recent Trends in Welding and Technology, eds. S. A. David and J.M. Vitek, ASM, 1990, pp. 19-23.
- [8] F Wang, W K Hou, S J Hu, E Kannatey-Asibu, W W Schultz and P C Wang, “Modelling and Analysis of Metal Transfer in Gas Metal Arc Welding”, Journal of Physics D: Applied Physics, Vol.36, No.9, 2003.
- [9] Gurpreet Singh Sidhu, Sukhpal Singh Chatha, “Role of Shielded Metal Arc Welding Consumables On Pipe Weld Joint”, International Journal of Emerging Technology and Advanced Engineering, Vol.2, No.12, 2012.
- [10] M. J. M. Hermans and G. Den Ouden, “Process Behavior and Stability in Short Circuit Gas Metal Arc Welding”, Welding Journal- New York-137-s, (1999).
- [11] K. L. Kenney, K. S. Miller and H. B. Smartt, “Heat Transfer in Pulsed Gas Metal Arc Welding”, Fifth International Conference on Trends in Welding Research, J. M. Vitek et.al., eds., ASM, 1998, pp.357-361.

- [12] Lee, Woei-Shyan and Tzay-Tian Su, "Mechanical Properties and Microstructural Features of AISI 4340 High-Strength Alloy Steel Under Quenched and Tempered Conditions", *Journal of Materials Processing Technology* Vol.87, No.1, 1999, pp.198-206.
- [13] L. P. Connor, *ed.*, "Welding Handbook (Eighth Edition)", Vol. 1, pp. 69, Miami, FLA: American Welding Society, 1987.
- [14] S. Subramanian, *et al.*, "Experimental Approach to Selection of Pulsing Parameters in Pulsed GMAW Welding Journal", Vol.78, 1999, pp.166-s.
- [15] J. C. Vaillant, B. Vandenberghe, B. Hahn, H. Heuser and C. Jochum, "C T/P23, 24, 911 and 92: New grades for Advanced Coal-fired Power Plants Properties and Experience", *International Journal of Pressure Vessels and Piping*, Vol.85, No.1, 2008, pp.38-46.

A Finite Element Investigation on Nonlinear Elastic Material for Anthropomorphic Robotic Fingertips

J. Pugalenti¹, M.Raguraman¹, L.Vijayakumar¹, S. Sankar¹, S. Yuvaraj¹, K. Venkatesh Raja²

¹Department of Mechanical Engineering, K.S.R. College of Engineering (Autonomous), Tiruchengode - 637 215, Namakkal District, Tamil Nadu

²Associate professor, Department of Mechanical Engineering, V.S.A. Group of Institutions, Salem - 636 010, Salem District, Tamil Nadu

Abstract

The investigation of soft materials is done for developing an anthropomorphic robotic fingertip in dexterous manipulation. Some of the soft materials are natural rubber, synthetic rubber, elastomer, polymer composite and nano-particulated polymer composite. The parametric relationships are investigated and some interesting results were found by using of Finite Element package ANSYS. The contact parameters of different materials are compared to the human skin values and the best soft material which behaves similar to the human skin was chosen for better grasping of anthropomorphic Robotic fingers.

Keywords: Anthropomorphic Robots, Contact Mechanics, Finite Element Analysis, Soft Finger Contacts

1. INTRODUCTION

In designing an anthropomorphic robot, fingertip design plays a vital role. In dexterous manipulations in anthropomorphic robots requires a soft material for good effective grasping. By nature, human skin can conform to the object easily. Mostly the robot has linear elastic material for grasping, which cannot conform to object easily and it may damage object while applying larger force. So the non-linear elastic materials are used recent decades.

In 1882, Hertz(6) studied the growth of contact area as a function of applied normal force N based on a linear elastic model. He conducted experiments using a spherical glass lens against a planar glass plate. From the results he concluded that the radius of contact was proportional to the normal force raised to the power of $1/3$ which was consistent with the analytical results based on the linear elastic model. In the theory of large elastic deformation, in 1949 Mooney derived the general stress relation for hyper-elastic materials.

In 1985 Jameson first used Hertzian contact theory to derive the relationship between the shear force and moment, later called limit surface. In 1969 Schallamach(16) and Cutkosky et al(4). In 1992 explored performance of various kinds of rubbers in their research for compliant materials that will provide ideal skin for artificial robot fingers. Contact mechanics for soft robotic fingers.

In 1989 Tataru(17) and 1991 Tataru et al(18).verified over experimentations that the Hertzian model is not effective for the modelling of non-linear elastic materials comprising large deformations and this theory proposed that non-linear elastic material show large deformation over small applied loads. In 1996 Han et al(5). also have done work in artificial finger design, using data obtained from experiments on human subjects. In 1999 Xydias and Kao(20) developed a power-law theory for soft hemispherical fingertips. This power-law was suggested for soft fingers, which behaved more like non-linear contacts. In 2000 Toru Omata et al (14). attempted to determine the static indeterminacy of the grasp force which is a fundamental problem in power grasping if static friction is considered in the contact points. In 2003 Byoung-Ho Kim et al(15). analysed the fundamental deformation effect of soft fingertip in two fingered object manipulation. In 2005 Seifert et al. applied Yeoh, Mooney-Rivlin and St-Venant-Kirchhoff(2,3,9) models for modeling of skeletal muscles. In 2011 Elango and Marappan(11) investigated the fundamental deformation effect of robot soft finger by analyzing the contact area, displacement and pressure. They used Ogden model for analysis. In 2013

K.Venkatesh Raja and R.Malayalamurthi(19) Assessment and influence of internal rigid core on the contact parameters for soft hemispherical fingertips.

From this literature review, very few authors compared the non-linear elastic materials to the human skin for best grasping which is very essential in robotic dexterous manipulation. The main purpose of this research work is to propose a best grasping material with comparison of human skin. From the comparison some interesting results were discussed using Finite Element Analysis.

2. REVIEW OF BASIC THEORIES FOR SOFT FINGERTIP MODELING

2.1. Hertz theory of Non-Linear Elastic Materials

Hertz studied the growth of contact area as a function of the applied normal force, based on the linear elastic model. He conducted experiments using a spherical glass lens against a planar glass plate. Using the experimental results from 10 trials, He concluded that the radius of contact is proportional to the normal force raised to the power 1/3.

The following equation relates the applied normal force (N) and the developed radius of contact.

$$N^{1/3} \quad (1)$$

2.2 Power Law Theory- Non Linear Elastic Materials

Xydas and Kao (20) extended the linear elastic contact model phenomena of soft finger were described by a power law theory more realistically.

$$a = CN^y \quad (2)$$

Here,

a= Contact Radius

C= Geometric Constant

N= Normal Force

=Material Dependent Constant

The varies from 0 to 1/3 for non-linear material and zero for an ideal soft finger.

3. SOFT FINGER CONTACT MODEL

The sectional view of the proposed soft hemispherical fingertip model is illustrated in figure 1. The fingertip is loaded in the normal direction to the rigid plane in contact with the tip, and is coupled in the UY direction in order to ensure that the normal load is being applied uniformly throughout the upper surface. A commercial finite element package, is applied for solving the non-linear contact problem.

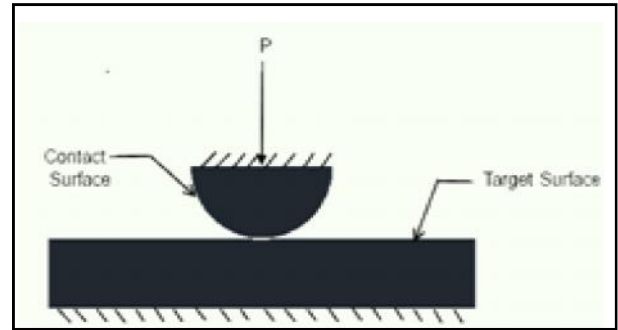


Fig.1 Hemispherical model of a fingertip

3.1 Fea Model

The element type is PLANE 183 and the condition is Axis Symmetry. The Surface to Surface contact was selected here. So that the fingertip is coupled on UY Direction and Target Surface is arrested in all directions. The selected materials in are Neoprene, Silicone Rubber, Natural Rubber, Tango Plus. The contact element used on the sphere surface area of type CONTACT 172. This type of contact element has three nodes, and six degrees of freedom. The three nodes allow the element to be a curved parabolic shape, thus matches more accurately to the surface of sphere. The single target element used on the flat surface is of type TARGET 169. The fingertip is passed by force on a Flat Surface material made up of Mild Steel ($E=2 \times 10^5 \text{ N/mm}^2$).

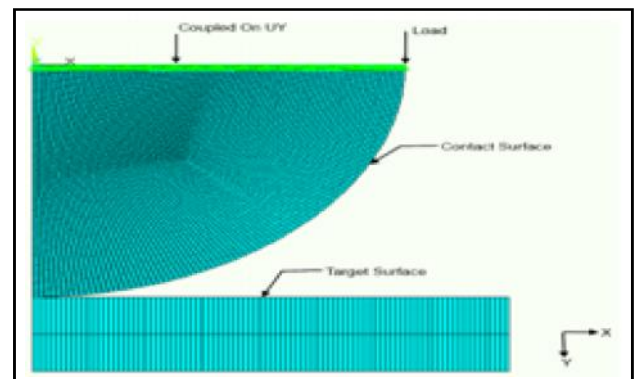


Fig.2 FEA model of soft-fingertip

4. RESULTS AND DISCUSSIONS

The results of Finite Element Analysis discussed in three parametric areas: The contact radius vs. normal force based on the power law theory, Contact pressure vs. normal force, vertical depression vs. normal force. The magnitude of the normal force is varied from 0 to 200N for simulation. The discussions on three parametric areas are presented in the following section.

Table 1 Ogden Constant values. (13,14)

Materials	Ogden Values
Neoprene	$\mu=0.167$ MPa, $\alpha=6.95$ MPa
Silicone	$\mu=0.4945$ MPa, $\alpha=0.7438$ MPa
Silicone R45	$\mu=0.7055$ MPa, $\alpha=1.0546$ MPa
Silicone 8000	$\mu=0.5571$ MPa, $\alpha=1.1609$ MPa
Natural Rubber	$\mu=1.12$ MPa, $\alpha=2.9$ MPa
Human Skin	$\mu=0.11$ MPa, $\alpha=9$ MPa

According to the values of the C and, the material are selected for anthropomorphic robots fingertip.

The neoprene material value is perfectly closer to the human skin value and also the slope of both materials is 90% matching with the human skin values.

Silicone values are also nearer to the human skin value. So it is optimal material for anthropomorphic robots manipulation. Natural rubber value is entirely different for human skin values. So the natural rubber is not directly used for manipulation.

4.1 Discussion on Contact Radius vs. Normal Force

Figure 3 illustrates the relationship between the radius of contact and the magnitude of the normal force.

Finally it was clear that the neoprene and silicone materials are perfectly suitable non- linear elastic material for the anthropomorphic robotics fingertip.

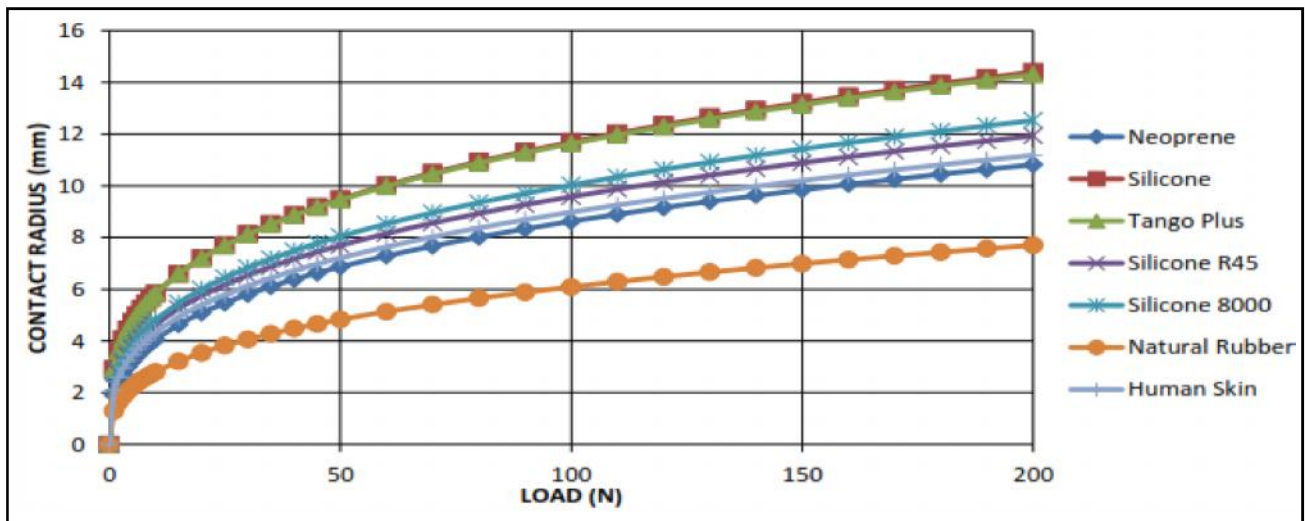


Fig.3 Relationship between the contact radius vs. the normal load.

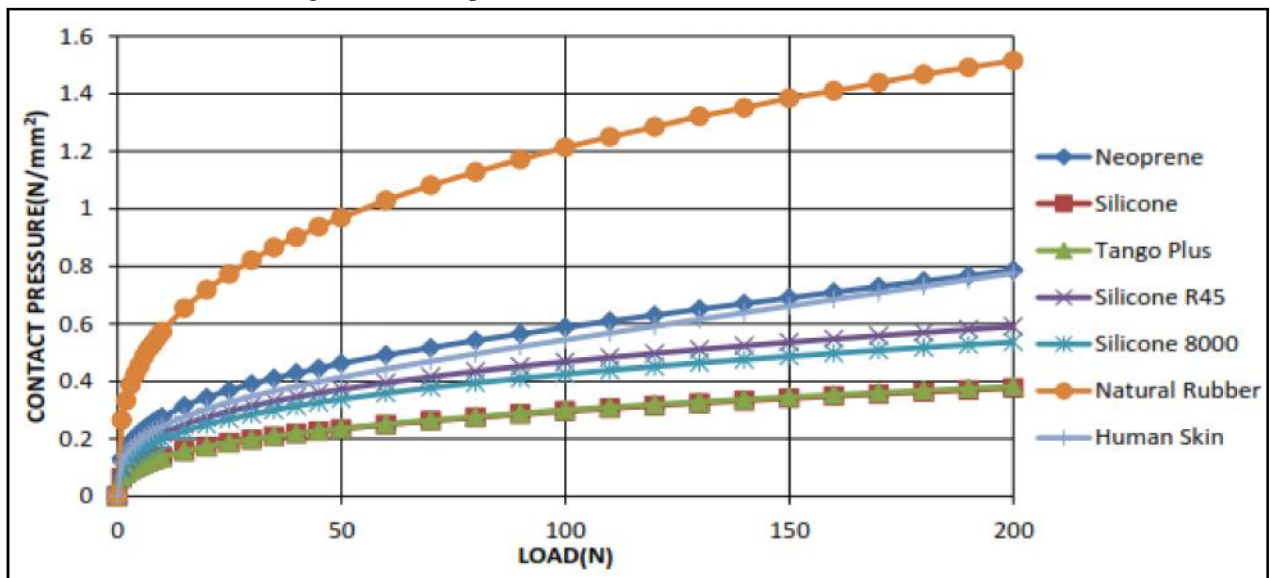


Fig.4 Relationship between the contact pressure vs. the normal load

4.2 Discussion on Contact pressure vs. Normal Force

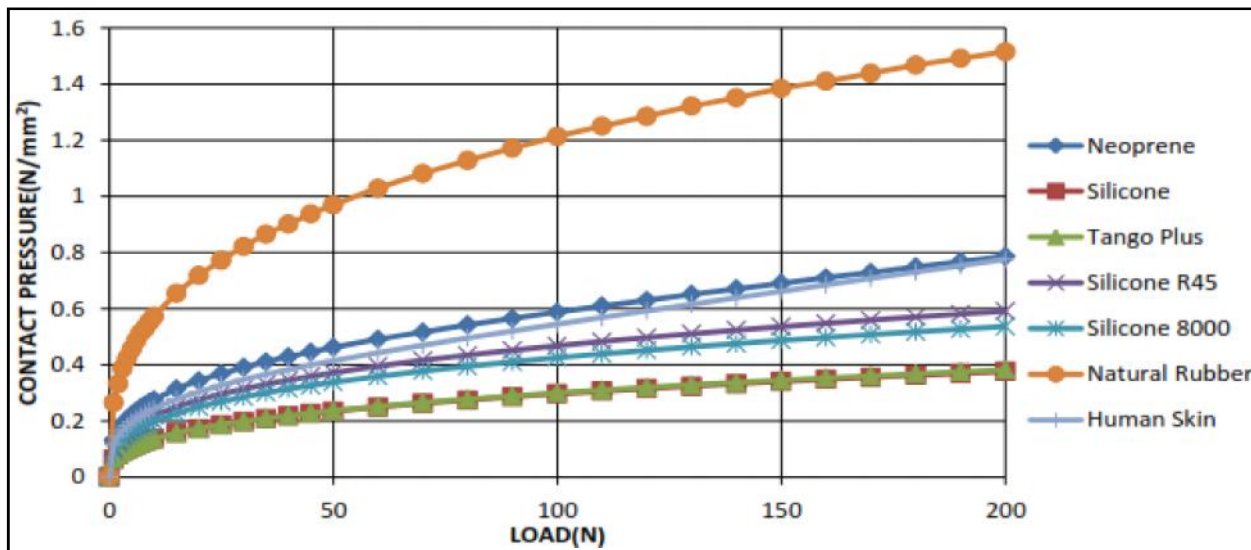


Fig.4 Relationship between the contact pressure vs. the normal load

Figure 4 illustrates the relationship between the contact pressure and the magnitude of the normal force.

Under low values of normal load, the contact pressure values of the neoprene and silicone materials are very closer to the human skin value.

As the normal load increase, the contact pressure is defers for all the materials. But the neoprene material is

perfectly suitable to the human skin values. So the neoprene materials are best suitable for the anthropomorphic robotic fingertip.

Under minimum load and maximum load conditions the natural rubber values are not matched with the human skin values. After some processes are done on the natural rubber, it will adopt to the anthropomorphic robots manipulation.

4.3 Discussion on Vertical depression vs. Normal Force

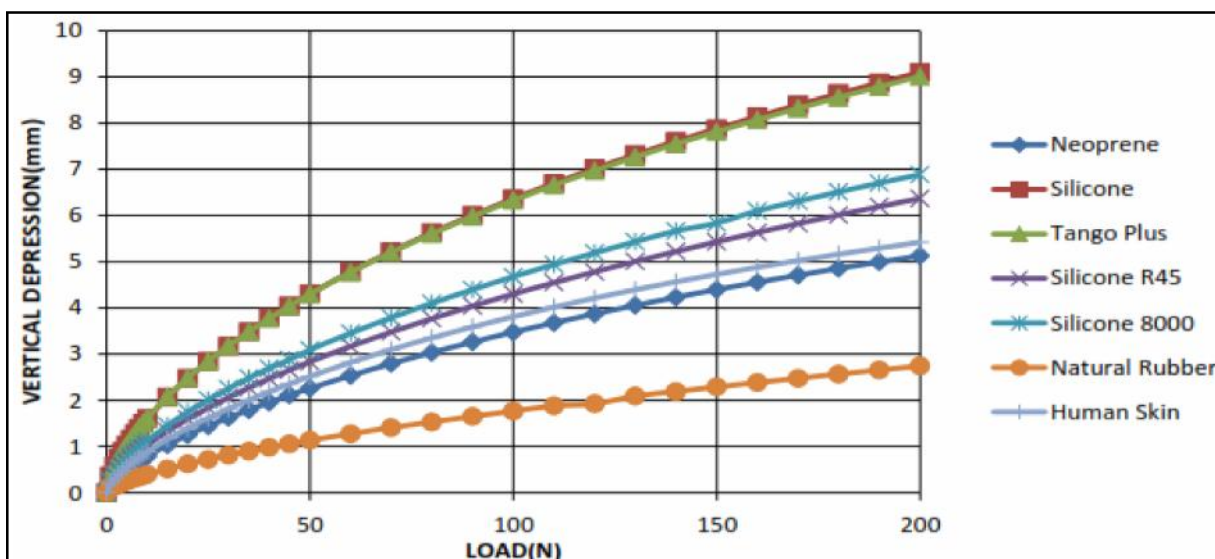


Fig.5 Relationship between the vertical depressions vs. the normal load.

Figure 5 illustrates the relationship between the vertical depression and the magnitude of the normal force.

On the grasping force from 0 to 50N, the vertical depression of the neoprene and silicone materials are exactly matched with the human skin values.

As the grasping force increases the vertical depression values are varied. Finally the neoprene material is perfectly suitable non-linear material for the anthropomorphic robot fingertip. Even though the natural rubber values are minimum range, it does not used for dexterous manipulation.

Silicone and Tangoplus material values are more than that of the human skin values. The neoprene and silicone, materials are optimal material for better anthropomorphic robots manipulation.

5. CONCLUSION

The modeling of the soft finger contact is the one of the most essential tasks in the dexterous manipulation. This proposed soft finger model will give rise to innovation of a more realistic artificial fingertip which emulates humans. The combination of various investigations presented in this study can be used to analyze and simulate contact behaviours of grasping and manipulation in robotics. Based on the power law theory for soft finger contacts, the parametric relationship is presented the contact radius, contact pressure and vertical depression. Contact parameters are done for six different soft materials (neoprene, silicone R45, tango plus, natural rubber, silicone 8000, and silicone). From this analysis, the silicone and neoprene materials are best optimal materials for anthropomorphic Robotic fingertip.

REFERENCES

- [1] ANSYS 11.0 Documentation. ANSYS Inc.
- [2] H.Abe, K.Hayashi and M.Sato, "Data Book on Mechanical Properties of Living Cells".
- [3] P.E.Allaire, J.G. Thacker, R.F.Edlich, G.J. Rodenhaever and M.T. Edgerton, "Finite Deformation Theory for In-vivo Human Skin".
- [4] M.R.Cutkosky, J.M. Jordain and P.K. Wright, "Skin Materials for Robotics Fingers,"
- [5] HY. Han, A.Shimada and S.Kawamura, Proc.1996. IEEE Int.conf.Rob.Autom.
- [6] H.Hertz, "On the Contact of Rigid Elastic Solids and on Hardness", chapter 6: Assorted papers by H.Hertz. MacMillan, New York, November 1882.
- [7] KL.Johnson, "Contact Mechanics", Cambridge University Press: Cambridge.
- [8] I. Kao and F.Yanga, "ICCC Transaction on Robotics and Manipulation".
- [9] S. Kuster and R.Dillmann, "Passive Modeling of Skeletal Muscles", Institute for Rechnerentwurf and Fehlertoleranz.
- [10] MT. Manson and JK.Salisbury, "Robot Hands and the Mechanics of Manipulation", MIT press, Cambridge, MA, 1985.
- [11] Natarajan Elango and R.Marappan, "Fundamental Deformation Effect of A Robot Soft Finger and its Contact Width during Power Grasping", 2009.
- [12] RW. Ogden and Rubb, "Chem Technology", 1986.
- [13] RW. Ogden, "Non-Linear Elastic Deformations", Courier Dover Publication. New York 1997.
- [14] T. Omata and K. Nagata, "Rigid Body Analysis of the Indeterminate Grasp Force in Power Grasps", 2000.
- [15] KH. Park, BH. Kim and S. Hirai, "Development of Soft Fingertip and its Modeling based on Force Distribution", IEEE Int Conf Robot Autom., 2003.
- [16] A. Schallamach, "The Load Dependence of Rubber Friction", Proc. Physical Soc.
- [17] Y.J. Tatara, "Eng.Mater.Technol.", 1989.
- [18] Y. Tatara, S.Shima and JC.Lucero, "Eng. Mater Technol.", 1991.
- [19] K. Venkatesh Raja and R.Malayalamurthi, "Influence of Internal Rigid Core on the Contact Parameters for Soft Hemispherical Fingertip".
- [20] N. Xydas and I.Kao, "Modeling of Contact Mechanics and Friction Limit Surface for Soft Fingers with Experimental Results", 1999.

Experimental Study on a Solar Water Desalination System

K. Selvakannan¹ and P. Prashanth²

¹PG Student, Department of Energy Engineering, ²Assistant Professor, Department of Mechanical Engineering, Kumaraguru College of Technology, Coimbatore - 641 049, Tamil Nadu
E-mail id:selvakannan29@gmail.com, prasanth.p.mec@kct.ac.in

Abstract

In the present scenario the provision of water terribly much reduced. plenty of work were undertaken to enhance the productivity of the still for distillation. Throughout the review on solar still performance, the results indicate that, there are some parameter that have an effect on the performance of solar still like depth of the still, quality of brine water, evaporation rate sensible heat storage medium used, variety of inner glass used. Four modifications for sun based desalination structures are shown in this assignment the first modification is, of addition of sensible heat storage medium, specified it will store the sun radiation and reemit throughout evening time. Some sensible heat storage materials are red brick items, quartzite rock, naturally washed stone. The properties of many sensible heat storage materials are given below The second modification is the addition of silver layer in the side of the basin such that it reflects the solar incident radiation inside the solar still effectively with minimum loss of heat. The third modification is, varying the depth of the solar still to find the optimum yield this is due to the increase in the capacity of the water in the basin. The Fourth modification is the addition of black die for mixing with the water in the in the still. Water with the addition of black die to the water inside the basin there is a increase in the absorbency of the solar energy entering the water itself. Thus, the water temperature in the presence of dye is much higher than that in the absence of the dye. Consequently by these change in sun oriented still, the productivity of water will be increased. The heat flows along with time interval is analyzed.

Keywords: Pure water, Solar Energy, Solar Distillation, Solar hotwater, TDS

1. SOLARENERGY

sun based vitality has the best capability of all the supply of renewable energy and if solely little quantity of this way of energy may will be used it will be one among the foremost necessary provides of energy, particularly once different sources within the country

This answer is solar water distillation. it's not a placement method, however it's not received the eye that it deserves. maybe this can be as a result of it's a such a low-tech and versatile answer to water issues. Nearly anyone is capable of building a still and providing in themselves with fully pure water from terribly questionable sources. of radiation is absorbed in earth and atmosphere payeryear. solar energy wherever sun hits atmosphere is 1017watts and also the total demands is 1013 watts. thus the sun offers U.S. one thousand times additional power than we want. If we willowed are able to } use five- hitter of this energy it'll be fifty time what the globe will needs. The energy radiated by the sun on a bright sunny day is four to seven KWh per money supply [2].

2. INTRODUCTION TO SOLAR STILL

Solar distillation may be a tried and true technology. the primary famous use of stills dates back to 1551once it absolutely was employed by Arab alchemists. alternative scientists and naturalists used stills over the approaching centuries together with Della passage (1589) Lavoisier(1862), and Mauchot (1869) [3]. the primary standard star still plant was in-built 1872 by the Swedish engineer Charles Wilson within the mining community of Las Salinas in what's currently northern Chile (Region II). This still was an oversized basin-type still used for supply H₂O victimization salt feed water to a nitrate mining community. The plant used wood bays that had blackened bottoms victimization logwood dye and alum. the whole space of the distillation plant was four,700 sq. meters. On a typical summer day this plant made four. 9 metric weight unit of H₂O per square measure of still surface, or quite twenty three,000liters per day. star water Distillation system conjointly referred to as "Solar Still". star Stillwell effectively purify H₂O & even raw sewerage. star Stills will effectively removing Salts

minerals, Bacteria, Parasites, Heavy Metals & TDS[2]. Basic principal of operating of star still is “Solar energy heats water, evaporates it salts and microbes left behind), and condenses as clouds to come back to earth as rain

2.1 Solar Still Operation

Water to be. The glass cowl permits the radiation to pass into the still, that is usually absorbed by the blackened base. This interior surface uses a blackened material to boost absorption of the sunrays. The water begins to heat up and also the wet content of the air at bay between the water surface and also the glass cowl will increase. The heated vapor evaporates from the basin and condenses on the within of the glass cowl. during this method, the salts and microbes that were within the original water square measure left behind. Condensed water trickles down the inclined glass cowl to an inside assortment trough and bent on a storage bottle. Feed water ought to be additional daily that roughly exceeds the distillation production to supply correct flushing of the basin water and to scrub out excess salts left behind throughout the evaporation method. If the still made three liters of water, nine liters of make-up water ought to be additional, of that half-dozen liter leaves the still as excess to flush the basin.

2.2 Forms of Star Still

Basin Type: It encompass shallow, bracken basin of saline impure water coated with a sloping clear roof radiation that passes through the clear roof heats the water in blackened basin. therefore evaporating water that gets condensed on the cooler beneath aspect of the glass and gets collected as liquid hooked up to the glass[4]. Wick sort star Still: It consists of a wick rather than a basin. The saline impure water is more matured the wick or absorbed by the wick at a slow rate by surface tension. A water-resistant liner is placed between the insulation and therefore the wick. Alternative energy is absorbed by the water with in the wick that gets gaseous and later condensed on the bottom of the glass and eventually collected with the condensation channel fastened on the lower aspect of all-time low surface (4)

The base of the solar still is made of G.I. box of dimension (4’ x 2’ x 10 cm). This box is embedded into another box of wood shown in figure 1. Here length L=

3. DESIGN OF SOLAR DISTILLATION PLANT

3.1 Construction of Solar Still

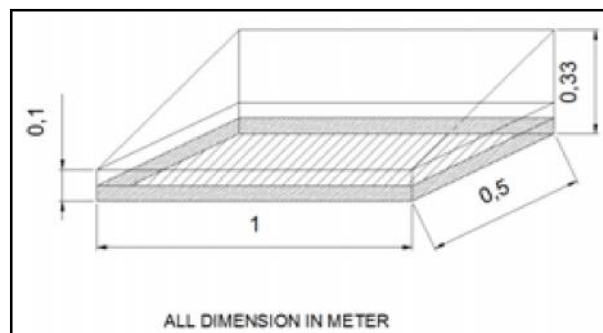


Fig.1 Construction of solar still

Table 1 Specifications of the Conventional Still

Sl.No.	Specifications of the Solar Still	Measurements
1	Length	29 inches
2	Width	19.inches
3	Glass cover inclination	25°
4	Depth of basin in front side	7 inches
5	Depth of basin in back side	14.inches
6	Thickness of Glass cover	4 mm

29cm, Breath B=125cm, Height H= 19 cm. and at opposite side = 14 cm, Angle Θ =150. This also contains same box of thermocol inside it between the G.I box. The thermocol is having 3 mm thickness. The half pipe is fixed such that the water slipping on the surface of the glass will fall in this pipe under the effect of gravity. A frame of fiber stick is fixed with the G’I box so that glass can rest on it. This completes the construction of the model.

The holes for the inlet of water, outlet of harse water and outlet of unadulterated pure water is made as per the convenience. We have made the outlet of brackish water at right bottom of the model (seeing from front of the model), outlet of the pure water at the end of the channel and gulf at the right divider over the outlet.

3.2 Details of Different Parts of the System

3.2.1 Still Basin

It is the a part of the system during which the water to be distilled is unbroken. it’s thus essential that it should absorb solar power. thence it’s necessary that the fabric have high absorbtivity or terribly less reflectivity and really less transitivity. These square measure the criteria’s for choosing the basin materials. Kinds of the basin materials that may be used square

measure as follows: one. animal skin sheet, 2. Gesilicon,3. steel plate, 4. RPF(reinforced plastic) five. G.I. (galvanized iron).

3.2.2 Side Walls

It usually provides inelasticity to the still. however technically it provides thermal resistance to the warmth transfer that takes place from the system to the encircling. thus it should be made of the fabric that’s having low worth of thermal physical phenomenon and may be rigid enough to sustain its own weight and therefore the weight of the highest cowl totally different forms of materials which will be used are: 1) stone 2) gravel 3) thermocol, 4) RPF (reinforced plastic).For higherinsulation we’ve got used composite wall of thermocol (outside) and glass fitting wood. (Size::thermocol (k= thermal conductivity=0.6W/m0C) eight metric linear unit thick, thermocol(k= thermal conductivity=0.02W/m0C) fifteen metric linear unit thick)

3.2.3 Top Cover

The passage from wherever irradiation happens on the surface of the basin is high cowl. Conjointly it’s the surface where ever atmospheric phenomenon collects. That the options of the highest cowl are 1)clear to radiation, 2)Non absorbent and Non-absorbent of water 3)clean and sleek surface.The Materials are often used are 1) glass, 2) synthetic resin. We’ve used glass (3mm) thick as high cowl having rubber tube as frame border

size(4’ X 2’ cm)

3.2.4. Pipe

The atmospheric phenomenon that’s fashioned slides over the inclined prime cowl and falls within the passage, this passage this passage, that fetches out the pure water is named pipe the materials which will be used are 1)G.I. 2)RFP 3)P.V.C We have used P.V. C Pipe (size:four.5x 1’’cm)

3.2.5 Supports for Top Cover

The frame provided for supporting the highest cowl is Associate in Nursing optional factor. I.e. it are often used if needed. we’ve got used fiber stick as a support to carry glass (size ::five millimeter X 5mm). the sole modification in our model is that we’ve got to form the model as vacuumed as attainable. thus we’ve got tried to form it airtight by sticking out tape on the corners of the glass and at the sides of the box from wherever the likelihood of the discharge of within hot air is most.

4. RESULTS AND DISCUSSION

Experiment is performed from 08:00am to 06:00pm in winter season.the more effective time condensation 12.00 pm to 3.30 pm.

4.1 Readings Taken for Still

Table 2 Represents the Reading Taken for Solar Still

TIME	BASIN TEMP (T)	OUTER GLASS TEMP (T)	SEA WATER TEMP (T)	AMBIENT TEMP (T)	SOLAR INTENSITY (W/m^2)	AIR VAPOURE TEMP (T)	CUMULATIVE YIELD (LITTER)
08.30AM	19	22	20	12	750	22	0.0235
09.00AM	20	23	21	15.1	768	30	0.239
09.30AM	22	28	23	17.3	820	35.6	0.225
10.00AM	26	32	27	18.6	848	40	0.39
10.30AM	28	38	30	19.2	868	46.2	0.49
11.00AM	33	40	35	20.6	898	52.6	0.545
11.30AM	39	45	40	21.4	915	53.5	0.465
12.00PM	50	52	52	20.5	956	55	0.495
13.00PM	52	61	62	19.1	990	57.4	0.498
13.30PM	59	63	63	18	1024	58.2	0.503
14.00PM	64	65	66	16	1056	62.3	0.498
14.30PM	65	67	66	14.5	1100	65.3	0.496
15.00PM	67	69	68	13.5	1058	67.5	0.396
15.30PM	65	66	65	12	1042	64.3	0.375
16.00PM	63	63	63	10.5	1031	61.1	0.302
16.30PM	59	58	59	9	1006	56.3	0.86
17.00PM	56	54	57	8.3	998	54	0.44
17.30PM	54	50	55	7	875	47	0.36
18.00PM	49	48	50	7.6	850	36	0.25
18.30PM	43	46	45	6.9	828	29.1	0.022

4.2 Observations

Time taken for drop to come to pipe = 1/2 hour
 Amount of brackish water poured initially = 16litter
 Time taken for drop to come out of pipe = 0.4
 Amount of pure water obtained at the end of the exp. = 1.75
 TDS of purified water =68.1
 Temperature of the condensate = 52

4.3 Graph

Figure 2 represents the temperature variation in the solar still during six hours. The maximum

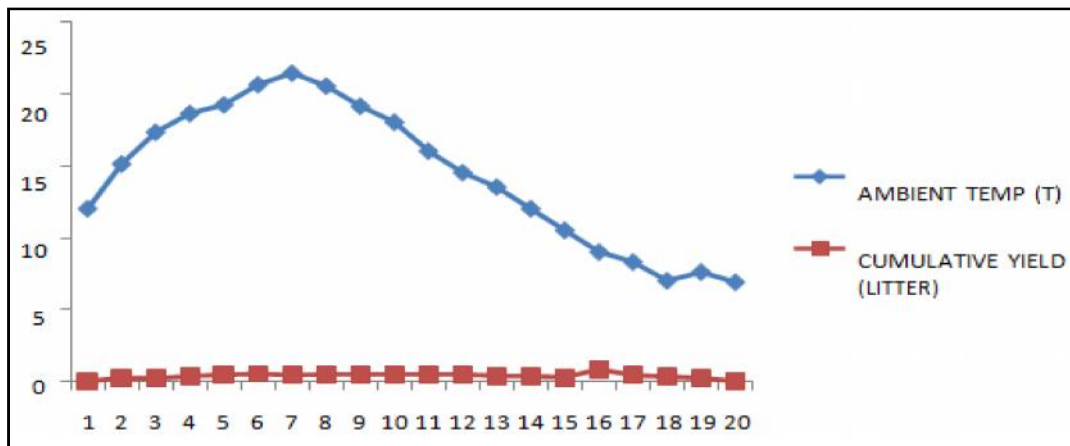


Fig.2 Temperature variation

5. CONCLUSION

From the graph 1, we can conclude that the increase in temperature and hence the evaporation is maximum in the period of 11:15 am to 2:45 pm. The maximum temperature achieved is 530c which is at 2:30 pm. then the temperature decreases. The aim of our experiment was to get pure water from the brackish water available. The brackish water we have supplied was 16liters and at the end of the experiment we got 1.7 liter. The experiment was carried out in winter season.

The TDS level of purified water obtained is 67.8 PPM. So the water obtained is potable. Theoretically, the experiment should fetch out 2.35 liter. So the efficiency of the system is 8%.

REFERENCES

[1] A. Kumar, A. Kumar, G.D. Sootha and P. Chaturvadi, "Performance of a Multi-stage Distillation System using a Flat-plate Collector", Extended Abstract, ISES Solar World Congress, Kobe, Japan, 1989.

temperature in the system is of 531C obtained at 01:35pm.

4.4 Efficiency of Still

The theoretically obtained amount of pure water = 2.33 liter. The practically obtained amount of pure water = 1.6 liter. Efficiency=(actual amount of pure water) / (theoretical amount of pure water)*100 (1.6 / 2.33) *100 68.66 %.

[2] BA. Akash, MS. Mohsen, O.Osta and Y. Elayan, "Experimental Evaluation of a Single-basin Solar still Using Different Absorbing Materials", Renewable Energy, Vol.14, No.1-4, 1998, pp.307-310.
 [3] B.B. Sahoo, N. Sahoo, P.Mahanta, L.Borbora, P.kalita, "Performance Assesment of Solar still Using Blackened Surface and Thermocole Insulation", Vol.33, No.17, 2007, pp.1703-1708.
 [4] H.P. Garg and J.Prakash, "Solar Energy", Tata McGraw Hill Publishing Co. 2008.
 [6] M.A.S. Malik, G.N Tiwari, A. Kumar and M.S. Sodha, "Solar Distillation", Pergamon Press, Oxford, UK, 1982.
 [7] R.K.Rajput, "Heat and Mass Transfer", S.Chand Publication.
 [8] G.N. Tiwari, "Solar Energy", Narosa Publishing House, 2002.

Indian Journal of Engineering, Science, and Technology (IJEST)

(ISSN: 0973-6255)

(A half-yearly refereed research journal)

Information for Authors

1. All papers should be addressed to The Editor-in-Chief, Indian Journal of Engineering, Science, and Technology (IJEST), Bannari Amman Institute of Technology, Sathyamangalam - 638 401, Erode District, Tamil Nadu, India.
2. Two copies of manuscript along with soft copy are to be sent.
3. A CD-ROM containing the text, figures and tables should separately be sent along with the hard copies.
4. Submission of a manuscript implies that : (i) The work described has not been published before; (ii) It is not under consideration for publication elsewhere.
5. Manuscript will be reviewed by experts in the corresponding research area, and their recommendations will be communicated to the authors.

Guidelines for submission

Manuscript Formats

The manuscript should be about 8 pages in length, typed in double space with Times New Roman font, size 12, Double column on A4 size paper with one inch margin on all sides and should include 75-200 words abstract, 5-10 relevant key words, and a short (50-100 words) biography statement. The pages should be consecutively numbered, starting with the title page and through the text, references, tables, figure and legends. The title should be brief, specific and amenable to indexing. The article should include an abstract, introduction, body of paper containing headings, sub-headings, illustrations and conclusions.

References

A numbered list of references must be provided at the end of the paper. The list should be arranged in the order of citation in text, not in alphabetical order. List only one reference per reference number. Each reference number should be enclosed by square brackets.

In text, citations of references may be given simply as "[1]". Similarly, it is not necessary to mention the authors of a reference unless the mention is relevant to the text.

Example

- [1] M.Demic, "Optimization of Characteristics of the Elasto-Damping Elements of Cars from the Aspect of Comfort and Handling", International Journal of Vehicle Design, Vol.13, No.1, 1992, pp. 29-46.
- [2] S.A.Austin, "The Vibration Damping Effect of an Electro-Rheological Fluid", ASME Journal of Vibration and Acoustics, Vol.115, No.1, 1993, pp. 136-140.

SUBSCRIPTION

The annual subscription for IJEST is Rs.600/- which includes postal charges. To subscribe for IJEST a Demand Draft may be sent in favour of IJEST, payable at Sathyamangalam and addressed to IJEST. Subscription order form can be downloaded from the following link [http:// www.bitsathy.ac.in/ijest.html](http://www.bitsathy.ac.in/ijest.html).

For subscription / further details please contact:

IJEST

Bannari Amman Institute of Technology

Sathyamangalam - 638 401, Erode District, Tamil Nadu Ph: 04295 - 226340 - 44

Fax: 04295 - 226666 E-mail: ijest@bitsathy.ac.in Web:www.bitsathy.ac.in

Indian Journal of Engineering, Science, and Technology

Volume 10, Number 1, January - June 2016

CONTENTS

Realization of Aging Aware Reliable Multiplier Design Using Verilog R.Rathna Devi and R.Ganesan	01
Bloom Filter Based Data Management With Error Detection And Correction V. K. Juvilna, S. Amalorpava Mary Rajee and R.Ganesan	08
Comparative Analysis of Different Wheeling Charge Methodologies N. Selvam and P.L. Somasundaram	14
Analysis on Various Optimization Techniques for Selecting Gain Parameters in FOC of an E-Drive Meher Anusha Vanapalli, Raja Sekhar Kammala and Sathish Laxmanan	20
Automated Gesture Recognition System Using Raspberry Pi N. Geraldine Shirley and Neethu Krishna	25
Assessment and Enhancement of Transient Stability in Power system using ETAP Software A.Maria Sindhuja and D.Raj Kumar	31
Antioxidant Activities of A Few Common Seaweeds from the Gulf of Mannar and the Effect of Drying As the Method of Preservation R.Charu Deepika, J.Madhusudhanan and T.Charles John Bhaskar	37
Optimization, Standardization of extraction and Characterization of Lutein S. Gayathri, S.R. Radhika Rajasree, L. Aranganathan and T.Y. Suman	44
Biopharmaceuticals and Nutraceuticals from Marine Species and Marine Waste T. Charles John Bhaskar	49
Analysis and Comparison of Mechanical Properties of Alloy Steel gr.22 Material Welded by GMAW Process with Conventional SMAW Process K. Karthikeyan, V. Anandakrishnan and R. Alagesan	53
A Finite Element Investigation on Nonlinear Elastic Material for Anthropomorphic Robotic Fingertips J. Pugalenthil, M.Raguraman, L.Vijayakumar, S. Sankar, S. Yuvaraj and K. Venkatesh Raja	59
Experimental Study on a Solar Water Desalination System K.Selvakannan and P.Prashanth	64